

**“DEVELOPMENT OF GRAPHENE PROMOTED CLICK
TRIGGERED SELF-HEALING NANOCOMPOSITES”**

**A thesis submitted to the
*University of Petroleum & Energy Studies***

**For the award of
DOCTOR OF PHILOSOPHY
in
*Mechanical Engineering***

BY

Sanka Rama Venkata Siva Prasanna

October 2019

SUPERVISOR (S)

**Dr. Sravendra Rana
Dr. Shyam Pandey**



**Department of Mechanical Engineering
School of Engineering
University of Petroleum & Energy Studies
DEHRADUN-248007: Uttarakhand**

**“DEVELOPMENT OF GRAPHENE PROMOTED CLICK
TRIGGERED SELF-HEALING NANOCOMPOSITES”**

**A thesis submitted to the
*University of Petroleum & Energy Studies***

**For the award of
DOCTOR OF PHILOSOPHY
in
*Mechanical Engineering***

BY

**Sanka Rama Venkata Siva Prasanna
(SAP ID- 500056860)**

October 2019

Supervisor

Dr. Sravendra Rana
Associate Professor
Department of Chemistry
University of Petroleum and Energy Studies

Co-Supervisor

Dr. Shyam Pandey
Professor
Department of Mechanical Engineering
University of Petroleum and Energy Studies



UNIVERSITY WITH A PURPOSE

**Department of Mechanical Engineering
School of Engineering
University of Petroleum & Energy Studies
DEHRADUN-248007: Uttarakhand**

DECLARATION

October 2019

DECLARATION

I declare that the thesis entitled “**Development of Graphene Promoted Click Triggered Self-Healing Nanocomposites**” has been prepared by me under the guidance of **Dr. Sravendra Rana**, Associate Professor of Department of Chemistry, University of Petroleum & Energy Studies and **Dr. Shyam Pandey**, Professor of Department of Mechanical Engineering, University of Petroleum & Energy Studies. No part of this thesis has formed the basis for the award of any degree or fellowship previously.

S. Rama Venkata Siva Prasanna

Sanka Rama Venkata Siva Prasanna

*Department of Mechanical Engineering,
School of Engineering
University of Petroleum & Energy Studies
Dehradun-248007: Uttarakhand
Date: May 6, 2020*

CERTIFICATE



CERTIFICATE

I certify that **Sanka Rama Venkata Siva Prasanna** has prepared his thesis entitled “**Development of Graphene Promoted Click Triggered Self-Healing Nanocomposites**”, for the award of PhD degree of the University of Petroleum & Energy Studies, under my guidance. He has carried out the work at the Department of Mechanical Engineering, University of Petroleum & Energy Studies.

Supervisor

Dr. Sravendra Rana
Associate Professor
Department of Chemistry
University of Petroleum and Energy Studies
Dt: May 6, 2020

Co-Supervisor

Dr. Shyam Pandey
Professor
Department of Mechanical Engineering
University of Petroleum and Energy Studies
Dt: May 6, 2020

CORPORATE OFFICE: 210, 2nd Floor,
Okhla Industrial Estate, Phase III,
New Delhi - 110 020, India.
T: +91 11 41730151/53, 46022691/5
F: +91 11 41730154

ENERGY ACRES: Bidholi Via
Prem Nagar, Dehradun - 248 007
(Uttarakhand), India.
T: +91 135 2770137, 2776053/54/91, 2776201
F: +91 135 2776090/95

KNOWLEDGE ACRES: Kandoli Via
Prem Nagar, Dehradun - 248 007
(Uttarakhand), India.
T: +91 8171979021/2/3, 7060111775

ENGINEERING | COMPUTER SCIENCE | DESIGN | BUSINESS | LAW | HEALTH SCIENCES

ABSTRACT

This work aims to develop composites materials having self-healing properties including enhance in mechanical and electrical properties. The principal weakness of polymer composites is damage from impact, where resulting micro-cracks can propagate to allow delamination and breakage of the composites, resulting in loss of physical properties of the composites. Strategies to compensate material fatigue including mechanical and conductive properties are among the most challenging issues, being prominently addressed by the use of nano- and microscaled fillers, or via new chemical concepts such as self-healing materials. Capsule based self-healing approach is dedicated to achieve the self-healing, in particular, Cu(I)-catalyzed Huisgen [3+2] dipolar cycloaddition “‘click chemistry’ (CuAAC)” based covalent self-healing was performed.

A robust approach to improve the dispersion, stability, and recyclability of a copper catalyst via immobilization of copper nanoparticles Cu(I) on N-doped reduced graphene oxide nanosheets was explored. Nitrogen-doped reduced graphene oxide (NRGO) stabilized copper nanoparticles based heterogeneous catalyst were synthesized to assist CuAAC for achieving it at low temperature without any external additive (oxidizing/reducing agent), and performs click reaction under both solvent and bulk conditions. The NRGO-Cu(I) catalyst is reusable ten times and observed around 90% yield after 10th cycle, whereas washing and recyclability of catalyst was performed under open air environment. DFT calculations were also analyzed to confirm the experimental findings.

Self-healing nanocomposites in response to external damage were developed using synthesized graphene based catalytic system, bearing embedded metal-nanoparticles, which after embedding into a thermoset-material displays self-healing ability up to 100 % at room temperature. The study also found the use of graphene as both, the nanostructured material (for enhancing the mechanical and conductive properties) and catalyst, helpful to trigger self-healing responses via ‘click chemistry’ at room temperature - a feature which often is not achieved in many reported self-healing materials, where healing is only accomplished at

significantly higher temperatures. Together with the embedding and distribution of the graphene-based catalyst, a capsule-based approach is used to embed the required components stable into a polymer matrix, where one capsule-sort is sufficient to prevent early mixing of the components. Triggered capsule rupture then induces contact of the healing agents with the graphene-based catalyst, in turn inducing "click"-reaction, able to fully repair damage onsite as determined by mechanical measurements. Given the enormous importance of autonomic repair of materials damage, this concept here reports a true and reliable chemical system, with a high level of robustness.

In consequence, graphene promoted composites materials based on 'click chemistry' demonstrates self-healing at low temperature. The low temperature self-healing materials open the window for preparing the composite materials for aircraft safety, anti-corrosion coatings, as well as for wind turbines.

ACKNOWLEDGMENT

I would like to express my heartfelt gratitude to my supervisors Dr. Sravendra Rana and Dr. Shyam Pandey, for their continuous encouragement and motivation throughout my thesis work. I am very thankful to them for presenting this promising area of research to me and for their supervision, which I have been getting all these years of my research.

In addition to my Supervisors, I would like to show gratitude to Dr. S. J. Chopra (Chancellor), Dr. Deependra Kumar Jha (Vice-Chancellor) and Dr. Kamal Bansal (Dean) at the University of Petroleum & Energy Studies for their cherished support for my research work.

I would like to express my gratitude to Dr. J. K. Pandey (Associate Dean R &D), Dr. S.M Tauseef (Assistant Dean SoE, R&D) and Dr. Ajay Kumar (Head of Mechanical Department) at University of Petroleum and Energy Studies, for his support during my research.

I would like to extend my special thanks to my dear faculty colleague and friend Mr. Balaji K who stood with me at each phase of my work.

My sincere gratitude to Dr. Yves Leterrier and Prof. Dr. Véronique Michaud from Laboratory for Processing of Advanced Composites (LPAC), (EPFL), Lausanne, Switzerland, Prof. Wolfgang H. Binder from Institute of Chemistry, Martin Luther University Halle-Wittenberg, Germany, Dr. Anurag Srivastava from Advanced Materials Research Group, ABV - Indian Institute of Information Technology and Management, Gwalior and Prof. Nanda Gopal Sahoo (Kumaun University, Nainital) for their research collaboration.

Thanks to Mr. Caneon Kurien, Mr. Debajoyti Bose, Mr. Pinniseti Swami Sai Ram, Mr. Raghunath, Ms. Meera CS, Ms. Aslesha and Ms. Manjusha. I also thank all my faculty colleagues at Department of Mechanical Engineering.

I express my sincere gratitude to my family for all their love, encouragement and support. I am greatly indebted to my loving friends Mr. Dheeraj, Mr. Sai Pradeep and Mr. Vipul Ram for their support whenever needed in every moment of life.

I would like to acknowledge in-house Central Instrumentation Centre (CIC) and Composite Lab facility; where I have carried out my research work. I also thank lab technicians Dr. Devendra Rawat, Mr. Charu Pant and Mr. Anuj Kumar.

I would like to express my gratitude to R&D Department and SRE Department for their support. I also thank Mr. SS Farmer (Deputy Registrar), Ms. Rakhi Ruhel, Mr. Amit Pandey and Team R&D.

TABLE OF CONTENTS

DECLARATION	3
CERTIFICATE.....	4
ABSTRACT.....	5
ACKNOWLEDGMENT.....	7
TABLE OF CONTENTS.....	9
ABBREVIATIONS.....	12
LIST OF FIGURES	14
LIST OF TABLES.....	17
CHAPTER 1: INTRODUCTION	1
1.1 COMPOSITES.....	1
1.2 SELF-HEALING COMPOSITES	2
1.3 TYPES OF SELF-HEALING.....	3
1.3.1 AUTONOMIC SELF-HEALING MATERIALS	4
1.3.2 NON AUTONOMIC SELF-HEALING MATERIALS	8
1.4 APPLICATIONS	20
1.5 OBJECTIVES.....	26
1.6 SUMMARY.....	26
CHAPTER 2: OVERVIEW AND BIBLIOGRAPHY SURVEY FOR NANO BASED COMPOSITE MATERIALS	28
2.1 OVERVIEW	28
2.2 CARBON BASED SELF-HEALING NANO MATERIALS	28
2.2.1 PREPARATION METHODS.....	29
2.2.2 SELF-HEALING APPROACHES USING GRAPHENE.....	31
2.3 ENCAPSULATION STRATEGIES.....	37
2.3.1 MINI-EMULSION POLYMERIZATION (OIL-IN-WATER).....	39
2.3.2 SOLVENT EVAPORATION PROCESS.....	40
2.3.3 INTERFACIAL PROCESS	41
2.3.4 SOL-GEL PROCESS.....	42
2.4 DIFFERENT CHEMISTRIES INVOLVED IN SELF-HEALING.....	44
2.4.1 DICYCLOPENTADIENE (DCPD).....	44
2.4.2 5-ETHYLIDENE-2-NORBORENE (ENB) BASED HEALING SYSTEM...	44
2.4.3 AMINE-EPOXY-BASED HEALING SYSTEM.....	45
2.4.4 THIOL EPOXY BASED HEALING SYSTEM.....	46

2.4.5 THIOL-ISOCYANATE BASED HEALING SYSTEM	47
2.4.6 CLICK (AZIDE-ALKYNE) BASED HEALING SYSTEM.....	48
2.4.7 SELF-HEALING BY SUPRAMOLECULAR	49
2.5 SUMMARY:.....	56
CHAPTER 3: DEVELOPMENT OF HETEROGENEOUS CATALYST TO PROMOTE CLICK TRIGGERED SELF-HEALING.....	58
3.1 INTRODUCTION	58
3.2 MATERIALS AND METHODS.....	59
3.2.1 MATERIALS.....	59
3.2.2 METHODS	60
3.3 PREPARATION OF GRAPHENE OXIDE (GO).....	60
3.4 PREPARATION OF COPPER IMMOBILIZED THERMALLY GRAPHENE OXIDE (TRGO/Cu(I)).....	63
3.5 PREPARATION OF NITROGEN DOPED COPPER IMMOBILIZED REDUCED GRAPHENE OXIDE (NRGO/Cu(I))	67
3.6 SYNTHESIS OF AZIDE FUNCTIONALIZED POLY DIMETHYLSILOXANE72	
3.7 SYNTHESIS OF ALKYNE FUNCTIONALIZED PDMS	72
3.8 TESTING OF CATALYTIC ACTIVITY	73
3.9 DENSITY FUNCTIONAL THEORY (DFT) ANALYSIS	77
3.10 SUMMARY	80
CHAPTER 4: DEVELOPMENT OF SELF-HEALING NANOCOMPOSITES	81
4.1 INTRODUCTION	81
4.2 PREPARATION OF SELF-HEALING AGENTS	82
4.2.1 PREPARATION OF TRIVALENT ALKYNE MOIETY	82
4.2.2 PREPARATION OF TRIVALENT AZIDE MOIETY	83
4.2 FABRICATION OF ENCAPSULATION.....	87
4.2.1 PREPARATION OF PRE-POLYMER SOLUTION	87
4.2.2 PREPARATION OF EMULSION	87
4.2.3 PREPARATION OF MICROCAPSULES	87
4.3 COMPOSITE PREPARATION	88
4.4 RESULTS AND DISCUSSION	89
4.4.1 TENSILE TEST.....	91
4.4.2 SELF-HEALING PERFORMANCE.....	95
4.4.2 CONDUCTIVITY	100
4.5 SUMMARY.....	101

CHAPTER 5: CONCLUSION AND FUTURE PERSPECTS	102
5.1 FUTURE PERSPECTS	103
REFERENCES	105
APPENDIX.....	120
BIO-DATA	127
PLAGARISM CERTIFICATE.....	129

ABBREVIATIONS

C	:	Carbon
CHCl ₃	:	Chloroform
CNT	:	Carbon nanotube
Cu	:	Cupperic Oxide
DCM	:	Dichloromethane
DFT	:	Density functional theory
DGEBA	:	Diglycidylether of bisphenol A
DMA	:	Dynamic Mechanical Analysis
DSC	:	Differential Scanning Calorimeter
E'	:	Tensile storage modulus
FAAS	:	Flame Atomic Absorption Spectrometry
FE-SEM	:	Field Emission Scanning Electron Microscopy
GO	:	Graphene Oxide
H	:	Hydrogen
H ₂ O ₂	:	Hydrogen Peroxide
H ₂ SO ₄	:	Sulfuric Acid
HB	:	Hyper-branched polymer
HCl	:	Hydrochloric Acid
HRTEM	:	High-Resolution Transmission Electron Microscopy
M _n	:	Number Average Molecular Weight
N	:	Nitrogen
Na ₂ SO ₄	:	Sodium Sulfate
NaHCO ₃	:	Sodium Bicarbonate
NaOH	:	Sodium Hydroxide
nm	:	Nanometer
NMR	:	Nuclear Magnetic Resonance
NRGO	:	Nitrogen Doped Reduced Graphene Oxide

NRGO/Cu(I) Oxide	:	Copper immobilized Nitrogen Doped Reduced Graphene Oxide
O	:	Oxygen
p	:	Volume fraction
PAA	:	poly(acrylic acid)
PDMS	:	Polydimethylsiloxane
PEI	:	poly (ethylene imine)
pH	:	Potential of Hydrogen
R_f	:	Retardation Factor
rGO	:	Reduced Graphene Oxide
ROMP	:	ring opening metathesis polymerization
SAP	:	superabsorbent polymer
TBAB	:	Tetra-N-Butylammonium Bromide
TDOS	:	Total density of states
TLC	:	Thin-layer chromatography
TMPTE	:	Trimethylolpropane tripropargyl ether
T_{onset}	:	Onset Temperature
T_p	:	Peak Temperature
TRGO	:	Thermally Reduced graphene Oxide
TRGO/Cu(I)	:	Copper immobilized thermally reduced graphene oxide
UV–Vis	:	Ultraviolet–visible spectroscopy
XPS	:	X-ray Photoelectron Spectroscopy
XRD	:	X-ray Diffraction Spectroscopy
σ	:	Current conductivity

LIST OF FIGURES

<i>Figure 1.1 Basic structure of composite material.....</i>	<i>1</i>
<i>Figure 1.2 Approaches for biological and synthetic system [9].....</i>	<i>3</i>
<i>Figure 1.3 Classification of self-healing system.....</i>	<i>4</i>
<i>Figure 1.4 Mechanism of capsule based healing system [12].....</i>	<i>6</i>
<i>Figure 1.5 Ring Opening Metathesis Polymerization (ROMP) [27].....</i>	<i>6</i>
<i>Figure 1.6 Mechanism of Vascular based self-healing [28].....</i>	<i>7</i>
<i>Figure 1.7 Various approaches used to synthesize physical and chemical interaction based self-healing materials.....</i>	<i>9</i>
<i>Figure 1.8 Classification of materials based on non-autonomic.....</i>	<i>10</i>
<i>Figure 1.9 (a) UPy-containing polymer. (b) Supramolecular hydrogel made of PEG-UPy polymer 15 wt% in water [40].....</i>	<i>11</i>
<i>Figure 1.10 Schematic representation of a) photo-switchable, dynamically crosslinked polymer network and b) the chemical structures of the crosslinkers, indicating the switchable reactivity for the reversible DA reaction and healability of the network [68]</i>	<i>16</i>
<i>Figure 1.11 (A) Healing Process; (B) Healing reaction [70].....</i>	<i>17</i>
<i>Figure 2.1 The ability of self-healing using IR, electricity and electromagnetic in FG-TPU composites [142].....</i>	<i>30</i>
<i>Figure 2.2 SEM image of rGO-PU a) cut crosssection b) healed after passing microwave [142].....</i>	<i>32</i>
<i>Figure 2.3 images demonstrating the self-healing property of tri-layered nanocomposite hydrogel. (a) Two pieces (one was in methylene blue color for better understanding) were separated in two halves, b) then the cut surfaces brought into contact by applying mechanical force, then (c) a single piece hydrogel can be found after few minutes and d) it displays that it can withstand high stretchable forces even after failure [156].....</i>	<i>34</i>
<i>Figure 2.4 (a) Graphical representation of the welding process of GF-HI, b) images taken during Joule-heated GF-HI, c) welded samples, d) SEM images of welded samples, yellow dashes indicates the strong bond between the graphene layers [151].....</i>	<i>35</i>
<i>Figure 2.5 self-healing system based on Click-triggered graphene nanocomposites [161].....</i>	<i>36</i>
<i>Figure 2.6 self-healing of polymer composite using oxidation-reduction process [139].</i>	<i>37</i>
<i>Figure 2.7 schematic representation of capsule parts a) polymer material in blue color and b) core material as green in color.....</i>	<i>38</i>

<i>Figure 2.8 Formation of Pre-polymer by reaction between urea and formaldehyde [162]</i>	40
<i>Figure 2.9 schematic representation of procedure adopted for preparing capsules using sol-gel and interfacial process [174]</i>	43
<i>Figure 2.10 5-ethylidene-2-norborene (ENB) based healing mechanism [127]</i>	45
<i>Figure 2.11 Nucleophilic ROMP using bisphenol A diglycidyl ether and diethylenetriamine [127]</i>	46
<i>Figure 2.12 Thiol Based self-healing system [127]</i>	47
<i>Figure 2.13 a) Healing procedure for poly(aroyltriazole)s films b) click reaction [198]</i>	49
<i>Figure 2.14 self-healing by supramolecular mechanism [202]</i>	50
<i>Figure 2.15 a) frequency measurement of PIB, b)supramolecular network formation, c) experiment procedure of self-healing behavior [209]</i>	52
<i>Figure 2.16 a) naphthalene-diimide rich in pi electron b) Prenyl end-capped weak in pi electrons c)Interaction between the naphthalene-diimide and prenyl pi-pi stacking [210]</i>	53
<i>Figure 3.1 'click' reaction using NRGO/Cu(I) catalyst</i>	59
<i>Figure 3.2 (a) XRD and (b) UV for Graphene Oxide (GO)</i>	62
<i>Figure 3.3 (a) TEM image of TRGO/Cu(I) and (b) Histogram of particle diameter of TRGO/CU(I)</i>	64
<i>Figure 3.4 (a) XPS of TRGO/Cu(I), (b) High resolution XPS of element C, (c) High resolution XPS of element Cu. (d) High resolution XPS of element O</i>	66
<i>Figure 3.5 (a,b) TEM images of the NRGO/Cu(I) catalyst. (c) Copper particle size and distribution</i>	68
<i>Figure 3.6 (a) XPS of NRGO/Cu(I). (b) High resolution XPS of element N. (c) High resolution XPS of element Cu. (d) High resolution XPS of element C. (e) High resolution XPS element of O</i>	71
<i>Figure 3.7 Scheme of azide functionalized PDMS</i>	72
<i>Figure 3.8 Scheme of alkyne functionalized PDMS</i>	73
<i>Figure 3.9 (a,b) catalyst recycling within ten reaction cycles for NRGO/Cu(I) and TRGO/Cu(I), respectively. (c,d) TEM image of Cu particles after 10 cycles for NRGO/Cu(I) and TRGO/Cu(I), respectively</i>	75
<i>Figure 3.10 DSC measurements for the bulk 'click' reaction with different catalysts at 5 °C/min heating rate</i>	76

Figure 3.11 (a, b) Cu ⁺ adsorption on TRGO and NRGO, respectively. (c, d) Band structure of Cu ⁺ adsorption on TRGO and NRGO, respectively. (e, f) NRGO with a cluster of 3 and 5 Cu ⁺ ions, respectively.....	79
Figure 4.1 Synthesis of trimethylolpropane tripropargyl ether (TMPTPE)	82
Figure 4.2 Structure of 2-(((6-(azidomethyl)nicotinoyl)oxy)methyl)-2-(hydroxymethyl)propane-1,3-diyl bis(6-(azidomethyl)nicotinate).....	85
Figure 4.3 ¹ H NMR for 2-(((6-(azidomethyl)nicotinoyl)oxy)methyl)-2-(hydroxymethyl)propane-1,3-diyl bis(6-(azidomethyl)nicotinate).....	86
Figure 4.4 ¹³ C NMR for 2-(((6-(azidomethyl)nicotinoyl)oxy)methyl)-2-(hydroxymethyl)propane-1,3-diyl bis(6-(azidomethyl)nicotinate).....	86
Figure 4.5 FE-SEM image for the synthesized capsules containing healing agent.....	88
Figure 4.6 (a) Pure Epoxy and (b) Epoxy composite	89
Figure 4.7 SEM image of capsules with a) 5wt%, b) 10wt%, c) 15wt% and d) 20wt%...	89
Figure 4.8 Presence of healing agents and catalyst in epoxy matrix	90
Figure 4.9 'click' reactions measured by DSC at 5 °C /min heating rate	91
Figure 4.10 Plot for Tensile stress Vs strain for prepared pure epoxy and composite samples measured at strain rate: 0.1mm/min, 25 °C	93
Figure 4.11 plot for tensile stress Vs strain curve for prepared pure epoxy and composite samples with different capsule loading (strain rate: 0.1mm min ⁻¹ , 25 °C)	94
Figure 4.12 Deformation curve for the applied load.....	96
Figure 4.13 DMA analysis (before and after crack) for the prepared nanocomposites (contain 15 wt% azide capsules) at 25 °C.....	96
Figure 4.14 Self-healing efficiency of prepared specimens obtained from DMA results .	97
Figure 4.15 Self-healing efficiency of epoxy specimen with heterogeneous catalyst determined at different temperature with time dependent.....	98
Figure 4.16 Self-healing efficiency of epoxy specimen with NRGO/Cu(I) and different wt% of capsules at room temperature with time dependent.....	99
Figure 4.17 TEM images of a) homogenous (Cu(PPh ₃) ₃ F) and b) heterogeneous catalyst TRGO/Cu(I) dispersion in epoxy matrix.....	100
Figure 4.18 Conductivity Vs Graphene volume fraction	101

LIST OF TABLES

<i>Table 1.1 Physical interaction based self-healing mechanism, healing efficiency, mechanical and electrical properties of nanocomposites.....</i>	<i>13</i>
<i>Table 1.2 Chemical interaction based self-healing mechanism, healing efficiency, mechanical and electrical properties of nanocomposites.....</i>	<i>18</i>
<i>Table 1.3 Demonstrated applications for self-healing nanocomposites and associated healing features.....</i>	<i>21</i>
<i>Table 2.1 Properties of healing and capsule parts.....</i>	<i>38</i>
<i>Table 2.2 Self-healing approach.....</i>	<i>54</i>
<i>Table 3.1 Elemental analysis of Go, TRGO/CU(I) and NRG0/CU(I).....</i>	<i>68</i>
<i>Table 3.2 Performance of different Cu-catalysts: phenyl acetylene and benzylazide in THF at room temperature.....</i>	<i>74</i>
<i>Table 3.3 Comparison of band gap with increasing size of Cu⁺ ion cluster.....</i>	<i>79</i>
<i>Table 4.1 Mechanical performance of prepared specimens.....</i>	<i>92</i>
<i>Table 4.2 Mechanical performance of prepared specimens with different wt% loading of capsules.....</i>	<i>94</i>

CHAPTER 1: INTRODUCTION

1.1 COMPOSITES

In recent years, nano/microscale filled polymer components have created many opportunities to overcome the limitations of traditional polymers. Furtherance in engineering structures like material development, testing, analysis, design, production and maintenance, provides direct benefits of development in material technologies. The unique composite materials possess corrosion resistance, permeability, higher strength to weight ratio, electromagnetic transparency, enhances fatigue life, wear resistance, acoustic and thermal insulation, high thermal conductivity, low thermal expansion which are difficult to achieve by individual materials[1]. According to the requirements of desirable properties, these materials can be tailored. By considering, the reliability, performance and cost effectiveness as a major contributing parameter for a composite material. Nevertheless, composite material enhances the material properties compared to blends and alloys; it can be achieved by combining more than one homogeneous materials having different properties [2].

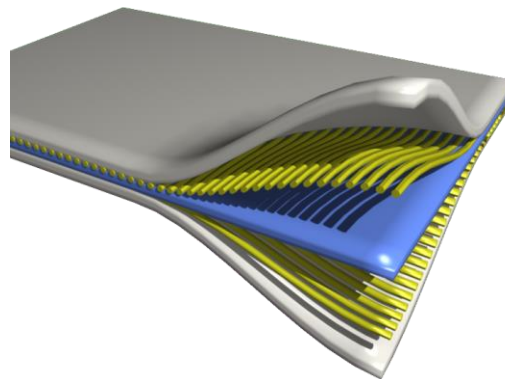


Figure 1.1 Basic structure of composite material

Figure 1.1 shows the basic structure of composite materials, made of two phases: continuous state known as matrix and discontinuous state known as filler. They are classified based on matrix, polymeric, ceramic or metallic. Among those polymeric materials are having more advantages compared to ceramic and metallic due to its properties such as light weight, more ductile in nature and the properties

can be varied by addition of different fillers like graphene, CNT, carbon black, etc [3].

Composite materials play vital role in the field of aerospace engineering, where one third of aircraft structures are built using metals which reduce the performance of craft and increase the maintenance cost[4]. By replacing, the existing materials with the composite materials, could be helpful to reduce the weight, and in turn, it reduces fuel consumption. The combination of polymer and fiber as a composite material possesses low density, high strength, higher stiffness to weight ratios and demonstrates better corrosion protection and fatigue resistance behavior[5]. The addition of multifunctional nanoparticles to the polymer materials is helpful to enhance the physical, chemical, mechanical, thermal, and electrical properties; and includes control in electrostatic discharge, conductive adhesives, and enclosures for electromagnetic shielding[6]. Nevertheless, the material degradation or damage due to impact loads and lightning strike owing to insulating behavior are the major concern, and can be improved by incorporation of self-healing concept and conducting (inducting) nanofillers inside the matrix[7].

1.2 SELF-HEALING COMPOSITES

The self-healing (SH) materials are prominent advancements in composite materials having the capability to restore their inherent structure in case of fracture. Irrespective of the crack size such as micro or macro on material, it can rebuild the gap without any manual influence. The basic idea of these self-healing is motivated from the living species, having the ability to heal themselves by presence of leukocytes when there is a physical damage[8]. In both biological and synthetic cases, the system initiated by the injury (Figure 1.2). In the biological systems, the first process is of inflammatory response or an immediate response when damage occurs like clotting of blood[9]. In the second stage cell proliferation means deposition of matrix in the repair site which may take some time to complete the process of deposition. In the third stage, matrix remodeling it leads to several months to appear like the base[10]. In the synthetic approach, first stage is of actuation: triggering the healing mechanism by damaging the embedded

microcapsules and in the second stage starts due to the activation of the mechanism which transport the species to the damage sites. Thereafter, the healing process completed *via* polymerization, crosslinking and entanglement processes in the final stage.

Generally, materials degrades naturally by aging which rise to micro cracks that ultimately promotes the failure of material. Therefore, SH approach is helpful to improve the durability and reliability of the material. The main aim of this approach is to provide the better or same performance behavior compared to virgin counterpart in an economical way.

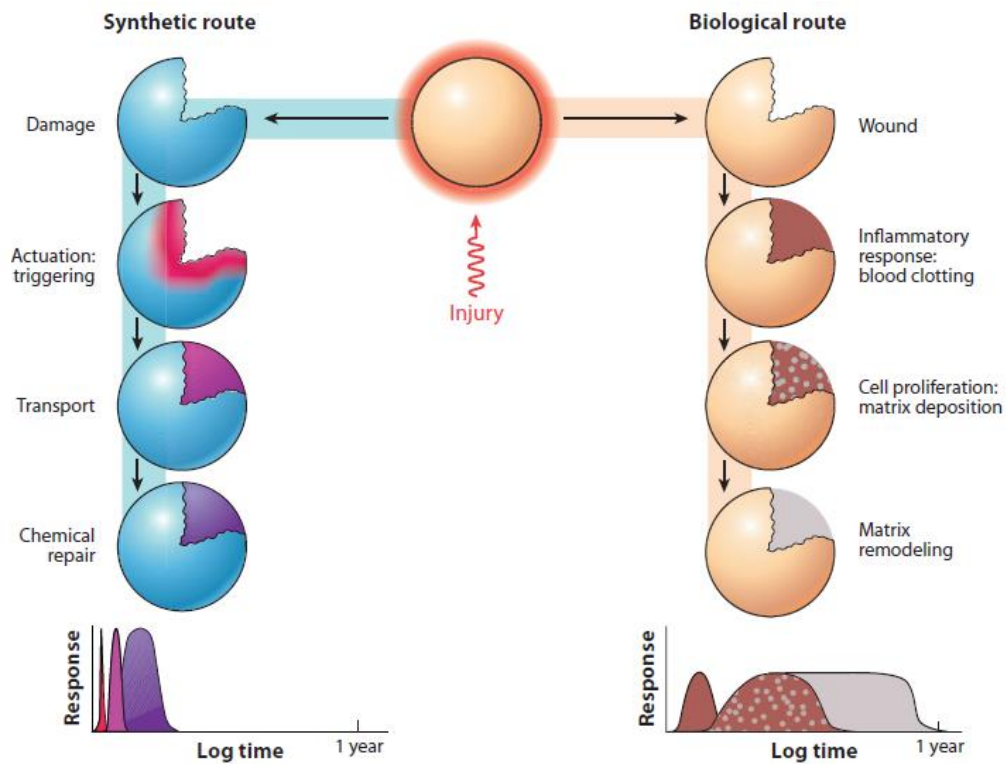


Figure 1.2 Approaches for biological and synthetic system [9]

1.3 TYPES OF SELF-HEALING

These are classified according to the type of chemistries involved in polymers/ polymer composites: a) autonomic and b) non-autonomic[11]. The healing performed by the interventions of external force, is known as non-autonomic, whereas, in case of autonomic self-healing, the process do not need any external force. However, based on the mechanism employed for autonomic self-

healing system, further this system is classified into extrinsic and intrinsic self-healing.

1.3.1 AUTONOMIC SELF-HEALING MATERIALS

In this process material is composed of self-healing capabilities, externally supplied by capsule/vascular network mechanism. The strategy used for designing these type of materials are a) microencapsulation, and b) microvascular network (Figure 1.3). In both the cases process starts by the external or internal damage.

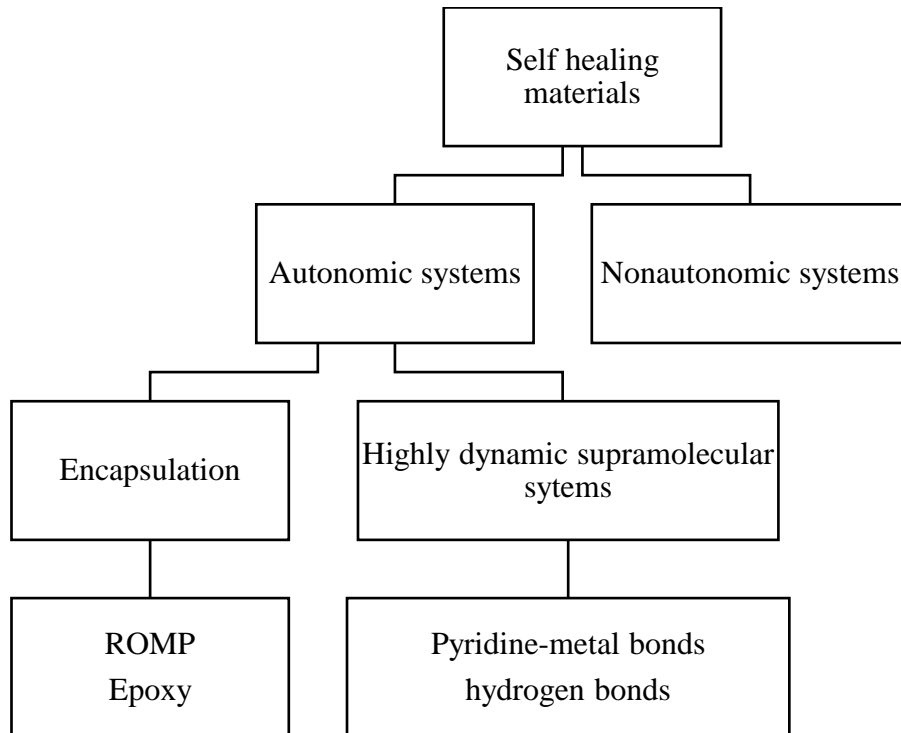


Figure 1.3 Classification of self-healing system

1.3.1.1 Capsule based self-healing

In capsule based self-healing systems, the capsules containing healing agents are dispersed in polymer matrix. Whenever the material is subjected to mechanical stress or damage, the capsules gets damage or rupture takes place, and healing agent in capsules gets triggered and transfer to the affected area and starts polymerization/crosslinking when it comes in contact with dispersed catalysts in the matrix as shown in Figure 1.4[12]. The capsules containing the healing agents are very small in size, ranges from is micro to nano meter. The encapsulation accomplish by the following methods: in-situ polymerization, interfacial

polymerization, sol-gel, coacervation, methods, meltable dispersion and extrusion. In-situ encapsulation is the most popular methods used by the researchers, since it is easy and economical. In-situ encapsulation reaction is proceeded by urea-formaldehyde (UF), melamine urea formaldehyde (MUF), melamine-formaldehyde (MF) and subsequent polymers used as the shell wall material interface between the droplets of oil/water emulsion[13]. The preparation of capsules using different strategies are discussed in subsequent chapter.

White et al. has reported the capsule based first generation self-healing material *via* ROMP based polymerization where dicyclopentadiene (DCPD) as the healing agent and Ruthenium based catalyst were used [14]. Brown et al worked for autonomic self-healing; using UF based capsules to determine the healing efficiency[15] and fatigue[16] of composite material. Moreover, the healing efficiency of composite material with the incorporation of DCPD/Grubbs catalyst of epoxy[17], epoxy vinyl-ester[18], fiber reinforced epoxy composites[19] and thermoplastic[20] was examined. The investigation of self-healing by different permutations was carried out such as; using various catalysts[21] and change in die monomer[22]. Tungsten hexachloride as a catalyst was tested and showed a better thermal stability in epoxy composite[23]. Rule et al. [24] used more innovative approach to preserve the catalytic activity by dispersing wax sphere balls containing Grubbs catalyst. Moo et al. explored the self-healing property in glass fiber-reinforced composite composed of DCPD and Grubbs catalyst preserved by wax[25]. Rong et al. [26] studied the effect of double capsules mechanism, in which one capsule contains the epoxy resin and the other contains the thermally triggered imidazole catalyst.

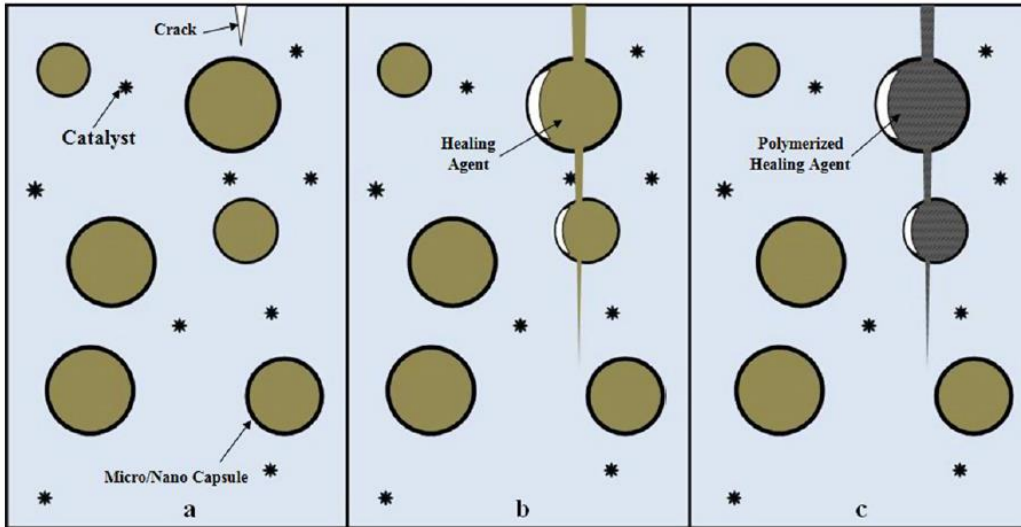


Figure 1.4 Mechanism of capsule based healing system [12]

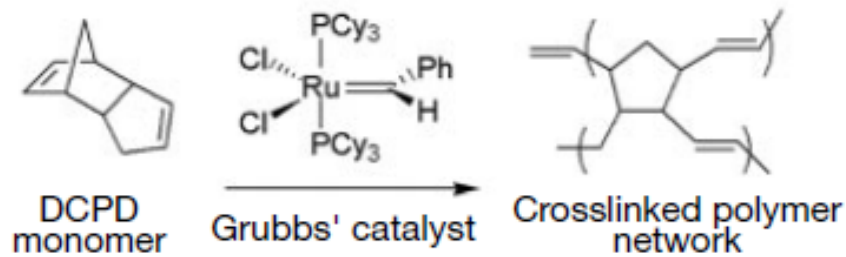


Figure 1.5 Ring Opening Metathesis Polymerization (ROMP) [27]

1.3.1.2 Vascular based self-healing

In vascular based self-healing system the healing agent is confined in a vascular network in the matrix, where in they are connected with each other in the form of network and these networks can be in the form of one dimension, two dimension and three dimension. The network will be in a closed loop until damage or rupture occurs to the network in Figure 1.6. After damage, the network delivers the healing agent to damaged portion and heals the site *via* crosslinking/polymerization of healing agent in contact of catalyst. At the damaged site, healing agents are refilled from undamaged site, which are connected; by this, thus allows the multiple healing events[28].

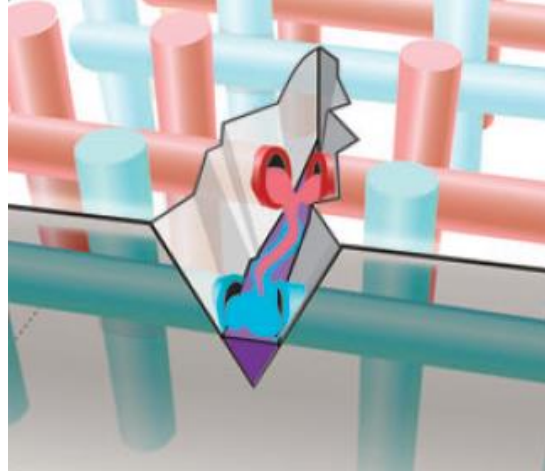


Figure 1.6 Mechanism of Vascular based self-healing [28]

Injection of healing agents into vascular system depends upon the wettability and it affects the diameter and network design. Mechanical properties are depend on the network volume fraction, uniformity, channel distribution, and bonding between the network & matrix; the vascular/channel system can be differentiate based on network dimension as follows[29].

One-dimensional channels: Investigation of self-healing in one-dimensional vascular self-healing system was carried out on epoxy by applying millimeter diameter pipettes made of glass containing two-part epoxy or cyanoacrylate[30]. Subsequently, authors investigated by varying different materials of pipettes, for identifying suitable fiber-reinforced materials among epoxy and vinyl ester[31]. They have investigated the effect of matrix by applying various loads on different specimens made of various thickness and volume fraction. Bleay et al.[32] prepared vascular system by incorporating 15 μm diameter Halex glass fiber (HGF), in unidirectional manner. These laminated fibers were filled with different fluids, which can be released whenever the damage sites were occurred. The release of fluid at damage site was observed by adopting X-radiography and ultrasonography methods.

Two-dimensional channel: These network acts as the intermediate between the piles and 3D networks and thus acts as the interface between the piles stacked

unidirectional; yields improvement in impact mechanical strength and connectivity. Agent transfer, optimize in network, channel diameter and shape of the network are the key factors need to consider while developing 2D channel based SH composites. H. R. Williams et al.[33] constructed sandwich panels of hierarchal network consist of polyvinyl chloride tubes, two-part epoxy system and obtained better results with complete recovery in flexural load and healing.

Three-dimensional channel: Construction of vascular system is a complex process, compared to 2D channel even though it follows the same chemistry[34]. The micro channels of 200 μ m containing DCPD healing agent were proposed. When the surface subjected to the damage then the vascular systems get damaged and releases the DCPD that reacts with Grubbs catalyst to polymerize and thus heal the crack. It was observed that authors could successfully pump the healing agents to damaged site for seven repeated cycles. The healing at the damaged site for every cycle was observed through microscope. Toohey et al.[35] fabricated the 3D vascular healing system based on two-part epoxy chemistry, where the both components were isolated. With this system the healing cycles were increased to sixteen. Hansen et al.[36] observed healing upto 30 cycles by making slight changes in the direct ink writing method. The author able to make the isolated interpenetrating network and optimized the mixing of two components using two-part epoxy system.

1.3.2 NON AUTONOMIC SELF-HEALING MATERIALS

In this process polymer repairs itself after it get damaged; by the utilization of dynamic/reversible interactions that can be broken and renewed under different physicochemical conditions[37]. Intrinsic self-healing presents several features such as, self-healing due to multiple times of healing at the same location without help of any healing agent and catalyst. Two main strategies, based on physical interactions and chemical interactions have been implemented to create intrinsic self-healing polymers (Figure 1.7). Reversible bonding can be either non-covalent, including host-guest interactions, π - π stacking, hydrogen bonds, ionic and hydrophobic interactions, metal coordination, or covalent, such as imine bonds,

disulfide and diselenide bridging, Diels-Alder reaction, reversible boronate ester, and acylhydrazones bonds. The reversibility of covalent bonds between different functional groups can be induced by external stimuli, and can be influenced by a change in temperature, pH, catalytic activity, irradiation, moisture, etc. [38].

The classification of intrinsic self-healing materials based on external stimuli is shown in Figure 1.8. Few of physical and chemical interactions are discussed in following sections.

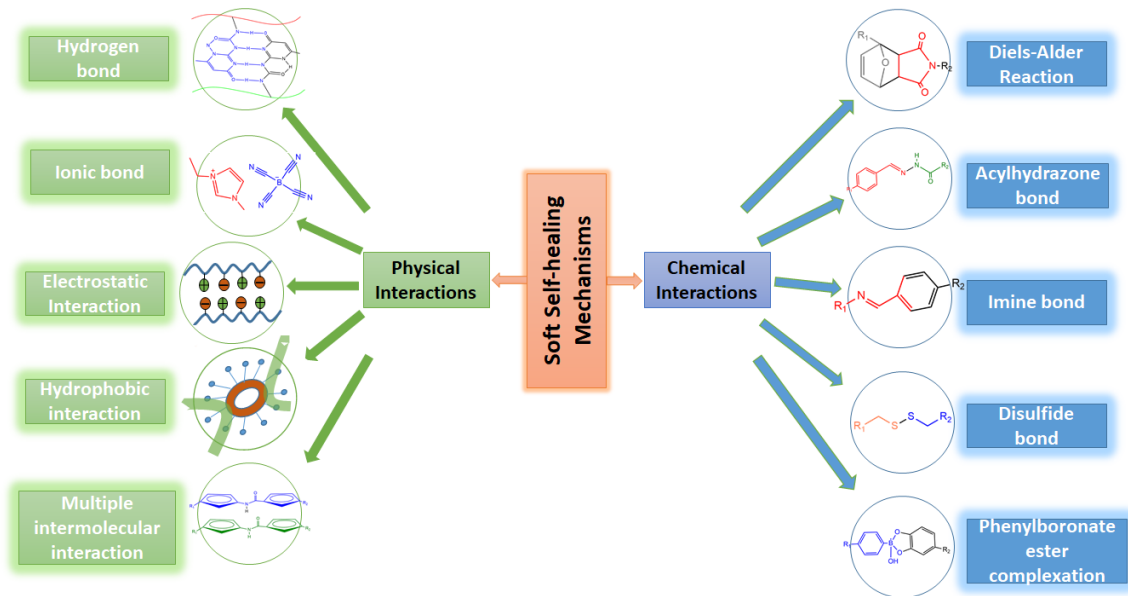


Figure 1.7 Various approaches used to synthesize physical and chemical interaction based self-healing materials

1.3.2.1 Physical interactions

Relying on transient bonds, physical interaction based materials are capable of exhibiting self-healing for multiple cycles, where the movement of polymer chains and the density of the network influences the life time of the reversible bonds [39]. For example, poly(ethylene glycol) based hydrogels were synthesized while functionalizing the prepolymer with quadruple hydrogen bond (UPy groups); due to their hydrophilic nature PEG-moieties can accommodate water, whereas the UPy groups give strength and elasticity while assembling into hydrogen-bonded arrays [40]. A heart shaped object demonstrated a shape persistent and self-healing behavior when cut into two pieces, which is joined by simply bringing both the halves together (Figure 1.9).

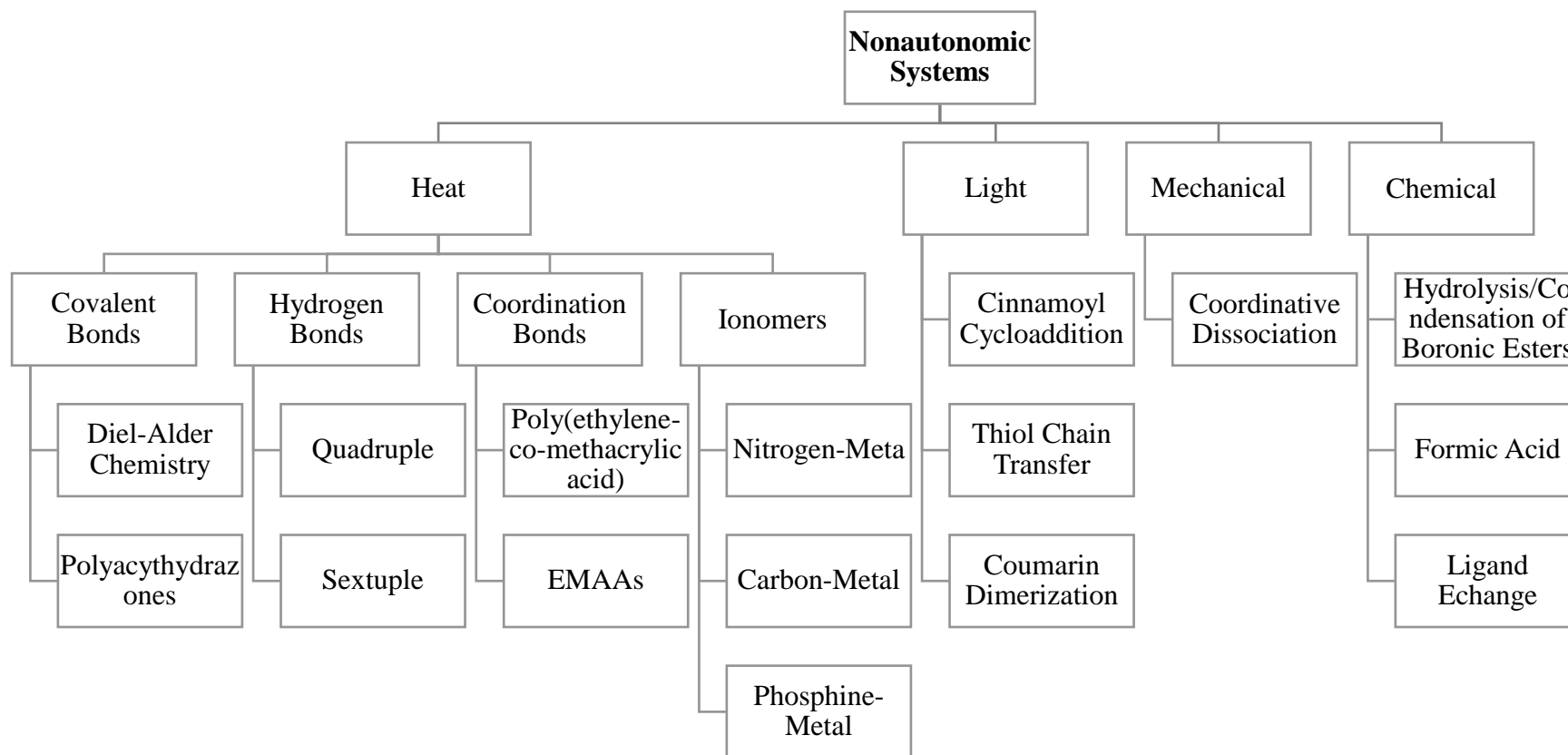


Figure 1.8 Classification of materials based on non-autonomic

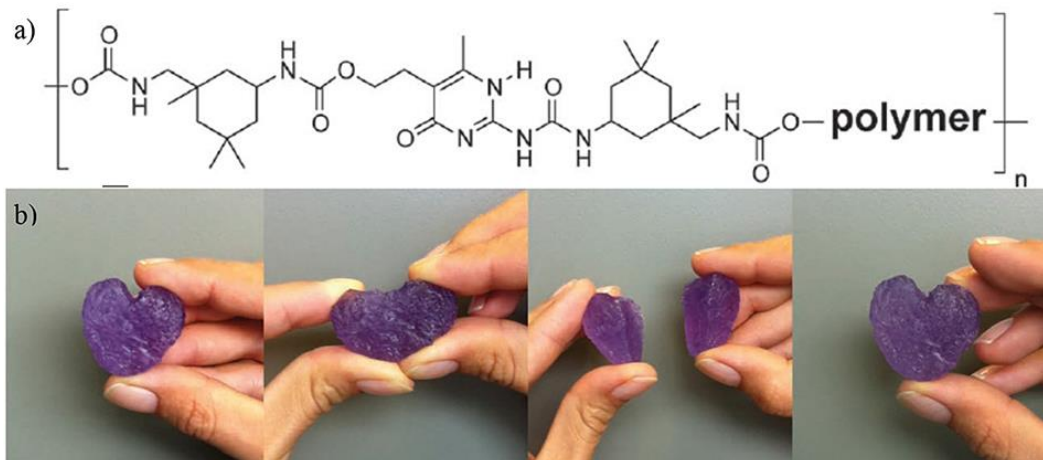


Figure 1.9 (a) UPy-containing polymer. (b) Supramolecular hydrogel made of PEG-UPy polymer 15 wt% in water [40]

In another example, an ionic self-healing mechanism involves charged polymer chains cross-linked with oppositely charged ions or polymer chains. Relative to organogels, ion gels exhibit high chemical stability and ionic conductivity, and are thus advantageous for different applications from soft actuators [41] to electrolytes for lithium ion batteries[42]. A self-healing and adhesive ionic gel was prepared by the mixing of polycation poly(allylamine hydrochloride) (PAH) with pyrophosphate (PPi) and tripolyphosphate (TPP)[43]. Due to highly dense ionic crosslinking, a high storage modulus was observed ($G'_{\infty} \approx 4 \times 10^5$ Pa). if the cut surfaces are not immediately joined, Due to stabilization and functional groups rearrangement, the self-healing performance of physically cross-linked hydrogels decreases [44].

A double-network (DN) based self-healing material with improved mechanical properties has been reported, where a symbiosis of covalent and non-covalent crosslinking network had been employed[45]. However, as the chemically covalent-cross-linked network cannot reversibly recover to its original state, the DN soft materials exhibit poor self-healing efficiency[46]. Thus, a multiple non-covalent cross-linked network could be more advantageous for preparing self-healing materials with high mechanical properties. A double network based poly(N-acryloyl glycinamide-co-N-benzyl acrylamide) containing a triple amide in

one side group was reported by Feng et al. The triple amide based soft material demonstrated a good shape memory ability, high mechanical strength (1.1 MPa) and about 95% self-healing efficiency occurred at room temperature[47].

Most of the widely explored non-autonomic based physical interactions materials are also now often combined with nanosized inorganic components to form nanocomposites, as summarized in Table 1.1. Describes the behavior of nanocomposite material with respect to healing efficiency, recovery, mechanical and electrical properties based on different physical interactions based self-healing mechanism. The addition of stiff nanofillers not only enhance the mechanical properties of the soft matrix [48] but also improve their self-healing properties [49]. Zhong et al. [50] proposed a tough and highly stretchable self-healing hydrogel based on silica nanoparticles, poly(acrylic acid) (PAA) and ferric ions. The hydrogel demonstrated excellent mechanical properties like tensile strength of 860 kPa and elongation at break ~2300%. It was suggested that the stretchability and toughness of a material is possible only by reversible cross-linking interactions between polymer chains, and helpful for energy dissipation through stress triggered dynamic process. Exfoliated sodium montmorillonite based self-healing hydrogel was formed by in situ polymerization of acrylamide monomers [51]. These hydrogels demonstrated good stretchability with a high fracture toughness (10.1 MJ m⁻³) and fracture strain up to 11800%, however, exhibited slow recovery of mechanical properties (RT, 5 days) and required multiple dry/re-swell handlings.

Table 1.1 Physical interaction based self-healing mechanism, healing efficiency, mechanical and electrical properties of nanocomposites.

Healing Mechanism	Materials	Self-healing conditions	Self-healing efficiency (Recovery %, obtained from tensile strength)	Mechanical properties (Tensile strength)	Electrical conductivity/resistance	Ref.
Hydrogen Bonding	AgNWs/branched poly(ethylenimine/poly(acrylic acid)-hyaluronic acid	RT, with a drop of water	100%	-	0.38 Ω sq ⁻¹	[52]
	Montmorillonite nanoplates/poly-dimethylacrylamide PDMAA	48 h, RT	100%	140 kPa	-	[53]
	Montmorillonite nanoplates/poly(acrylamide)	7 days, RT	100%	100-180 kPa	-	[51]
	Organoclay/poly(vinylpyrrolidone)	RT, 3h; pH 4-11	100%	0.210 Pa	-	[51]
	Zirconium hydroxide/Poly(acrylamide)	RT, 24 h	86%	404 kPa	-	[54]
	Graphene oxide/Polyacrymide	RT, 1 day	98%	180 kPa	10 S m ⁻¹	[55]
Hydrophobic Interactions	Graphite/polyethylenimine	RT, 10s	98%	200 kPa	190 S m ⁻¹	[56]
	Graphene oxide/poly(acrylamide)	3 days	53%	243 kPa	-	[57]
	Graphene peroxide/poly(acrylamide)	24 h, 30 °C	88%	350 kPa	-	[58]

Supramolecular Interactions	Cellulose nanocrystals/PVA	10-30 s, RT	100%	14.3 kPa	-	[59]
	SWCNT (10-20 wt%)/poly(2-hydroxyethyl methacrylate)	RT	100%	600 kPa	7.76 S m ⁻¹	[60]
Ionic Interaction	Fe ³⁺ / graphene oxide/ poly(acrylic acid)	48 h, 45 °C	80%	860 kPa	-	[53]
	Ferric ions/silica nanoplates/poly(acrylic acid)	70 °C	30%	1000 kPa	-	[50]
	Ferric ions/Silica/poly(acrylic acid)	50 °C, 24 h	70%	860 kPa	-	[50]
	Fe ions/PDMS/2,6-pyridinedicarboxamide	RT, -20 °C	90% at RT; (68% at -20 °C)	220 kPa	6.4 (Dielectric constant)	[61]
Multiple Interactions	Multi walled nanotube (MWNT)/Polyethylene polyamine (MWNT-0.5 wt%)	RT, 90 sec	100%	20 kPa	-	[62]
	Cellulose/polyvinyl alcohol (PVA)-borax (PB)	RT,	100%	~22000 MPa	3.65 S m ⁻¹	[63]

A symbiosis of shape memory and self-healing was also achieved for graphene oxide based polyurethane (GO-PU) nanocomposites [64], where fracture occurred in composite was effectively healed by exposure to direct sunlight and microwave (MW). The nanocomposites were effectively healed within 30-50 s under low MW power (360 W) and within 5-7 min under direct sunlight. During the healing process, GO absorbed energy from the stimulus, and then transferred this energy to the HPU matrix, where the soft segment of the hyperbranched polyurethane HPU melted (low $T_m \sim 50^\circ \text{C}$). Thus, the crack could repair with a higher mobility of the soft segment of HPU. the hyperbranched polyurethane (HPU)-TiO₂/reduced graphene oxide (TiO₂/RGO) nanocomposites exhibited combined attributes of shape memory, self-healing and self-cleaning properties were reported[65], where the fabricated nanocomposite exhibited composition and dose-dependent mechanical properties with excellent shape recovery ratio (91-95%) as well as shape recovery rate (1-3 min) under exposure to sunlight. The presence of a high amount of RGO (0.5-1 wt %) in the nanocomposite helps in rapid and efficient healing, whereas a high amount of TiO₂ nanoparticles (5-10 wt %) aids in achieving good self-cleaning properties.

1.3.2.2 Chemical interactions

This section covers the strategies for the preparation of chemical self-healing soft materials based upon dynamic networks of covalent interactions, including Diels-Alder reactions, disulphide, imine bond, boronate ester bond, acylhydrazones and nanocomposite interactions. The dynamic permanent covalent bonds can break and reform as per the prevailing conditions. For instance, a disulfide and acylhrazone bonds based self-healing network was developed, where in PEO based hydrogel, disulfide exchange reaction occurs at basic pH, whereas acidic pH is helpful for acylhydrazone exchange reactions[66]. The material did not show self-healing at neutral pH as the covalent bonds were not dynamic. In general, the broadly investigated temperature triggered reversible diene and dienophile based [4+2] cycloaddition and retro Diels-Alder (DA) mechanism make good candidates for healing networks.

A comprehensive study by Garcia et al. demonstrated the effect of reversible DA bonds in covalently cross-linked networks[67]. The study shows that due to retro-DA reaction at high temperature, an increased mobility in the network leads to the self-healing of the system. However, the required high temperature for DA/retro DA damages the properties of the parent material. A switchable ‘on’ and ‘off’ based photo-switchable DA dynamic network was developed by Hecht et al., where the incorporation of furan cross linker allows reversible (de- and re-crosslinking) in short and mobile maleimide-substituted poly(lauryl methacrylate) chains (Figure 1.10) [68]. In general, the common dynamic chemical interactions based self-healing is reversible upon temperature usage, thus limiting their application areas.

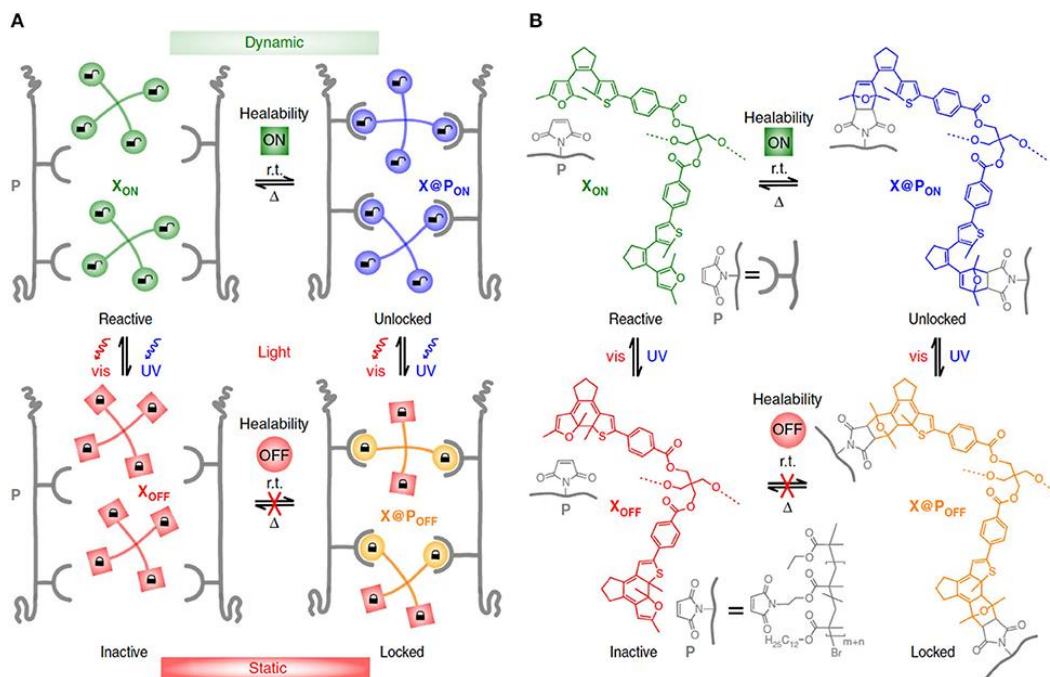


Figure 1.10 Schematic representation of a) photo-switchable, dynamically crosslinked polymer network and b) the chemical structures of the crosslinkers, indicating the switchable reactivity for the reversible DA reaction and healability of the network [68]

Table 1.2 highlights few recent works on the incorporation of nanofillers with chemical interaction based self-healing mechanism, healing efficiency, recovery, mechanical and electrical properties for better understanding. In particular conductive nanofillers are used to trigger and catalyze the self-repair

performance, owing to their superior heat absorption properties and resulting local heating under sunlight and microwave radiation. Indeed, due to their high photo-thermal conversion, conductive nanofillers enable to increase the temperature up to 200 °C in a very short time [69]. Shi et al. developed a dynamic reversible cross-linked organic-inorganic network via DA reaction between poly(styrene-butadiene-styrene) and CNT. The material demonstrated DA based self-healing with complete recovery of the mechanical properties in a time as short as 10 s due to the photo-thermal effect of CNT under laser irradiation (Figure 1.11) [70] whereas no self-healing occurred in absence of CNT.

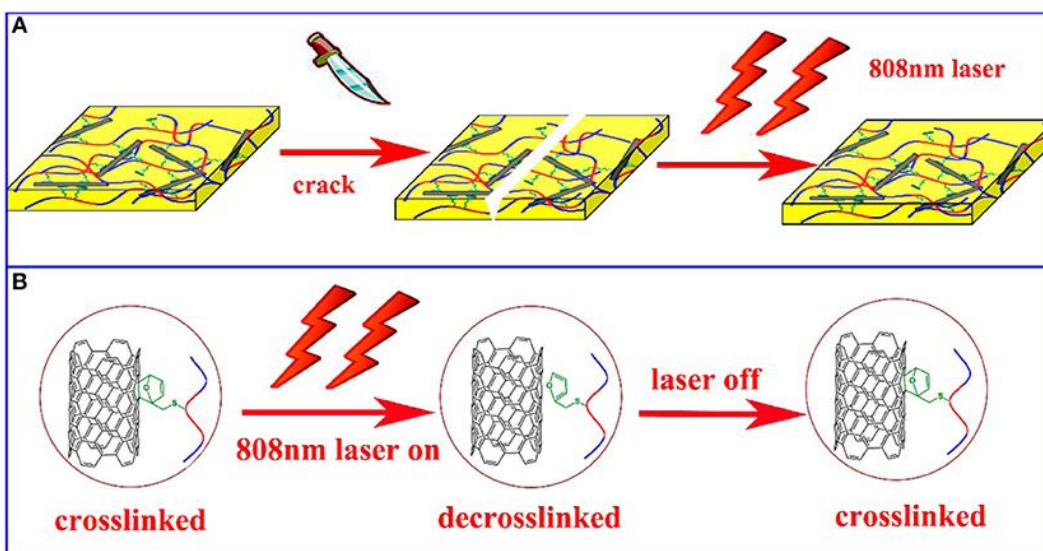


Figure 1.11 (A) Healing Process; (B) Healing reaction [70]

Table 1.2 Chemical interaction based self-healing mechanism, healing efficiency, mechanical and electrical properties of nanocomposites

Healing Mechanism	Materials	Self-healing Conditions	Healing efficiency (Recovery % obtained from tensile strength)	Mechanical Properties (Tensile strength)	Electrical Conductivity/Resistance	Ref.
Diels-Alder Reactions	C ₆₀ /Poly(styrene-b-butadiene-b-styrene)	80 °C (DA); 180 °C (rDA)	100%	19.8 MPa	-	[71]
	POSS/Siloxane	50 °C (DA); 110 °C (rDA)	100%	0.75 MPa	-	[72]
	Cellulose nanocrystal/Poly(ethylene glycol)	50 °C (DA); 90 °C (rDA)	78%	0.160 MPa	-	[73]
	Graphene oxide nanosheets/ Polyurethane	65 °C, 5h (DA); 120 °C, 30 min (rDA)	100 %	76 MPa	64 kΩ	[74]
	CNT/ Poly(styrene-b-butadiene-b-styrene)	80 °C, 6h; 80 laser (10 s, rDA)	100 %	18.5 MPa	-	[75]
	Boronate ester linkage	Cellulose-Polyvinyl alcohol	RT, pH	100%	-	-
Au particles/poly(vinyl pyrrolidone)		39 °C, 15 min	90 %	0.00055 MPa	-	[77]
MWNT-PDMS		Water vapor	90 %	1.81 MPa	1.21 S/cm	[78]

Disulfide bonds	Au particles/PEG/Bioactive glass	RT, 12 h	100%	0.35 MPa	-	[79]
Transesterification	Bentonite/Natural Rubber	150 °C, 3h	96%	4.5 MPa	-	[80]
Diselenide bonds	Graphene oxide/polyurethane	NIR light (5 min)	90%	6 MPa	-	[80]

1.4 APPLICATIONS

Self-healing materials find applications in engineering and bio-medical fields. The major uses of self-healing materials so far are in surface coating [81], drug delivery [82], [83], tissue engineering [84], [85], wound healing [86], [87], and soft robotics [88], [89]. Herein, some applications of soft self-healing nanocomposites in biomedical fields including drug, tissue adhesive, as well as in industry fields including actuators sensors, and coatings are gathered (Table 1.3).

Table 1.3 Demonstrated applications for self-healing nanocomposites and associated healing features.

Materials	Self-healing Mechanism	Self-healing conditions	Self-healing efficiency (recovery %)	Applications	Ref.
PF/DCPD	ROMP	24h, RT	81.4% (toughness) & 91.8% (fracture strength)	Coating	[90]
Isophrone diisocyanate/Isocyanate	Thiol-ene	72h, RT	100%	Coating	[91]
Isophrone diisocyanate/Isocyanate	Thiol-ene	72h, NaCl solution	100%	corrosion	[92]
DCPD/ENB	ROMP	50°C	95%	Structural	[93]
Epoxy/DCPD	ROMP	120°C	75% (elastic modulus)	Aerospace structure	[4]
DCPD	ROMP	RT	99% (fracture toughness)	Coating-corrosion	[94]
Epoxy	ROMP	24h, 80°C	81% (fracture toughness)	Aerospace structure	[95]
ENB/DCPD/Carbon fiber	ROMP	24h,RT	1155% (inter laminar structural strength)	Aerospace structure	[96]
Hydroxyl end-functionalized polydimethylsiloxane (HOPDMS) and polydiethoxysiloxane (PDES)	Phase separated	24h, RT	46% (fracture toughness)	Coating-corrosion	[97]
Hydroxyl end-functionalized polydimethylsiloxane (HOPDMS) and polydiethoxysiloxane (PDES)	Phase separated	24h, 20°C	100%	Coating-corrosion	[98]

ethylidene norbornene,SWCNT	ROMP	1min, 45°C	100%	Aerospace structure	[99]
Fibre reinforced polymer FRP	ROMP	1h, 45°C	119% (stiffness)	Aerospace structure	[100]
DCPD/ENB	ROMP	2h,105°C	100% (FESEM)	Aerospace structure	[101]
PAA/CNS NC	Hydrogen bonding	RT	91%(tensile strain) 98% (toughness)	Soft robotics	[102]
tannic acid-coated cellulose nanocrystals (TA@CNC)	Coordination bonding	RT	92.5% (fatigue and resilience) 70% adhesive strength 97.1% electrical resistance)	Wearable sensors	[103]
TiO ₂ /BMIMBF ₄ ionogel	Supramolecular interactions	100 to -10°C	98% (compression strength)	Electro-chemical actuators	[104]
PVAc/Graphene	Diffusion of polymer Chains	60°C	89% (mechanical properties)	Actuators and sensors	[105]
PAA-GO-Fe ³⁺	Ionic interactions	RT	100% (tensile strength)	Soft actuators	[106]
PPy/G-Zn-tpy	Metal-ligand supramolecular interactions	RT	100% conductivity	Electronics, biosensors, artificial skins	[88]
Li ₂ SO ₄ /CMC	Supramolecular	RT	94% (tensile strength) 88% (current density)	Lithium ion battery	[107]

GO/PAAM derivatives	Hydrophobic interactions	RT	66%	Waste water treatments, adsorbents	[57]
Graphene/SWCNT	Hydrogen bonding	Ambient temperature	98% (conductivity)	piezoresistive strain sensor	[108]
RFGO/PU	Diels-Alder	Microwave	93% (young's modulus)	Strains sensors, flexible conductors	[109]
rGO/SAP	Hydrogen bonding	RT	100% (resistance)	sensors	[110]
CNCs-Fe ³⁺	Ionic interactions	RT	98% (elastic modulus)	Soft Strain sensor	[111]
PPy/PAC/Fe ³⁺	Ionic interactions	RT	100% (tensile)	Soft sensor	[89]
PU/GO	Diels-Alder	Ambient conditions	90% (conductance)		
			96% (break strength)	Flexible electronics	[112]
			97% (elongation)		
			100% (young's modulus)		
rGO/polyacrylamide(PAM)	Mussel-inspired chemistry (non-covalent)	Ambient environment	95% (conductivity)	Bioelectronics	[55]
			60% (tensile strength)		
			80%		
			(Extension ratio)		
11-(4-(pyrene-1-yl) butanamido) undecanoic Acid/CNT/rGO	π - π stacking and Hydrogen bonding	RT pH=13.4	93% (strain)	Biomedical	[113]

GO/PAA	Diffusion of polymer chain	RT	88% (tensile strength)	Biomedical	[58]
PDA/Nanoclay/PAM	Hydrogen bonding Mussel-inspired chemistry (non-covalent)	Ambient environment	100% (compression strain for 20 cycles)	Wound healing	[114]
graphene oxide (GO)-hectorite clay-poly(N,N-dimethylacrylamide) (PDMAA)	Hydrogen bonding	Near-infrared (NIR) irradiation	96% (tensile strength)	Wound dressing	[115]
pDMAA/ β -CD/rGO	Hydrogen bonding	37°C	80%	Drug delivery	[116]
Graphene oxide(GO)/poly(acryloyl-6-aminocaproic acid) (PAACA)	double-network mechanism	RT pH<3	86%	Drug release	[117]
PDA/ Fe ₃ O ₄ / Carbon black/PAM	π - π stacking and Hydrogen bonding	RT	100% Tensile, conductivity and magnetic properties	Drug delivery and tissue engineering	[118]
Chitosan/Go	π - π stacking	RT	91% (compressive stress)	Tissue engineering	[119]
GO-UPy-PNIPAM	Supramolecular	RT	100% (elastic modulus)	Drug delivery	[120]
GO/DNA/SH	π - π stacking and Hydrophobic interaction	90°C for 3min	100% (adsorption)	Drug delivery	[121]
PDMAA-PVA/rGO	Hydrogen bonding	RT	100% (ultimate tensile strength and conductivity)	Artificial skin	[122]
p(HEMA-co-BA)-Fe ₃ O ₄	Host-guest interactions	RT	94.98% (electromagnetic	Coating-corrosion	[123]

lignin-modified graphene (LMG) and waterborne polyurethane (WPU)	Polymer diffusion	Infrared	absorption bandwidth) 40% (tensile) 171% (elastic modulus)	Coating-corrosion	[124]
PAA-MBAA-FeCl ₃	Covalent bond and ionic interaction	RT	99% (elastic modulus)	Coating-corrosion	[125]
CNT/PU/Ze ²⁺	Supramolecular	Near infrared (NIR) light (4.2 mW/mm ²)	93% (toughness)	Coating-corrosion	[126]

1.5 OBJECTIVES

Fast crosslinking process working under ambient/low temperature conditions in an autonomous fashion play a vital role in order to close damage-induced cracks, in turn it restore the mechanical and conductive properties without affecting functionality. To effectuate the strategy, following are the main objectives:

- Development of Heterogeneous catalyst to promote click triggered self-healing
- Development of graphene promoted “click” triggered self-healing composite material for aeronautical applications, helpful to overcome the drawbacks related to fatigue and conductivity of the composite materials
- Optimization of various process parameters to fabricate the composite material e.g., capsules content and graphene dispersion

1.6 SUMMARY

This chapter summarizes the feature of self-healing material including autonomic and non-autonomic self-healing mechanisms. The autonomic healing systems carry out in two ways, extrinsic and intrinsic healing systems, where the healing agent is externally supplied by capsule/vascular network systems. In both the capsule and vascular system the self-healing occurs in the similar fashion by polymerization of healing agents with/without catalyst after damage occur to dispersed capsule or vascular network. However, the construction of vascular network system is very tedious task even though it has an additional feature of multiple healing system, makes the capsule system in first place. In non-autonomic self-healing system, require external stimuli such as heat, light, mechanical and chemical for occurrence of healing. This system uses intrinsically self-healing mechanism offers features like multiple healing at the same location without help of any healing agents. This intrinsic system works in two ways; physical and chemical interactions, where the physical interactions are based on reversible bonding and occurs in the presence of external stimuli. Where chemical interaction

are based on the dynamic networks of covalent bonds. Indeed due to their weak interactions, it offers limited mechanical properties and electrical conductivity. Table 1.1 and 1.2 summarizes the efficiency, recovery, mechanical and electrical conductivity of self-healing nanocomposite materials due to physical and chemical interactions based on different healing mechanisms. Based on different strengths and weakness of healing systems we carry out the literature and experiments on capsule based healing system. The addition of nano materials gave provision for various applications listed in Table 1.3 based on different healing mechanisms.

CHAPTER 2: OVERVIEW AND BIBLIOGRAPHY SURVEY FOR NANO BASED COMPOSITE MATERIALS

2.1 OVERVIEW

Polymer based composite materials are frequently used in different applications due to their inherent properties like lightweight, flexibility, ease in production, copious availability and lightness. The incorporation of nanoparticles showed higher mechanical properties, and physical properties compared to ceramic and metal based materials. Nevertheless, due to complex loading, small impact damage, micro/nano size cracks are generated in the matrix, which decrease the lifetime of the material. Since self-healing concept, provides new opportunities towards the development of multifunctional materials. This chapter focuses on the different carbon based nano materials, encapsulation strategies and different chemistries involved for healing autonomously[127].

2.2 CARBON BASED SELF-HEALING NANO MATERIALS

The progress in the development of self-healing materials increased enormously by using different strategies. However these self-healing materials lack in some properties including mechanical, electrical, thermal and lower in healing efficiency, especially low in conversion efficiency, energy absorption and response to external trigger. Researchers are paying more attention towards improving the self-healing performance of polymeric materials and interestingly extending the range of healing systems. The incorporation of carbon materials possess excellent mechanical properties, thermal/electrical conductivity, absorption property[128], [129] and photo thermal effect[130]. Especially graphene is good in mechanical properties, electrical properties, thermal properties, quick response to external trigger and energy efficiency. Therefore, the addition of graphene enhances the mechanical properties and conductivity property of self-healing polymeric material. There are several notified methods for the preparation of graphene like epitaxial growth[131], mechanical exfoliation[132], chemical vapor deposition[133] and hummers method and modified hummers method are most

welcoming methods[134], [135]. In progress, the graphene based self-healing nanocomposite materials attracted in many of the applications like supercapacitors, sensors, biological applications, coating, artificial skin, adsorbent, self-cleaning, biomimetic material, flexible electronic devices and actuators.

2.2.1 PREPARATION METHODS

Different approaches have been applied for the preparation of graphene based polymeric self-healing composites including layer-by-layer assembly[136], hydrothermal method[110], solution mixing method[137], in situ polymerization[65] and wet-fusing assembly method[138]. Sun j et al. [139] explored self-healing polymeric film (RGO-CD&PAA/bPEI-Fc) prepared using layer-by-layer assembly approach. The composite comprises of β -cyclodextrin in modified RGO (RGO-CD) nano-sheets and poly(acrylic acid) (PAA) branched with poly(ethylenimine) embedded ferrocene (bPEI-Fc). In the similar fashion Ge L et al. [140] synthesized the self-healing material with the same polymeric material (PAA/bPEI-Fc) with graphene. Interestingly the authors found good ability of self-healing along with enhanced electrical conductivity for the synthesized composites.

The composite materials fabricated by hydrothermal method uses the difference in pressure and temperature of solution in autoclave at higher temperature and pressure to form a supersaturated crystals[141]. Tang Y et al. [110] prepared a hydrogel composite composed of reduced graphene oxide (RGO) embedded in superabsorbent polymer (SAP) and hyper-branched polymer (HB). Initially the RGO was well dispersed in Milli-Q water using bath sonicator to acquire the uniform suspension. Subsequently, it was thoroughly mixed after the addition of SAP and HB in prepared suspension. This mixture was heated at 100°C for 10h in autoclave lined with Teflon and stainless steel, thus formed conductive composite material; exhibit 100% healing within 20s even at room temperature.

The solution mixing method is most commonly used for preparing the graphene based or its derivative based self-healing composite materials, Huang Y et al. [142] developed an innovative strategy for fabricating self-healing nano

composite material using the polyurethane (PU) and few-layer graphene (FG) using the solution mixing. The developed composite materials exhibit excellent mechanical properties and the showed the healing using electricity, infra light (IR) and electromagnetic as external stimulus gave the good healing efficiency up to 98% shown in Figure 2.1. Beckert F et al.[143] developed a PGDAT/PG-CA films embedded with TRGO, which allows breaking of hydrogen bonds for the free motion and relaxation of bonds using the NIR laser. This is obtained by the reduction process with the application of temperature. Therefore, the TRGO has good water-dispersible quality with good conductivity and laser/light absorption capacity. For instance, Qu L et al. [144] fabricated different variety of graphene oxide in three different dimensions as 1D, 2D and 3D for self-repairing applications using moisture.

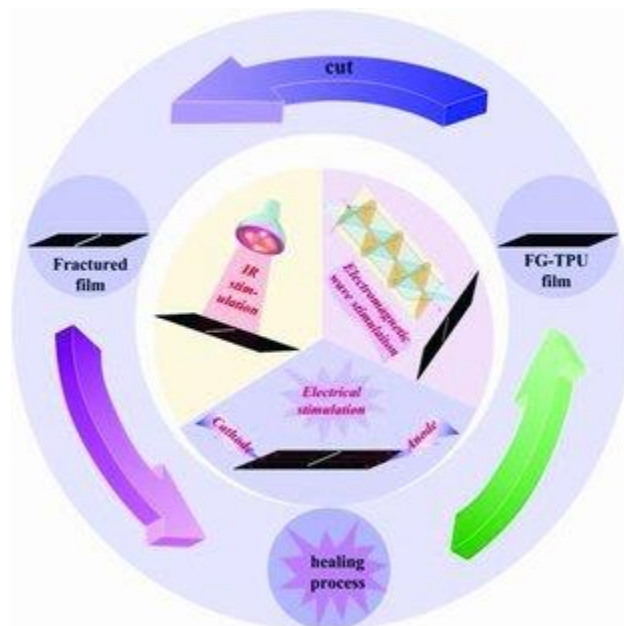


Figure 2.1 The ability of self-healing using IR, electricity and electromagnetic in FG-TPU composites [142]

Graphene based polymeric materials are prepared by dispersing the graphene nano particles in monomer and later allow to in situ polymerize at definite conditions[145]. This method made possible to prepare nanoscale composite materials using the nano materials having higher weight[2]. In simple words, mixing all the ingredients initially and allowing it to in-situ polymerize. Many

articles published on graphene based-self-healing materials using this in-situ polymerization technique[65]. Whereas, many graphene derivatives are functionalized to monomers to prepare composite materials using in-situ technique such as MGN [146], GO [119], FAGS [74], mGO [147], RFGO [109], GPO [58], TiO₂/RGO [65] etc. Wong C-P et al. [148] synthesized polyurethane (PU) and graphene oxide (GO) based self-healing composite materials on the principal of Diel-alder chemistry. The graphene nano particles are well dispersed in the mixed reagents and allowed to polymerize in-situ. In extension, the authors developed RFGO-DAPU composite as well[109]. Li Y et al. [149] fabricated nano composite hydrogel based on Poly(N,N-dimethyacrylamide)-graphene, which has capability to self-heal in-situ at 37°C in air for 12h. and found more suitable for biological applications.

The wet-fusing assembly process developed by Gao et al. [150], based on continuous wet spinning method for preparing the graphene staple fibers. This process uses the self-fusing principle to attain the self-healing by the graphene oxide fibers. It indicates that water has an ability to weld the sample for attaining healing. The non-woven fabric was fabricated with pure graphene oxide fibers by using wet-fusing technology. The wet fusing method showed highest interaction between the graphene fibers during overlapping period. It clearly indicates, this technique have great potential to prepare the graphene fibers. The self-healing by graphene fibers using the water and electric heaters were also reported[151].

2.2.2 SELF-HEALING APPROACHES USING GRAPHENE

Autonomous self-healing materials are highly appreciable for their life long repairing feature, and for achieving self-healing it requires external stimulus such as light, heat, mechanical force, moisture, electromagnetic wave, electricity and pH. Interestingly the pure graphene demonstrates the self-healing properties. Acharyya et al. [152] demonstrated graphene based self-healing material using molecular dynamic simulations. With the application of tensile load on the material reaches to its maximum tensile strength causes the cracks on its surface for 0.3-0.5nm, with the presence of graphene the material healed due to the elastic behavior of graphene

and the moment of C atoms closer caused the self-healing. The self-healing obtained in the material without any external stimulus.

The performance of graphene based self-healing composite materials showed improved efficiency with external stimulus as compared with alone graphene. Dong et al. [147] developed graphene/polyurethane based self-healing polymeric nanocomposite material, where self-healing approach works *via* retro-Diels-Alder (DA) reaction with the application of temperature. The developed material highlighted excellent mechanical and self-healing behavior. Wong et al. [74] developed low temperature based self-healing material based on Furfurylamine Graphene structures/Diels-Alder Polyurethane (FAGS/DAPU) works on the retro-Diels-alder mechanism. They achieved self-healing using the reversible cross-linking of thermally reversible covalent bonds and the movement of chains in polymeric materials by heat causes the bond reconstruction of hydrogen bonds.

Wong C-P et al. [109] prepared self-healing composite material based on RGO and PU, where microwave was used as an external trigger, by heating the material for self-healing based on DA mechanism. Graphene with microwave energy causes the heat propagation throughout the material, where DA bonds rapidly change reversibly and cause movement in polymer chains for achieving self-healing[142] (Figure2.2).

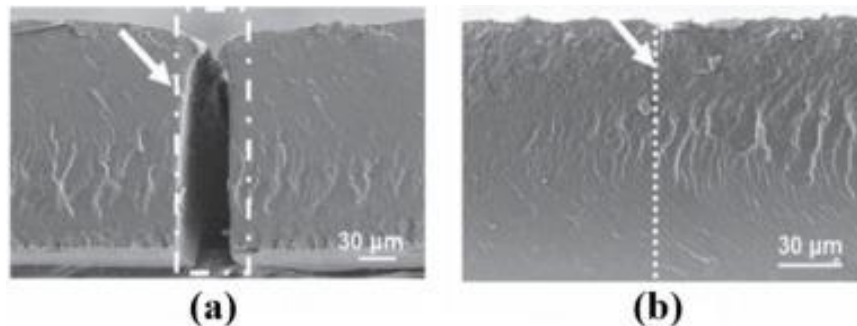


Figure 2.2 SEM image of rGO-PU a) cut crosssection b) healed after passing microwave [142]

Light as a source of energy can be controlled using remote/wireless control, moreover, it can be converted into heat energy as well[153]. More interestingly, the

graphene has a unique feature that it can absorb light using the photo-thermal effect and, thus promotes the heat generation. The self-healing using the different lights such as green light[154], sunlight[65] and infrared light[115], [142], [155] turn to be advantageous for graphene incorporation. For instance, Karak N et al. [65] demonstrated self-healing based on sunlight (within 10mins) and also the material demonstrates self-cleaning capability. In the similar fashion, Sun R et al. [112] developed self-healing nano composite material having 96% healing using infrared light. The developed nanocomposite heals based on DA in PU/graphene nano sheets composite material. The self-healing occurred after passing 980nm infrared light for 1min. Fei et al. [154] developed self-healing nanocomposite by polycaprolactone (PCL) incorporated rGO/silver nanowires (AgNWs) and gold nanoparticles (Au NP). The self-healing made possible using light having wavelength of 532nm, owing to photo thermal effect.

The self-healing can be achieved under mechanical force, and bringing the separated pieces closer [156]. Babaahmadi M et al. [156] developed tri-layered nanocomposite composed of agar polysachharide as first, PVA as second and graphene Nano-platelets as final layer networks. The process of self-healing in the hydrogel composite material demonstrated in Figure 2.3. where two-piece were brought back in contact and applied some mechanical force/pressure with hand for 10 mins, with the release of mechanical force the pieces formed into single one. The obtained hydrogel is subjected to force which demonstrated good stretchability even after the failure. Bao Z-N et al. [157] demonstrated the similar work but using the graphene oxide alone, where the authors have observed that the application of mechanical force causes the moment for hydrogen bonds reconstructing.

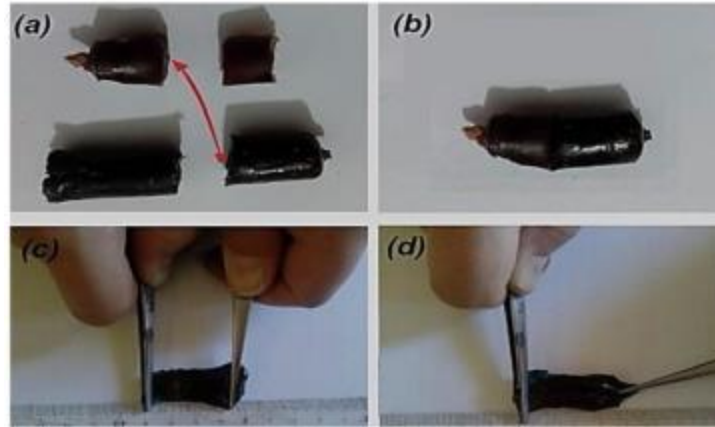


Figure 2.3 images demonstrating the self-healing property of tri-layered nanocomposite hydrogel. (a) Two pieces (one was in methylene blue color for better understanding) were separated in two halves, b) then the cut surfaces brought into contact by applying mechanical force, then (c) a single piece hydrogel can be found after few minutes and d) it displays that it can withstand high stretchable forces even after failure [156]

The self-healing is possible in many other ways like moisture, electricity, catalysts, autonomously, pH stimulus, oxidation-reduction and bionic process. For an example Szpunar J et al. [158] proposed an anticorrosion coating which has self-healing feature. The composite graphene layer, cerium layer, PAA and poly (ethylene imine) (PEI) were coated on magnesium alloy (AZ31) as a multilayer. The PAA/PEI alone used for the self-healing and GO is used for the corrosion inhibitors. More the number of bilayers of PAA/PEI causes increased mobility of chains due to the swelling ration of polymers. Ge L et al. [140] reported similar work, demonstrated the self-healing using the branched PEI and PAA incorporating GO in it, at higher humidity where the material performs better self-healing ability.

The self-healing based on electricity is possible only for electrical conductive materials, useful for the field of electronic device applications. The incorporation of few graphene layers on PU causes self-healing by applying the electricity and showed 98% healing efficiency[142]. Gao et al. [151] fabricated the self-weldable/solder-free weld graphene material using the electrical Joule heating effect. The results demonstrate that the welded graphene sheets has higher strength at joints, improved electrical conductivity without disturbing any structural integrity of the material (Figure 2.4).

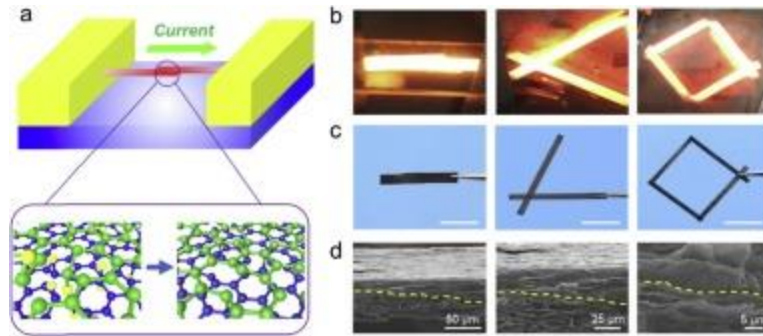


Figure 2.4 (a) Graphical representation of the welding process of GF-HI, b) images taken during Joule-heated GF-HI, c) welded samples, d) SEM images of welded samples, yellow dashes indicates the strong bond between the graphene layers [151]

The self-healing materials based on capsules and microvascular are typically catalytic based self-healing approach. The Binder WH et al. [159] demonstrated the ‘click chemistry’ based self-healing materials with copper and TRGO as catalyst. The low molecular azide and alkyne cross-linked in the presence of TRGO-CU₂O for self-healing applications. This system even demonstrated that the catalyst used in system served as catalytic activity as well as the reinforcement agent helpful to improve the conductive and mechanical properties of composites (Figure 2.5). It opens the great potential for click based self-healing approaches even at low temperature.

The material that self-heals without any external intervention generally known for autonomous self-healing. Saiz E et al. [160] developed a supramolecular-based self-healing polymer composite material made of PDMS, rGO, and Boron oxide (B₂O₃) at 200° C for 6h. The material is robust in construction, electrically conductive, helpful to restore the mechanical properties and heal multiple times without any external aid and interestingly it can sense the pressure as well. The self-healing occurred within 24h due to the dynamic bonds reformation of boron and oxygen, the hydrogen bonds react with unreacted OH group polymer chains.

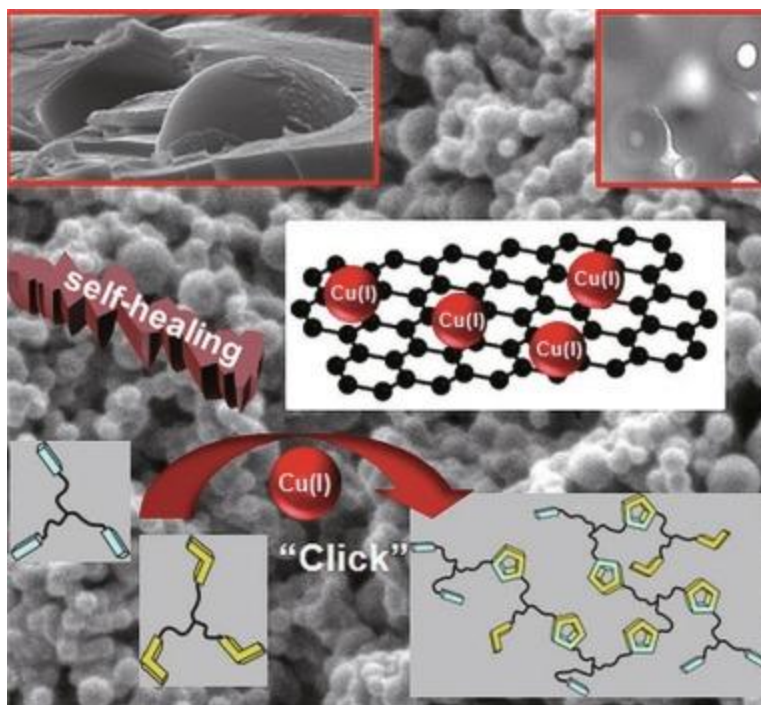


Figure 2.5 self-healing system based on Click-triggered graphene nanocomposites [161]

Yu S-H et al. [117] explored a pH stimulus self-healing nanocomposite hydrogel of GO/poly(acryloyl-6-aminocaproic acid) (PAACA). The GO/PAACA double networks initiated due to the existence of calcium ions, which acts as a cross linker agent and GO acts as a triggers. The opaque degree is prolonged with the time of hydrogel in HCL solution with $\text{pH} < 3$. Hydrogel surface starts crumpled within 10min. interestingly this process is reversible when the neutral or basic solution having $\text{pH} > 7$ was introduced. This is due to the re-inter-connection of hydrogen bonds with the calcium ions as response to pH. The hydrogel demonstrated the fast self-healing within seconds when the broken pieces of hydrogel were introduced into acid solution of $\text{pH} < 3$ and as reversible nature, the hydrogel got separated with higher pH solution.

Sun J et al. [139] developed a self-healing system with oxidation-reduction process work on host-guest interactions between the polymers matrix and rGO nanofillers. The self-healing was achieved even after several cuts and separated for long distance. This healing occurred in few steps (Figure 2.6), initially when the material subjected to cut and recombine the films of bPEI-Fc and RGO-CD got

healed in oxidation solution due to host-guest interactions. Secondly, it restores the mechanical properties of the film by reduction process (GSH solution). The self-healing occurred using the oxidation-reduction process are very efficient in self-healing properties including mechanical properties.

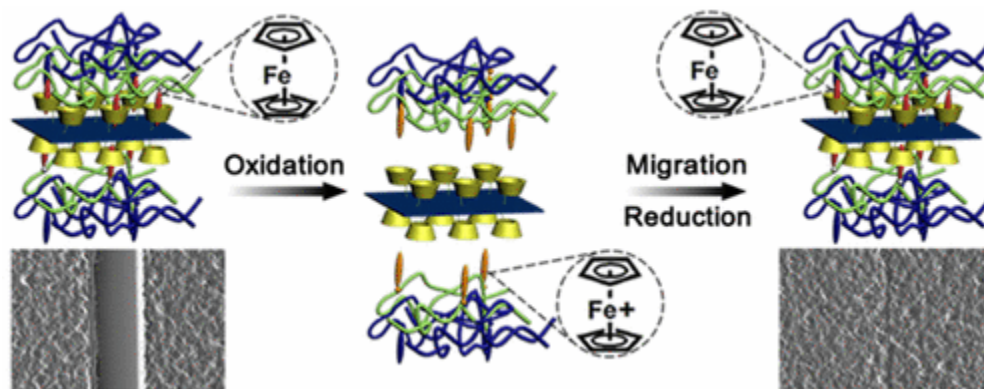


Figure 2.6 self-healing of polymer composite using oxidation-reduction process [139]

2.3 ENCAPSULATION STRATEGIES

The micro/nano-encapsulated self-healing approaches having various competences to perform self-healing alone without aid of any external triggers or any catalyst based on the mechanism used. This capsule based self-healing system is appropriate when it is easy in synthesis, mass production, longer life environmentally stable and can modify surfaces which requires for good dispersion in polymeric matrix[27]. The healing system using the capsule based has shown the prominent results which is effective and recommended in various field of applications[162] . Generally, the capsules size ranging from nano to micro size in diameter. The capsule contains the healing agent or core material and has the shell wall made of polymer materials as shown in Figure 2.7. The healing ability used by capsules was most successful in maximum of matrices even in vinyl ester[163]. The capsules expected to be viable in coating, stable in both chemical and mechanical properties, should be non-porous, and should be able to sense the damage and quick response by releasing the healing agent onsite.

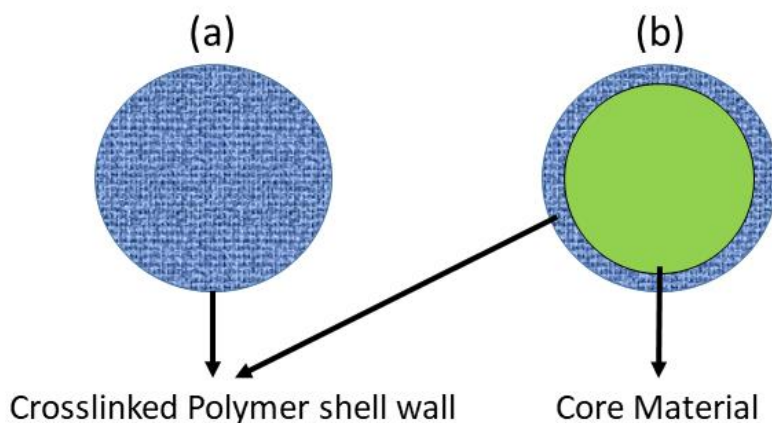


Figure 2.7 schematic representation of capsule parts a) polymer material in blue color and b) core material as green in color

There are several methods and procedures for synthesizing and preparing capsules according to the size and properties required as per design/requirement. There are few characteristics and properties required for capsules and healing compounds, which will fulfill the needs of healing, are given in Table 2.1.

Table 2.1 Properties of healing and capsule parts

Healing process and parts of capsule	Properties
Encapsulation process	<ul style="list-style-type: none"> • Easy and simple • Less time for preparation • Easily available
Shell wall	<ul style="list-style-type: none"> • Stable in chemical and mechanical states • Stable in acid/base • Compatible with matrix • Strong in interfacial strength • Size should be according to the application • Robust in construction
Capsule	<ul style="list-style-type: none"> • Longer in life • Able to easily rupture based on the matrix rupture • Strength of the matrix should be least effective • Be able to easily encapsulated
Core material	<ul style="list-style-type: none"> • No side reaction to be occurred on polymer shell material • Low in melting and freezing point

Healing reaction mechanism	<ul style="list-style-type: none"> • Non-toxic and stable • To be react with only wanted compounds • Able to flow (low T_g) • Fast and rapid even at low temperatures • Should possess least shrinkage during reaction • Able to make multiple reaction • Only reactive with monomer/healing agent
Catalyst used for healing	<ul style="list-style-type: none"> • Convenient in dissolving monomers • Able to disperse uniformly and easily throughout matrix for availability to react • Stable in chemical and mechanical states

The production of microcapsules is generally of two types a) chemical and b) physical, depends on the requirement and application of capsules. In general chemical procedures include in-situ emulsion and interfacial polymerization, submerged nozzle and centrifugal force processes and phase separation process. The physical methods are spray drying, spinning disc method, centrifugal extrusion, fluid bed coating and solvent evaporation method. In general, the micro/nano capsules required for self-healing are prepared using miniemulsion process (oil-in-water)[164], solvent evaporation[165], interfacial polymerization[166], sol-gel technique[167] and hollow micro capsules.

2.3.1 MINI-EMULSION POLYMERIZATION (OIL-IN-WATER)

The mini-emulsion polymerization process for encapsulation, the occurrence of polymerization initially starts from an emulsion consists of water, surfactants, core material, shell material. Water contains the core and shell material present in the form of immiscible and miscible phase. There are near similarities between interfacial polymerization and mini-emulsion, except dissolving in core monomers or no monomer added, and rest process happens in continuous phase. For an instance, the encapsulation of DCPD in UF using the in-situ polymerization use the pre-polymers occur by reacting urea with formalin in aqueous phase (Figure 2.8). With time this pre-polymer in low molecular weight gains the weight by forming interface layer in between DCPD and water. It is a form of progressive polymerization using the shell wall material[168]. The miscible shell material in

water starts forming wall by phasing out and starts covering the core material to form encapsulation [169]. It is possible only when there a change in anyone of the factor like including pH, temperature and presence of chemical species, those promotes precipitation process. This mini-emulsion process is commonly used, mainly because of its simplicity and effectiveness especially to encapsulate the healing agents in the liquid form.

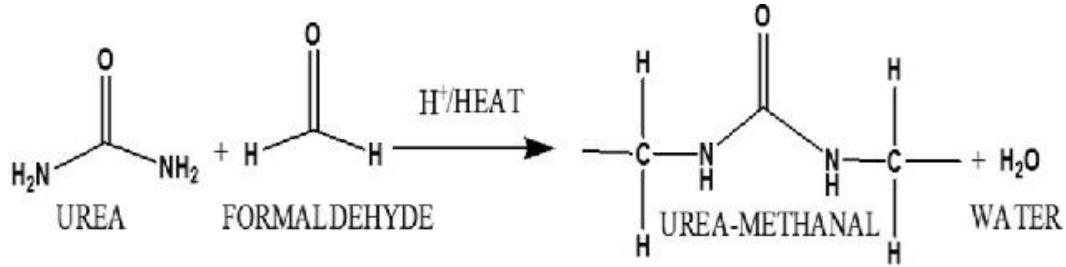


Figure 2.8 Formation of Pre-polymer by reaction between urea and formaldehyde [162]

2.3.2 SOLVENT EVAPORATION PROCESS

In the solvent evaporation process, the shell material is dissolved in solvent (chloroform/dichloromethane) and the dissolved solution is immiscible in water. The core material is dissolved completely in polymer solution. The formed mixture is continuously agitated with polyvinylpyrrolidone or PVA surfactants to obtain emulsion in the form of capsule. To obtain the microcapsules the shell material should diffuse into continuous phase and allows water to vaporize. With the instance of time or progress in evaporation, the capsules get harder and thus filtered out by evaporation[170]. Generally, this method is very useful when the species are having insolubility in continuous phase and yield of microcapsule is entirely dependent on the entrapment of core material in capsule. Moreover, with this solvent evaporation technique the capsules formed are having higher in porosity [171]. Li et al. encapsulated polyether amine inside PMMA by optimizing various parameters to obtain microcapsules for self-healing applications[165]. The encapsulation of epoxy resin along with polyether amine inside the PMMA was also encapsulated using the same approach[172]. This process can be used for healing agents having hydrophobic nature with many available shell materials like polymethylmethacrylate, polyvinyl fluoride (PVF), poly(L-lactide), polyvinyl

cinnamate etc. [173]. This process is simple, no harsh conditions are required and the complete process is straight forward, therefore it is superior among all other encapsulation techniques. However, due to solubility of shell material in solvent restricts its applications [174].

2.3.3 INTERFACIAL PROCESS

In this interfacial encapsulation process, the shell material is completely dissolved in core material/healing agent and the mixture is supplemented to aqueous phase. Additional curing agent is appended in aqueous phase to form a shell wall by polymerization of shell material around the core material to make capsule. Predominantly this interfacial process is used for synthesizing the larger capsules ranging from 3-30 μ m. For instance, the encapsulation of DCPD is possible by forming a polymer between the DCPD and water interface [169].

The majority of researchers used urea and formaldehyde in the process of preparing the capsules. Certainly, there are few complications in making capsules based on urea and formaldehyde:

- Mostly the formation of debris is high and followed by agglomeration. It also causes the incomplete healing because of formation of debris at the rupture site severally.
- Causes reduction in adhesion between matrix and capsules, due to the formation of agglomerated debris results into non-porous surface.
- Shell wall thickness ranging from 160-220nm is only possible[17].

The material with this type of capsule will never store the core material for long run due to the porosity[175]. Interestingly the capsule made of Melamine-urea-formaldehyde showed comparatively better shell properties. The procedure for making capsule is very simpler and no need of pH adjustment, which is very crucial in UF capsules[176]. Moreover, the double wall capsules made of UF have more enhanced properties of capsules compared to single wall UF capsules[177]. The first layered internal coating provides flexible property and the second outer layer provides the enough strength to the capsule shell wall[178].

2.3.4 SOL-GEL PROCESS

The most feasible process for preparing the capsules with organic core material is sol-gel process, since it happens due to low temperature hydrolysis reaction therefore it cannot withstand the elevated temperature. The capsules prepared by sol-gel process, commonly happens at low-temperature hydrolysis which is highly feasible for preparing the capsule with organic core materials, which cannot withstand the elevated temperatures[179]. In the sol-gel process, the organic moieties and emulsifier/surfactants dispersed in aqueous phase and the emulsified droplets are formed by controlling the agitation rate. Therein this emulsion is combined with silica, enables the formation of droplets suitable for hydrolysis conditions and starts condensing the alkoxide of silicon, leads to the formation of colloidal particles. The sol-gel process and oil-in-water emulsion process combined enables the formation of capsules by controlling the morphology and size of microcapsules preparation [180]. Mostly, methoxysilicate (TMOS) and tetraethoxysilane (TEOS) are used with silicon, which is easily soluble in ethyl alcohol. These precursors get condensed upon the gel formation which is known as gelation. The silicon alkoxides are commonly used in the preparation of microcapsules. Most of the researcher are interested in producing the hollow microcapsules that is the capsule without any core using evaporation, thermolysis and extraction processes[180]. The microcapsule production using the silica is most viable and easily available. Most of the industries uses the TEOS due to its availability and economical, but the production of capsules using the TMOS is much faster in production and gelation in comparative to TMOS due to the presence of small methoxide side groups. Yang et al prepared self-healing composite material for cementitious applications made the use of sol-gel and interfacial methods in the preparation of capsules[174], where the methyl methacrylate (MMA) acts as a healing agent and triethylborane (TEB) as a catalyst in the preparation of shell wall as depicted in the Figure2.9.

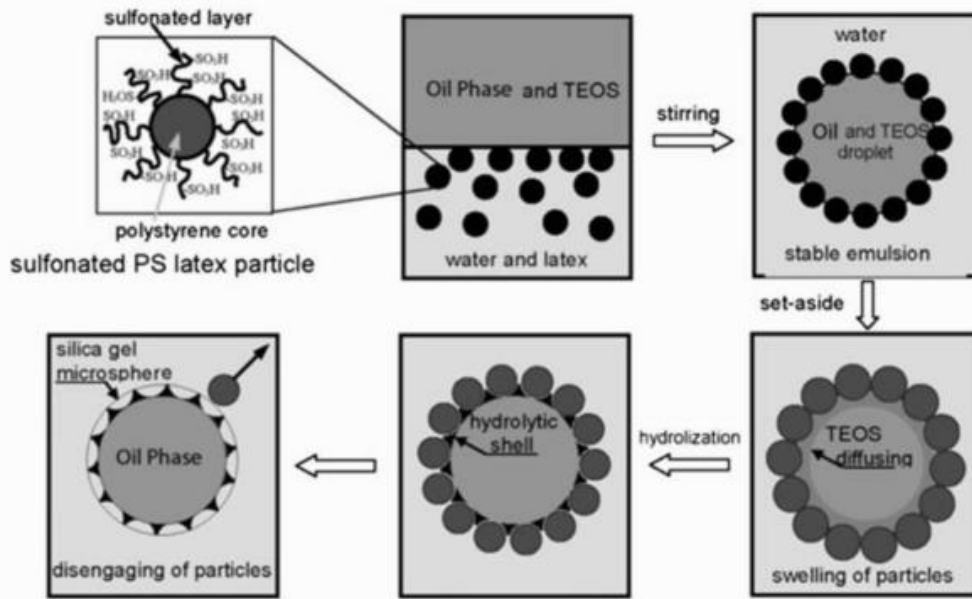


Figure 2.9 schematic representation of procedure adopted for preparing capsules using sol-gel and interfacial process [174]

Generally, this procedure is adopted to encapsulate enzymes[181], pancreatic islets[182], proteins[179] and many more for medical applications. The silica as a unique feature particularly in self-healing like, it acts as a diffusive barrier which restricts alteration of healing agents functionalities[174]. The sol-gel process uses very limited solvents and make much difficult to handle which showcase the limitation of sol-gel process. The Stober chemistry is majorly involved in sol-gel process, where this process is used to encapsulate sustainable solvents in thermoset polymers using the silica capsules. Few research was done even with the use of PVA in silica microcapsules containing the glycerol solvents which are capable of welding properties[174]. Based on the Stober chemistry, majorly ethanol-water are used for the preparation of capsules. If the healing agent used comprise of good solubility in water and ethanol can be easily emended and even acidic and basic conditions are also the major concern. The current requirement of nano-size capsules, which limits the core content presence, limits the process of sol-gel procedure for capsule preparation [174].

Most evidently there are several factor, which majorly influence or affect on the size of capsules such as temperature, propeller geometry, agitation rate,

emulsifier/surfactant, pH, and sonication rate, those significantly influence the morphology and size of the capsule apart from the above procedure adopted.

2.4 DIFFERENT CHEMISTRIES INVOLVED IN SELF-HEALING

2.4.1 DICYCLOPENTADIENE (DCPD)

White et.al has proposed the DCPD capsules based self-healing concept, where ring opening metathesis polymerization (ROMP), of DCPD was performed using Ruthenium (Grubb's) based catalyst [8], [27]. A variety of Grubbs catalyst includes grubbs 1st, 2nd & 3rd generations has also been discussed[183]. A comparative study of different monomers of DCPD (Exo and Endo) has also been performed[184]. The results, shows that exo DCPD has 20 times faster activity/polymerization compared to Endo DCPD. 2nd generation Hoveyda Grubbs catalyst showed better performance, faster kinetics including good thermal stability compared to 1st and 2nd generation Grubb's catalyst[183].

There are difficulties while using DCPD capsules and Grubbs catalyst, especially a uniform dispersion of catalyst into the matrices. In addition, there is a chance of deactivation of smaller crystal due to the presence of amine hardener in epoxy resins. Moore et. al has developed a new technique for the fine dispersion of crystals and for activation of catalyst by amine hardener, crystals are shielded by embedding them using paraffin wax[24].

2.4.2 5-ETHYLIDENE-2-NORBORENE (ENB) BASED HEALING SYSTEM

ENB is an alternative monomer for DCPD as it shows faster polymerization (self-healing) compared to DCPD [185] (Figure 2.10). The reaction kinetics of healing agent can be fine-tuned with the use of ENB. The mixture of DCPD and endo-ENB were also proposed better self-healing and structural applications[186], [187]. The self-healing based on the combined mixtures showed more than 95% healing efficiency at 170°C (curing temperature). The prepared epoxy composite material exhibited higher modulus even at -50°C and 70°C and has low glass

transition temperature (T_g), which suits for the requirement aeronautical structural application[188].

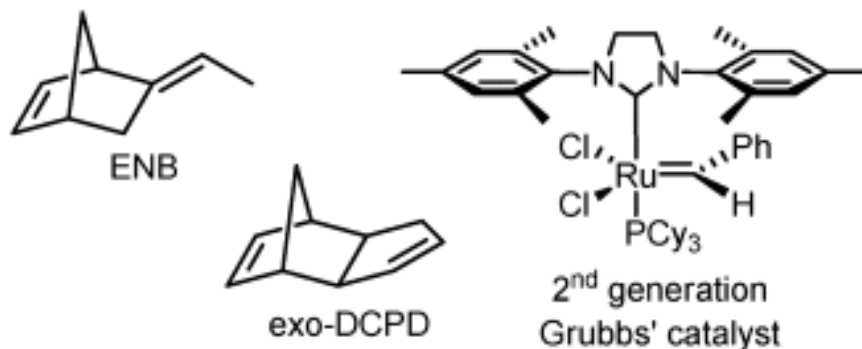


Figure 2.10 5-ethylidene-2-norbornene (ENB) based healing mechanism [127]

2.4.3 AMINE-EPOXY-BASED HEALING SYSTEM

An amine-epoxy based self-healing concept has been used for fibre & thermoset composites due to its good adhesive ability. Both the amine and epoxy resins were embedded in separate capsules and were arranged in pairs for better spatial and uniform distribution and mixing [189]. Whenever these tends to fracture, it fails and releases the healing agent in damaged site and react using nucleophilic ring opening polymerization (Figure 2.11) to heal and reform the original properties at room temperature. However to reduce the time for healing, additional heating is preferred. Toohey et. al introduced the vascular network using amine epoxy concept in a ductile epoxy[35]. A 60% fracture load was recovered after observing the 16 consecutive cycles and giving healing time for 48h at 300 °C for every cycle.

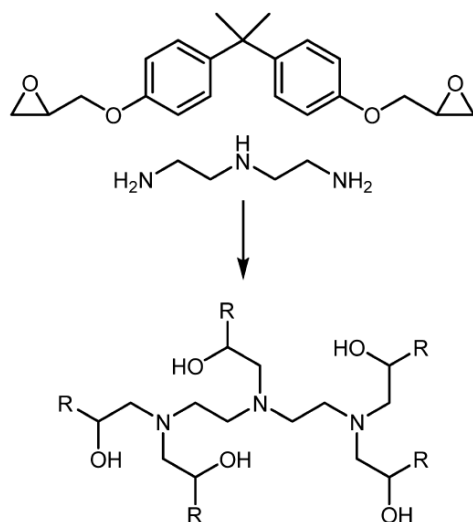


Figure 2.11 Nucleophilic ROMP using bisphenol A diglycidyl ether and diethylenetriamine [127]

2.4.4 THIOL EPOXY BASED HEALING SYSTEM

This system requires thiol multifunctional agents, epoxy resin as healing agent, (Figure 2.12), and elaborates the good thermal stability and healing concept. This is an exothermic thiol epoxy reaction, which happens very fast and an efficient manner. One of the major concern of this reaction is that, it needs catalyst for fast reaction process. The basic compounds required for this system are diglycidyl - 1,2,3,6-tetrahydrophthalate (DTP) as epoxy resin of low viscosity, combines with pentaerythritol tetrakis (Tetra Thiol) and catalyst of benzyl -N, N-dimethylamine(BDMA) [190].

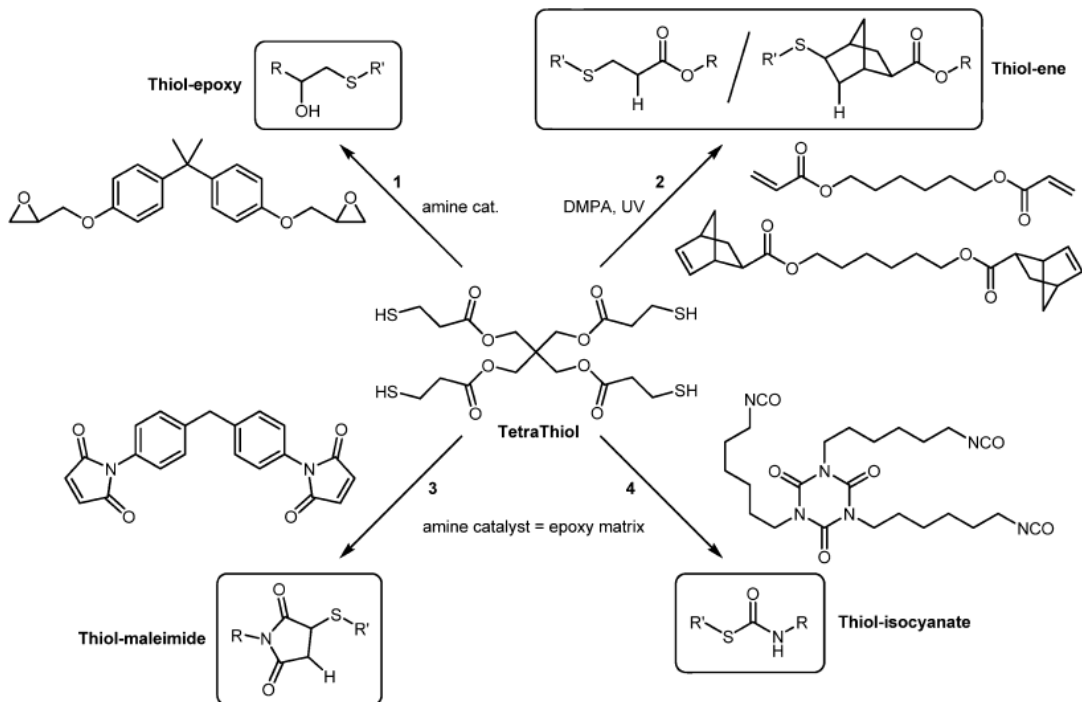


Figure 2.12 Thiol Based self-healing system [127]

This rises to deprotonation of thiol groups using amine, which rises the nucleophilicity, as a result it initiate the nucleophilic ring opening polymerization at room temperature with epoxide. A decrease in recovery percentage was observed when the temperatures are allowed to fall below room temperature, this is due to the low freezing point of dicyclopentadiene DTP healing agent.

2.4.5 THIOL-ISOCYANATE BASED HEALING SYSTEM

Combination of Thiol and Isocyanate is a recent advancement in self-healing systems using dual microcapsule method. It uses the nucleophilic reaction for healing purpose. Where thiol gets add on to isocyanate when it deprotonated and thus forms thio-urethane bonds[191]. A reaction between isooctyl 3-mercaptopropionate and hexamethylene diisocyanate (HDI) shows the isocyanate conversion within one minute by the addition of tertiary amine catalyst. Moreover, from the observation, it was observed that without the addition of catalyst the reaction yielded 40% within 10days. It was noticed that even without the catalyst the reaction is happening at slow rate, so both the healing agents requires separate

encapsulation. From TDCB test, a 54% recovery was found in fracture load at room temperature within 5 days.

2.4.6 CLICK (AZIDE-ALKYNE) BASED HEALING SYSTEM

In this system azide and alkyne as healing agents and Cu(I) as catalyst perform the cycloaddition (CuAAC) reaction for PIB materials (Poly(isobutylene)) [192]. Huisgen 1,3 dipolar cycloaddition with Copper Cu(I) as catalyst is defined as “Click” reaction [193]. By the presence of Cu(I) catalyst the 1,2,3 triazole ring reaction takes place by the combination of azide and alkyne. Polymers of various functional groups having different molecular weights and densities, of were synthesized using living polymerization technique. Click reactions are accelerated by correlating to the clustering effect by triazole rings which are formed near the active copper(I) center [194].

The μm sized three arm star azide-telechelic and multivalent alkynes are encapsulated and finely dispersed along with $\text{Cu}^{\text{I}}\text{Br}(\text{PPh}_3)_3$ catalyst in PIB (poly(isobutylene)) matrix, and the components were released by rupture caused by shear force [195]. Subsequently the network formation *via* CuAAC was proceeded and showed 91% recovery in tensile property by dynamic mechanical analysis (DMA) at room temperature have been observed the fast reaction at the different elevated temperature, also it requires enough time for self-healing (40, 60, 80 °C for 380, 60, 10 min respectively). Even at low temperature reaction were observed by the auto catalyst for the 1,2,3 triazole rings by the azide and alkyne reaction [196]. With the help of dual capsule technique CuAAC reaction for higher molecular weight of 250,000 g/mol for self-healing is investigated [195]. A similar result was observed with the same catalyst $\text{Cu}^{\text{I}}\text{Br}(\text{PPh}_3)_3$ using Bisphenol-E based dyes and Bisphenol-A based bisazide (healing agent), thus ensures components flow towards crack and recover the structure and properties [197].

By using trisazides and bis(arylacetylene)s, a thin film formed on hyper branched poly(aryltriazole)s *via* metal free click reactions (Figure 2.13). Repeatable healing events were observed by the extra azide and alkyne groups present at the periphery by heating up to 110 °C [198].

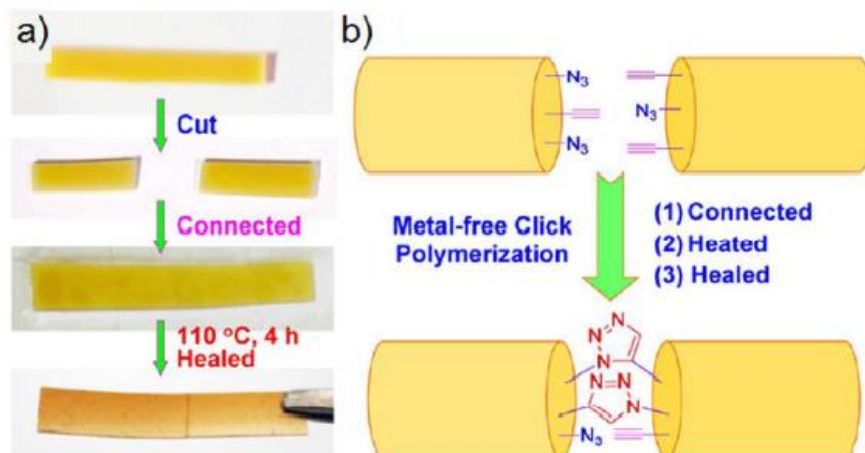


Figure 2.13 a) Healing procedure for poly(aroyltriazole)s films b) click reaction [198]

2.4.7 SELF-HEALING BY SUPRAMOLECULAR

The basic concept of supramolecular self-healing is based on reversible bonding, non-covalent bond like hydrogen bond, metal ligand bonds, ionomer bond, and π - π staking between compounds of low molecular weight and modified polymers with higher molecular weight polymers. Moreover, use of supramolecular concept affects the properties of material like viscosity, strength and flow[199], [200]. The major factors affecting the self-healing assembly is the geometry and shape of hydrogen bond. Even more, degree of polymerization is easily tunable by its nature in semi flexible and reversible nature for choosing the supramolecular materials [201]. The general concept of self-healing by supramolecular is shown in Figure 2.14 demonstrates undamaged material *i.e.* supramolecular bonds are attached with the network, after the conventional damage to the material causes crack. The crack surface consists of unbounded supramolecular bonds which seems to be sticky in nature and during the stipulated time the recombination of two crack surface leads to reconnecting the unbounded bonds to form a network, it causes self-healing autonomously. The formation of network or self-healing mainly depends on time required for the formation of sticky on the interface and dynamics of chains at individual polymer level [202]. The main advantage by using the supramolecular mechanism is multiple healing events are possible by their weak supramolecular bonds [203].

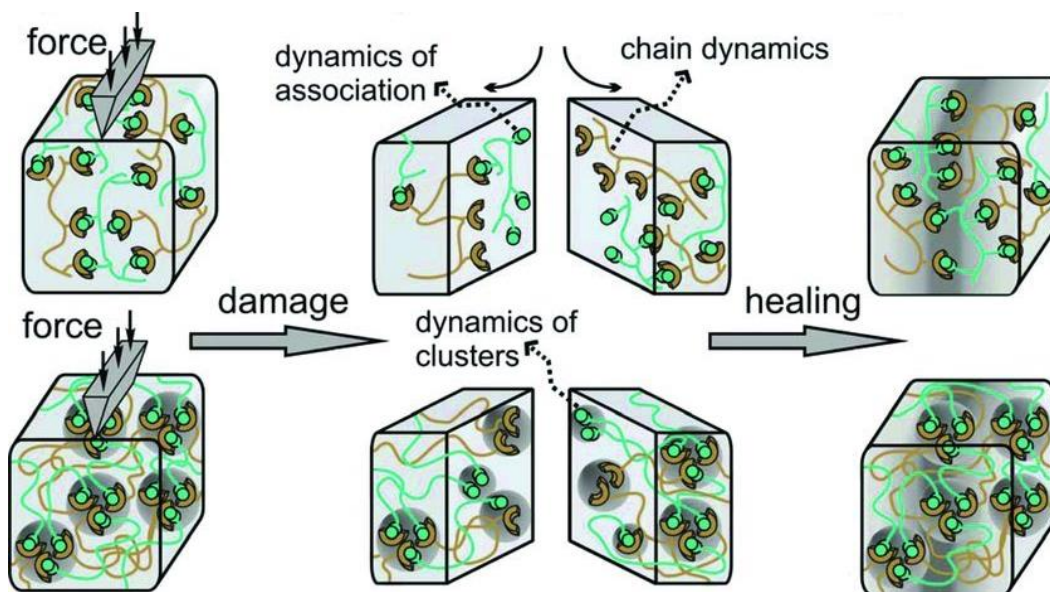


Figure 2.14 self-healing by supramolecular mechanism [202]

For the linear supramolecular or small building blocks, the formation of chain is happened due to associative groups or within the groups of polymers. In case of bigger building blocks, polymer chains are associated with two or more functional groups for the formation of network by crosslinking. For the supramolecular network, association constant (10^3 - 10^{12} M^{-1}) value is more than the dimerization constant (less than 100 M^{-1}) which can be neglected in many cases[204]. The lifetime of bond is inversely proportional to the rate of dissociation happened by diffusion controlled process. For the formation of strong and efficient bond by supramolecular network, degree of polymerization (DP) must be quite high, increase in concentration and decrease in temperature, or also by incorporating the multivalent monomers for crosslinking.

It is considered as a big challenge for transferring characteristic during self-assembly and self-interactions in bulk materials. It happens due to, more strong hydrogen bond results into slow dynamic behavior. By the contrast, weak interaction produces the strength in bulk materials. Care needs to be taken during designing and tuning the supramolecular polymer in choosing the solid-state properties and morphology are the major factors affects the performance of self-assembly[205]. It depends upon the dynamic chain mobility, good in bulk mechanical properties, hydrogen interactions and crystallization of supramolecular

moieties. Majorly this healing response time depends on two factors a) recombination of supramolecular moieties, and b) chain dynamics[199] for supramolecular bulk material to reform new chain under constraints[206].

2.4.7.1 Self-healing by hydrogen bond

In this system, the polymer matrix consists of hydrogen bonding groups, where there are many factors, which effects the self-healing and supramolecular aggregation, fiber formation, stacking, cluster formation, crystallization of polymer group and secondary effects such as secondary hydrogen bonds and dipole-interactions. Sivakova et al investigated on lower molecular weight telechelic poly (THF) of less than 2000g mol^{-1} with different nucleobases end groups. The interaction between the polymer and end groups is off very weak ($<50\text{ M}^{-1}$) which form film and formation of fiber is observed. Results showed high thermo-sensitive films of supramolecular [207].

Herbst et al. investigated on poly(isobutylene)s (PIB)s with 2,6-diaminotriazine (DAT) and thymine groups. Poly(isobutylene) is of lower $T_g = 70\text{ }^\circ\text{C}$. various combinations of DAT and THY were investigated: THY-THY, DAT-DAT and THY-DAT. The combination of PIB and THY showed the strongest effect during the melt [208]. The polymers at higher temperature ($> 70\text{ }^\circ\text{C}$) shows the lower viscous due to the deaggregation of groups. They also investigated the bivalent poly(isobutylene)s by changing the molecular weights (3,8,14,and 30K g mol^{-1}) by barbituric acid groups [209]. From the rheology it was observed that during high and low frequency ranges leads to rubbery plateau and low viscous respectively (Figure 2.15 (a)). Rubbery plateau is high for higher molecular weights of PIB, clearly shown by the formation of tie-points contains several barbituric acid groups. At small interval or high frequency, these tie-points are closed and at higher interval or small frequency these tie-points opens due to the viscous and elastic behavior. The timescale for the dynamic behavior of supramolecular is in the range of 31s-51s which depends upon the strength of interaction between the supramolecular, size of aggregate and polymer chain mobility. In Figure 2.15 (c) shows the autonomous self-healing behavior within the

ambient temperature range after the damaged portions were brought into contact with each other.

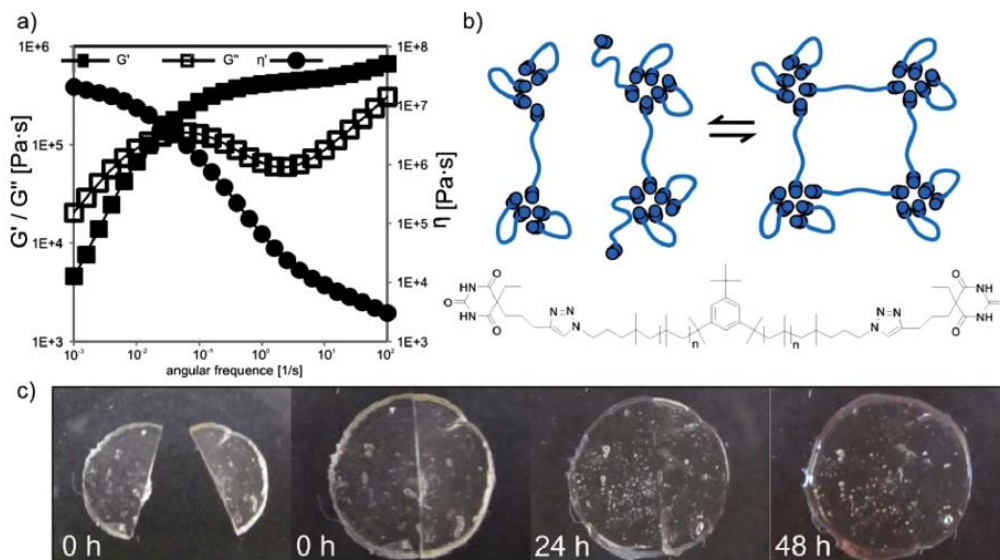


Figure 2.15 a) frequency measurement of PIB, b) supramolecular network formation, c) experiment procedure of self-healing behavior [209]

2.4.7.2 Self-healing by π - π stacking

S Burattini et al. introduced the self-healing based on π - π stacking or interaction[210]. This is an attraction between the π electron poor and π electron rich[211]. For the maximum amount of interactions to happen, conversion of low molecular weight to medium molecular weight is necessary in higher dynamic manner. In addition, with the chain folded secondary structures should be present in the supramolecular for possible interactions. The obtained product shows higher in tensile strength, which generally observed in covalent bond and used for self-healing applications as well.

S Burattini et al. S Burattini et al. developed π - π stacking based self-healing by choosing polyamide as a polymer has naphthalene-diimide and pyrenyl compounds, which contribute to π - π stacking. Where naphthalene-diimide is poor in π electron and pyrenyl end-capped as rich in π electron to develop π - π stacking leads to self-healing (Figure 2.16). The interaction between the naphthalene-diimide and pyrenyl showed the locking of end cap i.e. chain folding of polyamide were observed by cry stallographic and spectroscopic methods (Figure 2.16 c) leads

to the supramolecular network [210]. The interaction between the rich and poor electron mixing is obtained by mixing the pale yellow color of polyamide and as well with colorless polyamide, it gives red color, which indicates the charge transfer between the electrons, also after cooling, it converts into deep red color. Moreover, the resultant association constant was 130M^{-1} , hence reveals reversible character by the formation of supramolecular network.

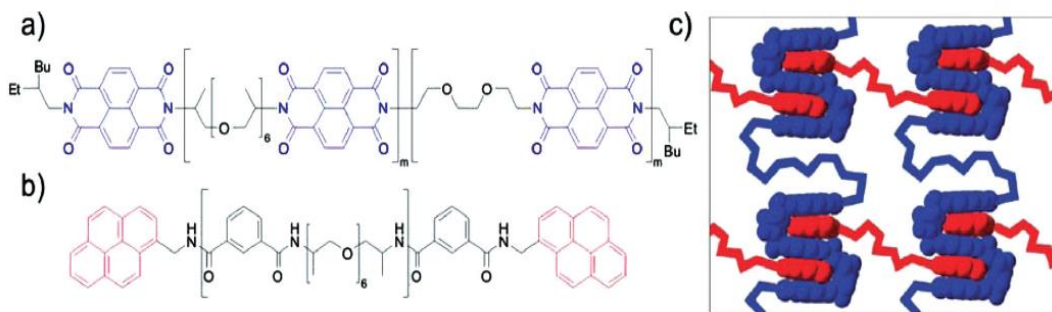
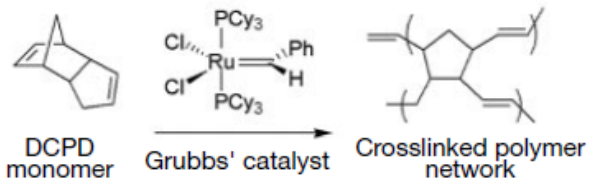
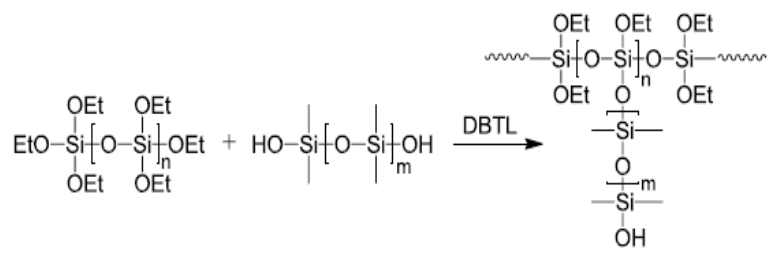
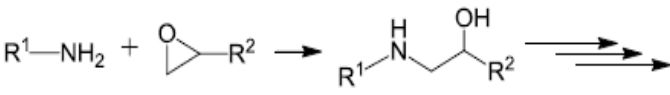
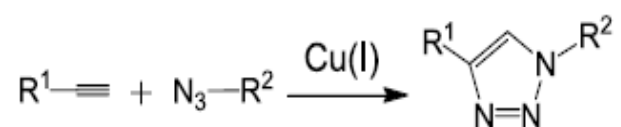
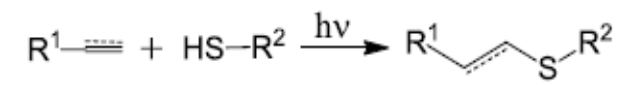
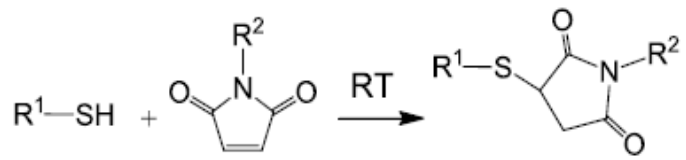


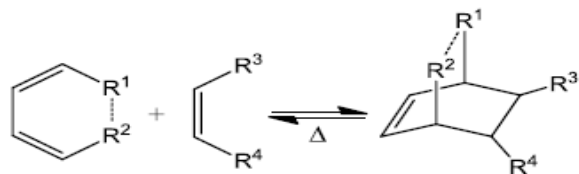
Figure 2.16 a) naphthalene-diimide rich in pi electron b) Prenyl end-capped weak in pi electrons c) Interaction between the naphthalene-diimide and prenyl pi-pi stacking [210]

2.4.7.3 Self-healing based on ionomers

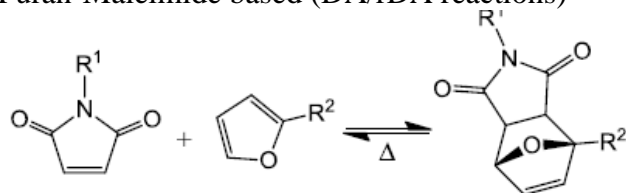
Self-healing for polymers can also perform using ionic groups, which is an advantage for clustering which do needful for crosslinking and reformation of supramolecular network [212]. Presence of ionomer is not enough for self-healing and the presence of polar acid groups within the material propagates the reversible hydrogen bonding was confirmed [213]. Self-healing is promoted by high heat generation during the reversible bonding along with higher energy. It produces the localized molten polymer, which is necessary for filling the damage and further process proceeded by inter-diffusion process. The entire process depends mainly on the inter-diffusion, crystallization; time given for regenerating the network and parameters like viscous and elastic behavior, comes into role for supramolecular network. This can happen even at low temperature when material subjected to local heating which is necessary for melting. The healing efficiency mainly depends on the temperature, impacting projectile and speed of impacting.

Table 2.2 Self-healing approach

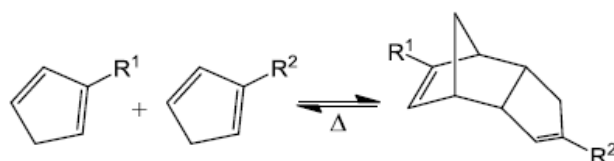
S.no	Self-healing concept	Temperature (°C)	Healing efficiency	Ref.
1	<p>Ring opening Metathesis Polymerization (ROMP)</p>  <p>DCPD monomer + Grubbs' catalyst → Crosslinked polymer network</p>	22	99%	[214]
2	<p>Polycondensation reactions of poly(siloxane)s-based self-healing approaches</p> 	20	24	[215]
3	<p>Epoxide curing</p> 	150-120	100	[216]
4	<p>CuAAC “click” reactions</p> 	30	100	[217]
5	<p>Thiol-ene/ thiol-yne “click” reactions</p> 	80	93	[218], [219]
6	<p>Michael addition</p> 	25 (3-5 days)	121	[220]
7	<p>Diels-Alder/retro-Diels-Alder reactions (DA/rDA reactions)</p>	50	100	[221]



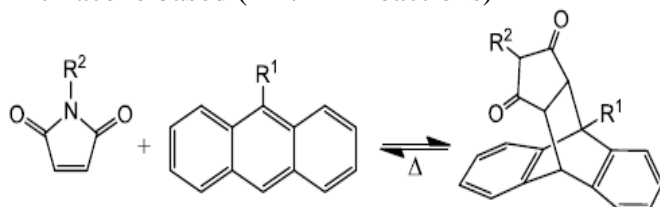
a) Furan-Maleimide based (DA/rDA reactions)



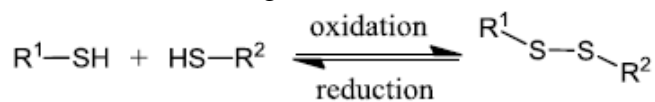
b) Cyclopentadiene based (DA/rDA reactions)



c) Anthracene based (DA/rDA reactions)



8 Thiol disulfide linkages 60 50-104 [222]
(25h)

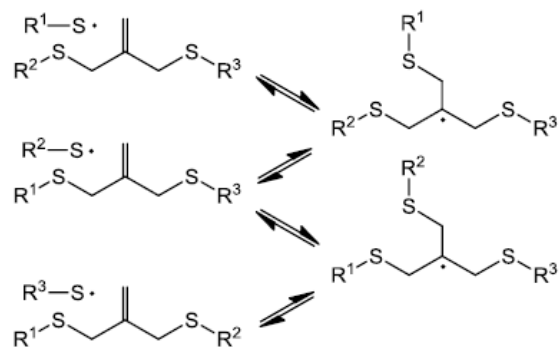


9 Disulfide exchange 80 50-104 [223]
(5min)

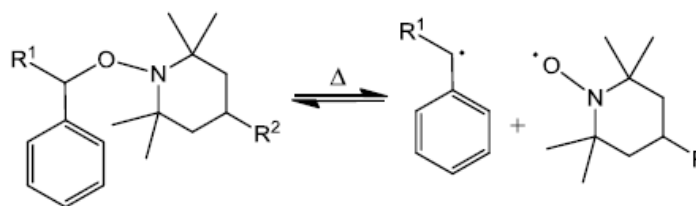


10 Radical based self-healing approach 50 60-105 [221]
(24h)

a) RAFT-like reactions



b) Alkoxy-amine based approach



11 Photo-induced self-healing

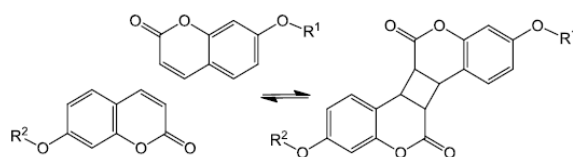
90-120

Up to 95

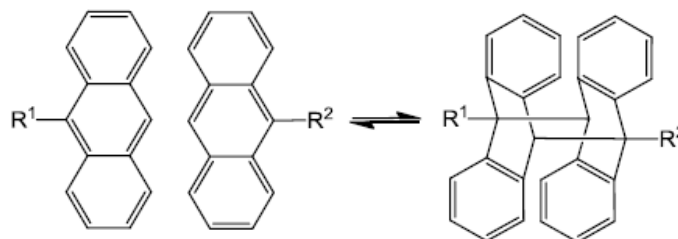
[213],

a) [2+2] Cycloaddition reaction

[224]



b) [4+4] cycloaddition reaction



2.5 SUMMARY:

Self-sealing *via* autonomous showed a great impact on self-healing potential of polymer and fiber reinforced materials. Table 2.2 shows the outline of few self-healing mechanisms for better understanding. Out of different chemistries involved in self-healing, few showed a greater contrast in self-healing and recovery in mechanical properties as well, such as DCPD, epoxy, Thiol-epoxy, amine-epoxy and azide-alkyne systems. The selection of polymer matrix also plays crucial role in self-healing out of different polymer matrices and chemistries, where PIB and PDMS matrices using azide-alkyne chemistry showed good healing efficiency. Recovery of matrix depends on how the agent's are interacting with external environment and dynamics involved in reformation of matrix. Factors affecting are viscosity and flow of healing agents at damaged site. Self-healing efficiency does not depend upon the type of delivery systems (microcapsules and vascular-based systems) moreover; it effects the mechanical properties (tensile strength, fracture toughness, fatigue and young's modulus) of composites. Further researchers should investigate on the effect of delivery system on mechanical properties of matrix. Most of the systems are slow down in crack propagation *via* hydrodynamic and

crosslinking reaction which effects the compressive strength after crack. Fatigue torsion, wear and tear due to the friction healed significantly up to some extent.

Therefore, to the best of my knowledge , self-healing composites including enhanced conductive and mechanical properties required for structural applications has not been explained yet.

CHAPTER 3: DEVELOPMENT OF HETEROGENEOUS CATALYST TO PROMOTE CLICK TRIGGERED SELF-HEALING

3.1 INTRODUCTION

This study is focused on the synthesis of Cu-graphene conjugate with high catalytic activity works as an effective catalyst in “click chemistry”, as well as could be effective to prepare the high dispersed graphene based composites including self-healing properties. The ‘click’ based self-healing is an efficient method used to crosslink the components even at room temperature. The ‘click’ reactions are regioselective, functional-group-tolerant, and can be performed under different reaction conditions using wide range of solvents[225]. However, after completion of reaction, the removal of copper catalyst as well as used oxidizing/reducing agent remains a challenge and thus hampering its utilization, in particular in electronics and biological applications[226]. The separation of catalyst from the reaction mixture was strongly facilitated by synthesizing the heterogeneous copper catalyst prepared using commercially available scaffolds, including resins, linear and cross-linked polymers[227], charcoal, graphene[228], or other-solid supports[229]. The support materials are also helpful to reduce the agglomeration as well as to achieve a uniform distribution of particles over a large area. However, catalyst recyclability and the necessity of an external ligand/base often limits their applicability.

Owing to their attractive properties such as high stability, electrical conductivity, porosity, and their performance for electron capture and transport, graphene supported catalysts have represented outstanding catalytic activity compared to other carbon/polymer supported catalysts[192]. To tune the intrinsic reactivity of the metal particles, the doping of heteroatom effectively alters the nature of the designed catalytic systems. N-doping of graphene oxide (GO) is cooperative to make a stronger interaction of metal particles and thus prevents the agglomeration as well as helpful to enhance the catalytic performance of

nanoparticles[192]. The role of N species on graphene decreases the surface energy, improves surface area in terms of functionality, higher in chemical active sites, and enhances electrical conductivity, which enforces to form a strong uniform dispersion of metal nanoparticles. Interestingly, the N-doping strongly influences the catalytic activity of metal nanomaterials to be occur at lower temperatures compared to alone copper. Additionally, of N-spices acts as an interacting layer between the copper and graphene, which promotes the enhanced catalytic action[230].

Only a few reports have appeared for using the N-doped carbon nanomaterials supported catalyst and their relevance in different applications. However, according to our knowledge the NRGO/Cu(I) (N-doped reduced graphene oxide) catalyzed “click” chemistry has not been explored yet. Here we explore a robust approach to improve the dispersion, stability, and recyclability of copper catalyst via immobilization of copper nanoparticles Cu(I) on N-doped reduced graphene oxide nanosheets and the synthesized heterogeneous catalyst (NRGO/Cu(I)) performs ‘click’ reaction at room temperature without addition of any co-catalyst (oxidizing/reducing agent) (Figure 3.1).

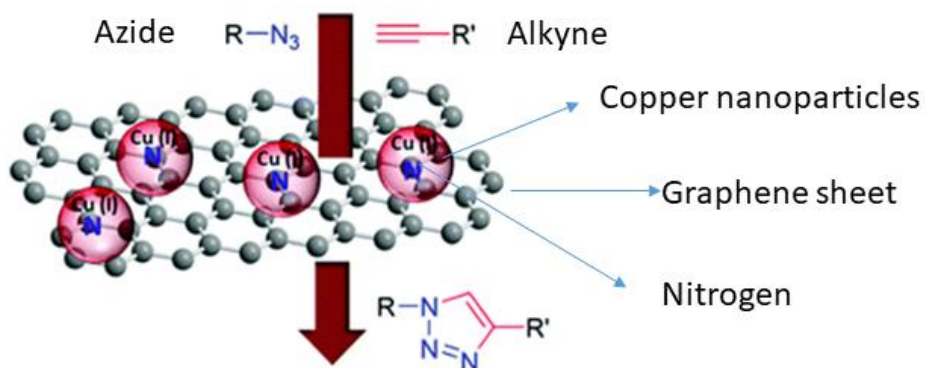


Figure 3.1 ‘click’ reaction using NRGO/Cu(I) catalyst

3.2 MATERIALS AND METHODS

3.2.1 MATERIALS

The materials used for the preparation heterogeneous catalyst as follows: Graphite Powder, Sodium Azide (purity >99.5%), Epoxy-Terminated Polydimethylsiloxane (PDMS) ($M_n=800$), Hydroxyl Terminated

Polydimethylsiloxane (PDMS) ($M_n=550$), Tetra-N-Butylammonium Bromide (TBAB) (purity >99.0%) and Propargyl Bromide (80 wt. % in toluene) were purchased from Sigma-Aldrich (Merck) with highest purity. Sulfuric Acid (H_2SO_4), Sodium Nitrate, Potassium Permanganate, Hydrogen Peroxide (H_2O_2), Ethanol, Hydrochloric Acid (HCl), Copper (II) Acetate, Melamine, Propan-2-ol, Sodium Bicarbonate ($NaHCO_3$), Sodium Sulfate (Na_2SO_4), Sodium Hydroxide (NaOH), Chloroform ($CHCl_3$) and Dichloromethane (DCM) were purchased from RANKEM

3.2.2 METHODS

The High-Resolution Transmission Electron Microscopy (HRTEM) analyses were performed on a FEI Titan³ 80-300 electron microscope with a c_s image aberration corrector (FEI Company) at 300 kV acceleration voltage. X-ray Photoelectron Spectroscopy (XPS) analysis was performed using a XPS PHI Versa Probe 5000 spectrometer. The pressure in the analysis chamber was typically $1.1 \cdot 10^{-9}$ Torr. The XPS measurements were performed using a monochromatic AlK α radiation at 1486.6 eV. A neutralizer with an Argon (Ar) gun was used during the XPS analysis to compensate charging effects. All NMR spectra were recorded on a Varian spectrometer (Gemini 400) at 400 MHz at 27 °C. Differential Scanning Calorimeter (DSC) measurements were performed on a 204F1/ASC Phoenix from Netzsch. Crucibles and lids made of aluminum were used. Measurements were performed in a temperature range from -20 to 250 °C using heating rates of 5 K/min. As purge gas, a flow of dry nitrogen (20 mL/min) was used for all experiments. C, H, N and O content analysis of the samples was performed using CHN PE 2400 SeriesII from Perkin Elmer. For evaluation of data the Proteus Thermal Analysis Software (Version 5.2.1) and OriginPro7 was used.

3.3 PREPARATION OF GRAPHENE OXIDE (GO)

The graphene oxide is prepared from the graphite by a slight modification in the modified Hummer's method [135]. The typical procedure, 1g of graphite powder and 39mL of sulfuric acid (H_2SO_4) (99%) sonicated for 15min for uniform

dispersion of graphite. later on 0.5g of sodium nitrate is added at 0 °C and allowed stirring for 30min. followed by the addition of 3g potassium permanganate slowly for 30min to avoid increment in temperature. This mixture is allowed stirring for 6h at room temperature until the mixture become dark green. Additional 3g of potassium permanganate is added to the reaction mixture and allowed stirring for 10-12h. Then the reaction mixture is slowly added to cold distilled water (DI) and 3% excess hydrogen peroxide (H₂O₂) to remove excess permanganate allowed for few minutes for settlement of heavy particles. The decanted supernatant layer washed with ethanol/hydrochloric acid (HCL)/ DI water 3times at 10,000 rpm. The obtained GO precipitate is dried at 80 °C for 24h. The obtained powder is graphene oxide. The presence of graphene oxide is analyzed using the X-ray Diffraction Spectroscopy (XRD, D8 ADVANCE ECO – Bruker) and UV-Vis Spectro Photometer (LAMDA 35, Perkin Elmer) characterization techniques were adopted. The peak at 12.187° was observed by XRD, which indicates the complete formation of graphene oxide shown in Figure 3.2 (a). UV spectroscopy was also performed to obtain the presence of graphene oxide and the characterization has been performed by dispersing graphene oxide powder in ethanol using ultrasonication. The absorbance peak at 221 nm perceived the presence of graphene oxide shown in Figure 3.2 (b). The Figure 3.2 (b) shows the two distinctive peaks, where 221nm shows the C=C, that indicates the amorphous carbon systems and a small narrow peak at 275nm is of C=O bonds[231].

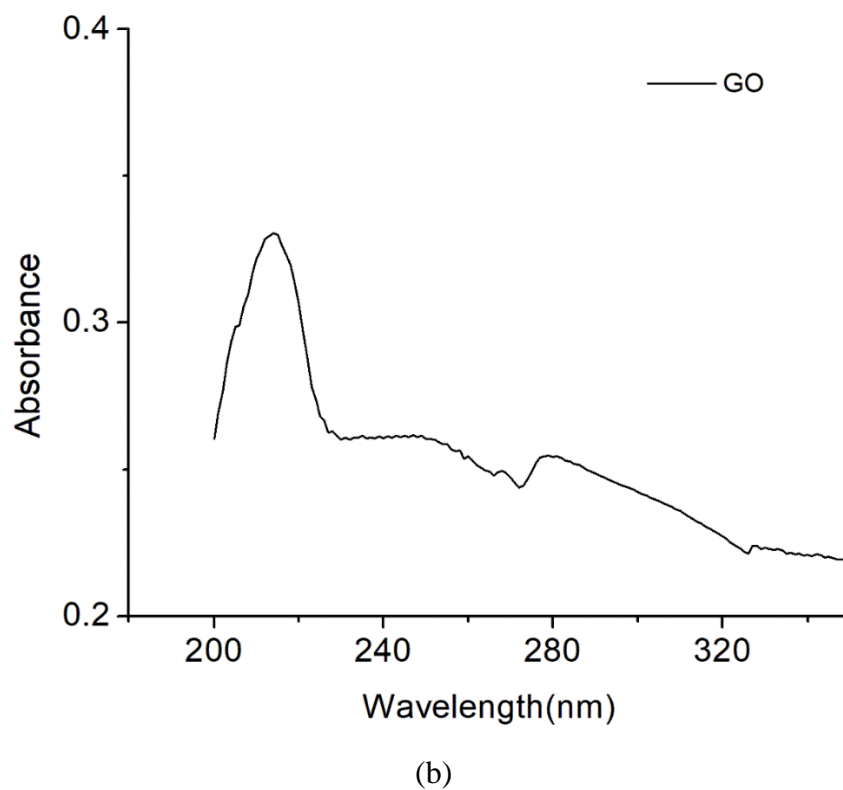
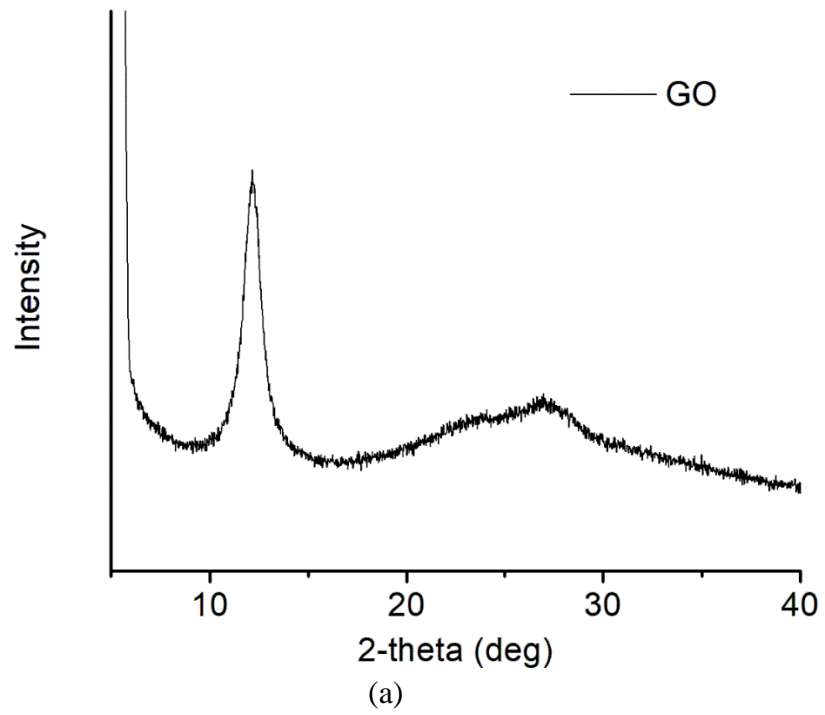
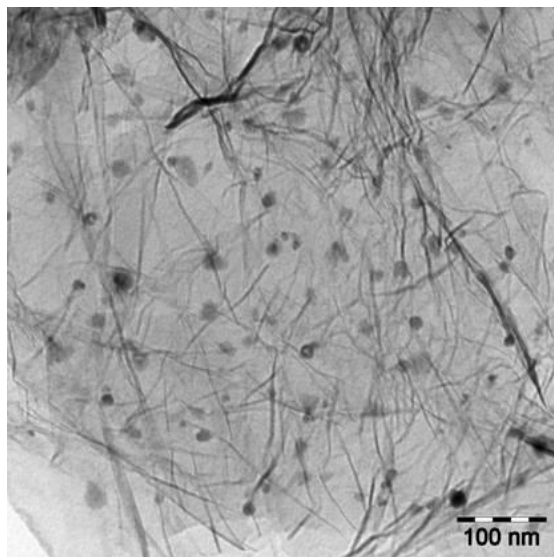


Figure 3.2 (a) XRD and (b) UV for Graphene Oxide (GO)

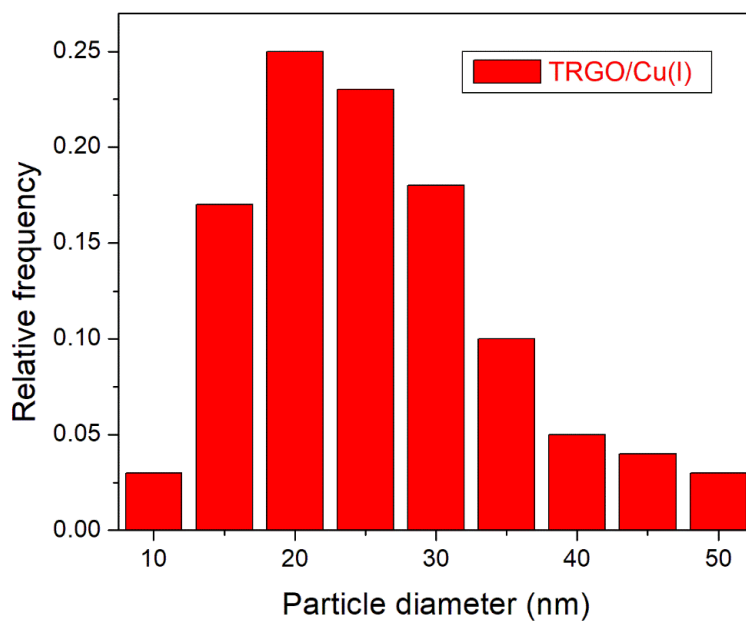
3.4 PREPARATION OF COPPER IMMOBILIZED THERMALLY GRAPHENE OXIDE (TRGO/Cu(I))

Further, the obtained GO was modified using the copper (II) acetate for immobilization. The immobilization of copper on GO (100mg) is performed by dispersing GO in water, followed by the addition of copper (II) acetate (20mg) under stirring for overnight at room temperature. After several washings with water and acetone, the Cu^{2+} -GO was dried in vacuum oven at 40 °C [232]. The TEM analysis was performed for TRGO/Cu(I) showed in Figure 3.3 (a), the sample was prepared by taking 1 mg of TRGO/Cu dispersed in 5 mL isopropanol using a water bath sonicator (15 min) and 1 drop of suspension was spread onto carbon film coated copper grid. After drying (overnight in desiccator), the sample was used for TEM measurement. The TEM images shows the highly dispersed TRGO/Cu(I) and the same TEM images are also used to detect average copper particle size (~20nm for TRGO/Cu(I)). Where a histogram shows the particle size distribution for the TRGO/Cu particles (Figure 3.3 (b)).

Here we further investigated the chemical composition of prepared catalyst *via* X-ray photoelectron spectroscopy (XPS) as shown in Figure 3.4. From the XPS investigation strongly shows the presence of C 1s (285.1 eV), O 1s (531.6 eV) and Cu 2p were observed, where the high resolution XPS confirms the presence of Cu(I) at peak satellites 932.3 eV and 952.3 eV (Figure 3.4 (c)). Furthermore, the data clearly denotes the absence of Cu(II), as no peak satellites at 942 eV and 962 eV was observed. The amount of copper content was determined using the FAAS analysis as 7.16×10^{-7} mol mg^{-1} loading of Cu content for TRGO/Cu(I).

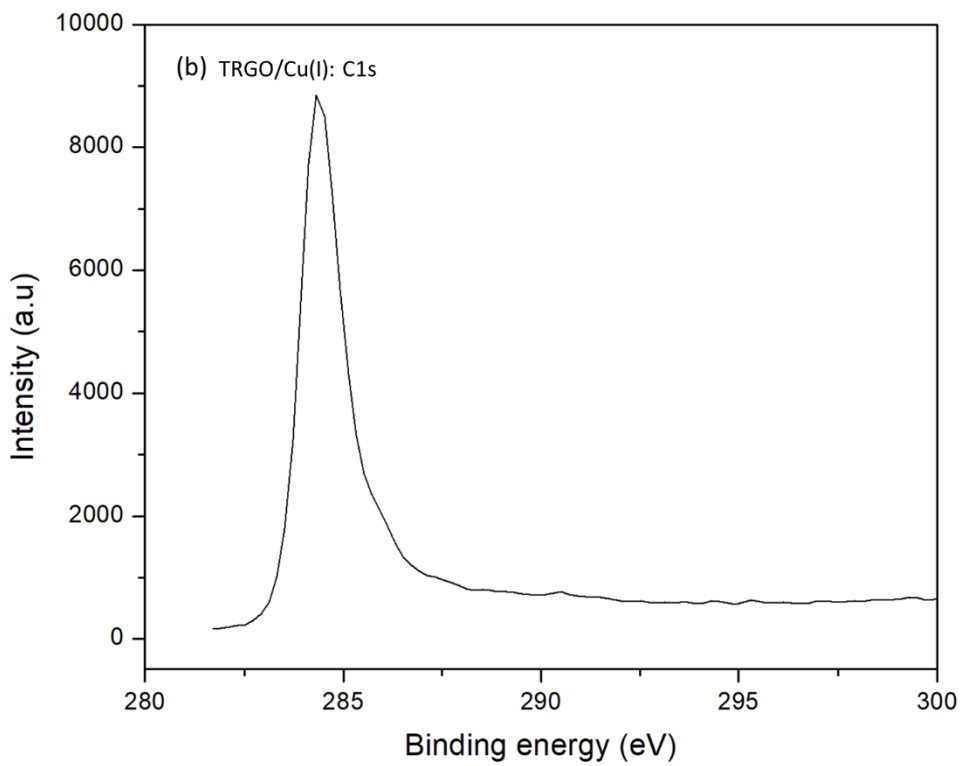
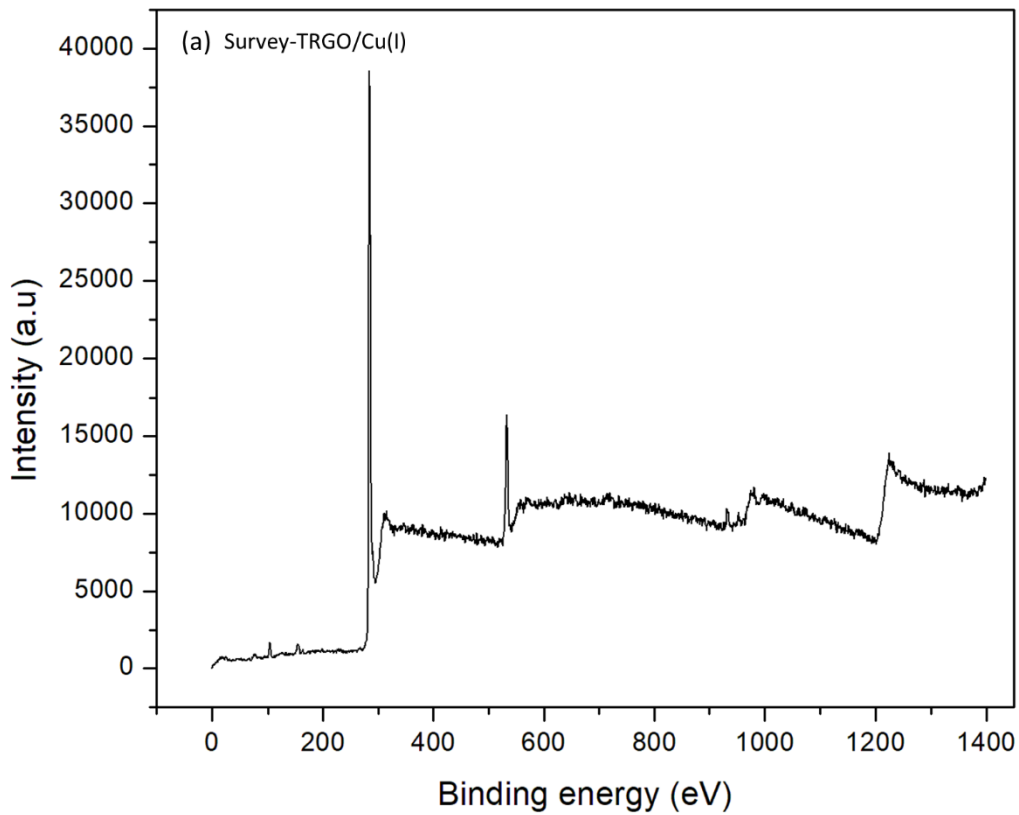


(a)



(b)

Figure 3.3 (a) TEM image of TRGO/Cu(I) and (b) Histogram of particle diameter of TRGO/CU(I)



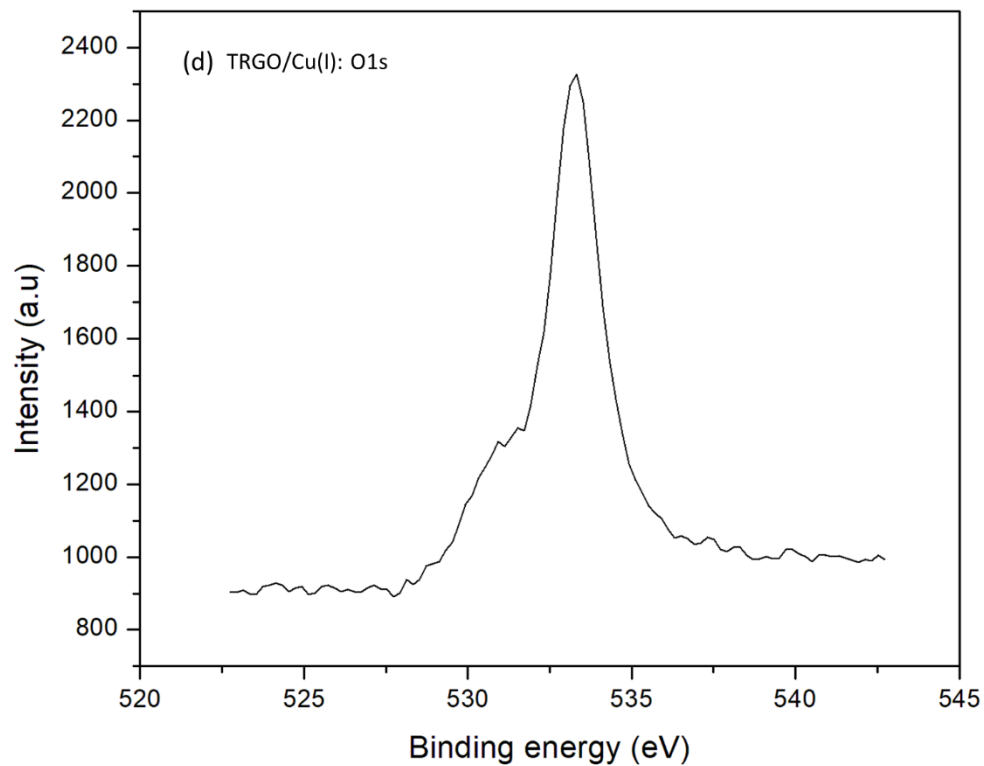
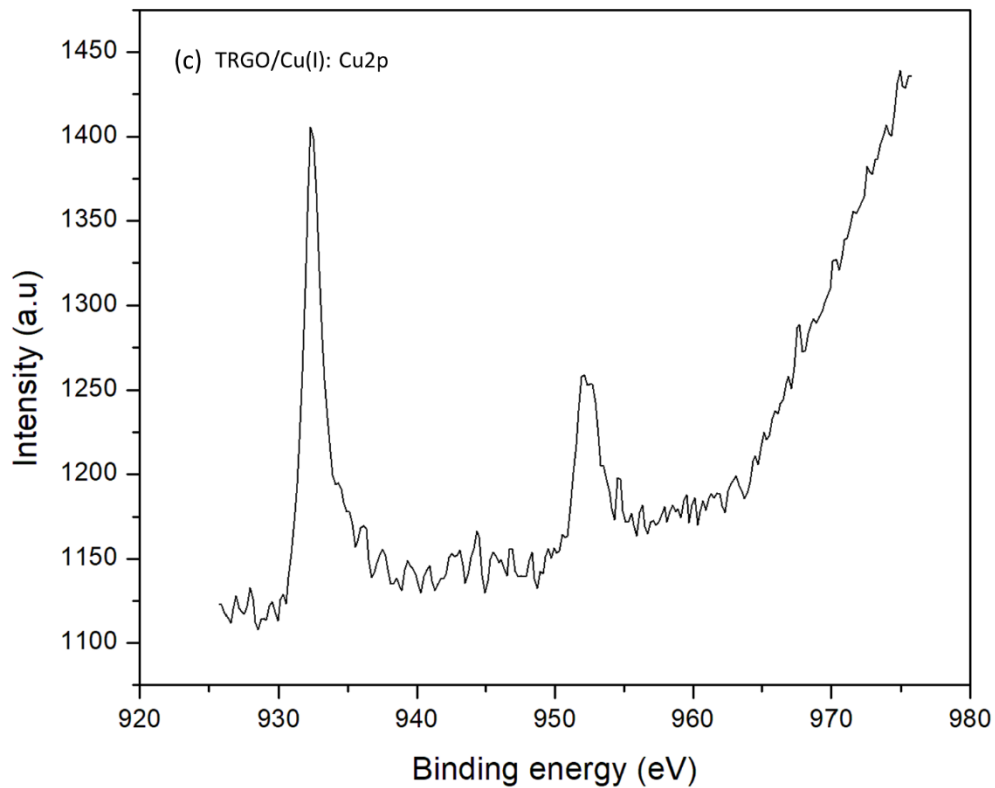


Figure 3.4 (a) XPS of TRGO/Cu(I), (b) High resolution XPS of element C, (c) High resolution XPS of element Cu. (d) High resolution XPS of element O

3.5 PREPARATION OF NITROGEN DOPED COPPER IMMOBILIZED REDUCED GRAPHENE OXIDE (NRGO/Cu(I))

The nitrogen doping on copper immobilized reduced graphene oxide is prepared by sonication of Cu^{2+} -GO in ethanol resulted in a uniform suspension. Followed by addition of melamine (2:1) to the above suspension and sonicated (~ 15 minute) further to obtain a uniform suspension. This uniform suspension kept for constant stirring until the ethanol from the resulting suspension was evaporated at room temperature itself to obtain a powder residue. Residue has to be grinded and then dried. The dried powder was heat treated in a tubular furnace under Ar atmosphere (4L/h). The temperature is raised from the room temperature to 600 °C at a rate of 10 °C /min and holding for 20min at 600 °C. Later on it allowed to cooled down to room temperature to obtain NRGO/Cu(I). The obtained powder from tubular furnace is washed with distilled water and dried.

From the Figure 3.5 (a, b) shows the TEM image of NRGO/Cu(I), displaying uniformly dispersed copper nanoparticles onto the surface of N-doped reduced graphene oxide. The TEM images were also found helpful to observe the average copper nanoparticles size (~20 nm for NRGO-Cu), where a histogram shows the particle size distribution for the NRGO-Cu particles Figure 3.5 (c). A 7.35×10^{-7} mol mg^{-1} loading of Cu content for NRGO-Cu(I) determined *via* FAAS analysis.

Elemental analysis was also made for the prepared catalysts (Table 3.1). XPS technique was performed to further evidence of the chemical composition of the nano-conjugates including the oxidation state of copper as well as copper interaction with doped nitrogen (Figure 3.6). The XPS peaks correspond to C 1s (285.1 eV), O 1s (531.6 eV) and Cu 2p were observed, where the high resolution XPS (Figure 3.6 (c)) reveals the peak energy of Cu(I), confirmed by the presence of peak satellites at 932.3 eV and 952.3 eV. Furthermore, the data confirms the absence of Cu(II), as no peak satellites at 942 eV and 962 eV was observed. A small associated peak observed at 932.7 eV (higher by 0.3 eV than that for N-free carbon;

((NRGO/Cu(I), Figure 3.6 (c)), could be attributed to a stronger interaction of the Cu(I) with N-doped RGO.

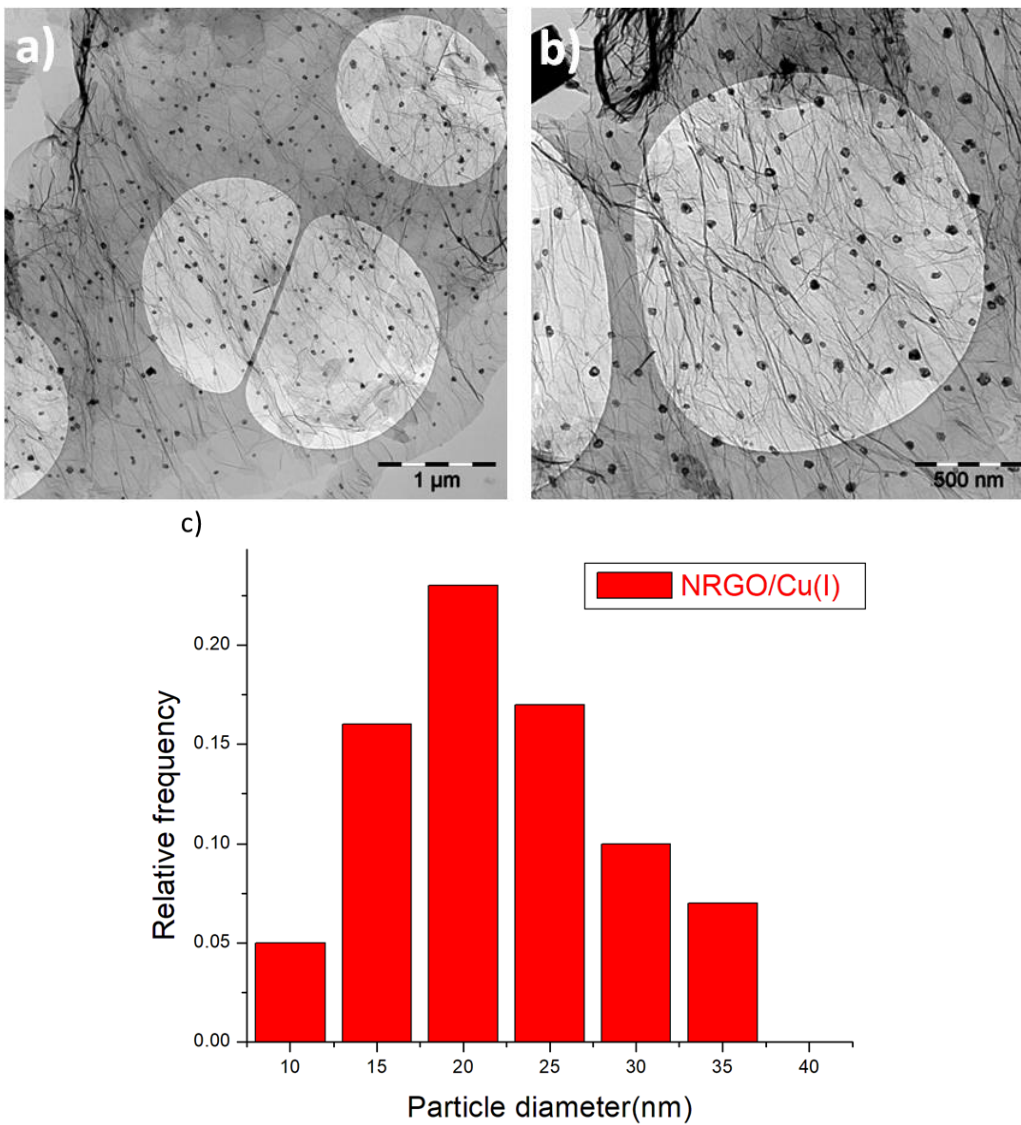
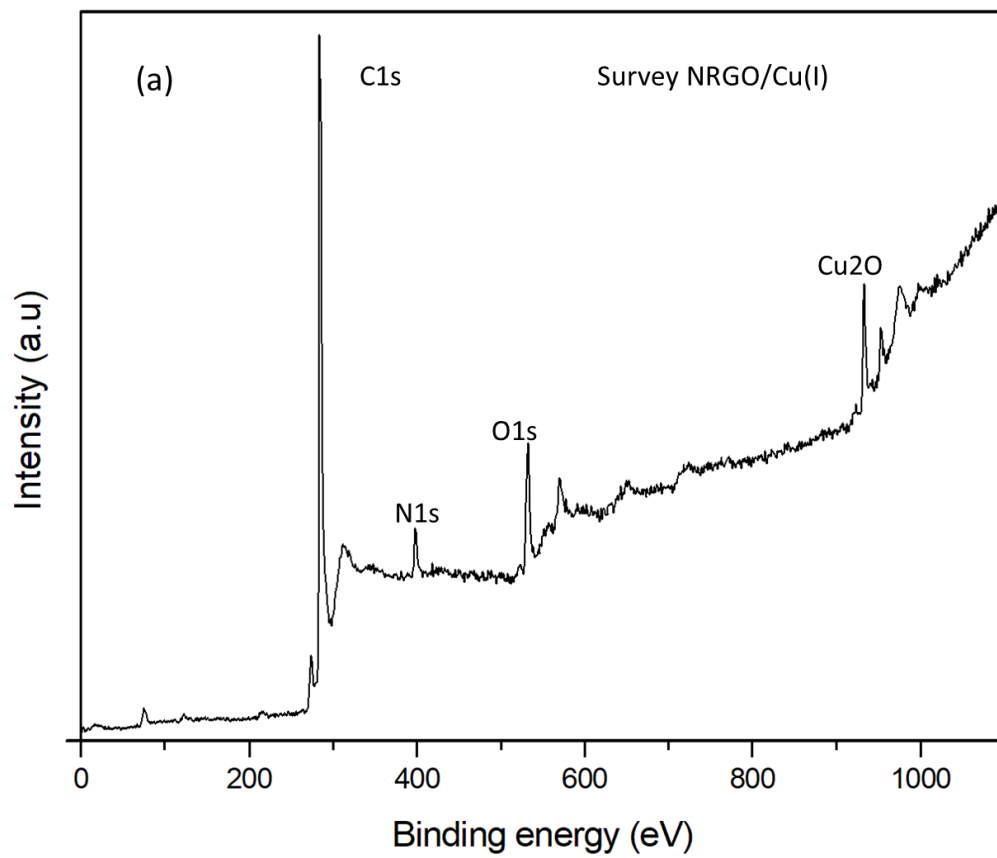
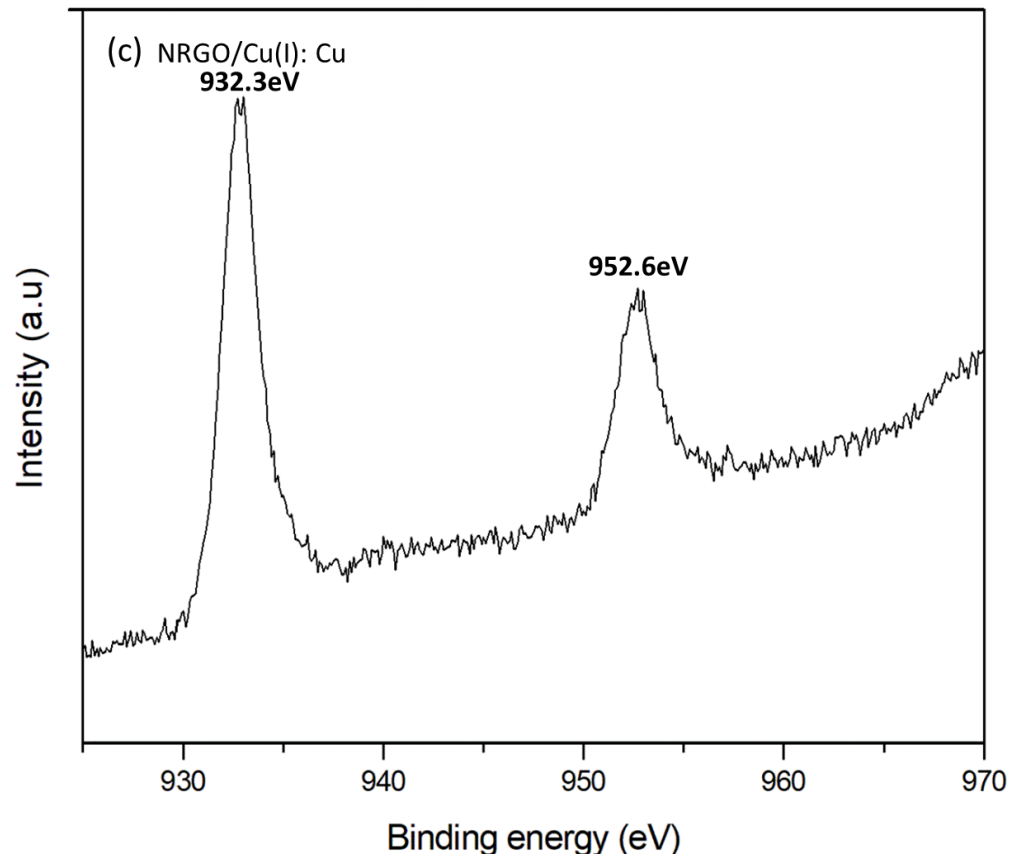
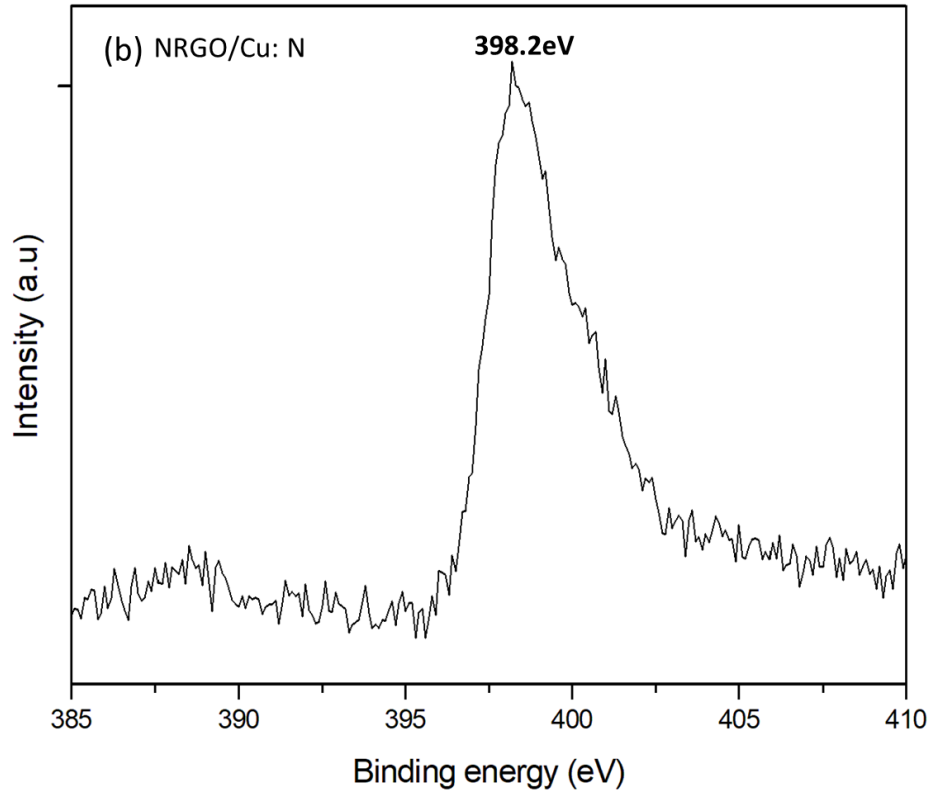


Figure 3.5 (a,b) TEM images of the NRGO/Cu(I) catalyst. (c) Copper particle size and distribution

Table 3.1 Elemental analysis of GO, TRGO/CU(I) and NRGO/CU(I)

Sample	C %	H %	N %	O %
GO	76.27	2.16	-	21.57
TRGO/Cu(I)	91.06	1.18	-	7.76
NRGO/Cu(I)	85.93	0.93	9.28	3.86





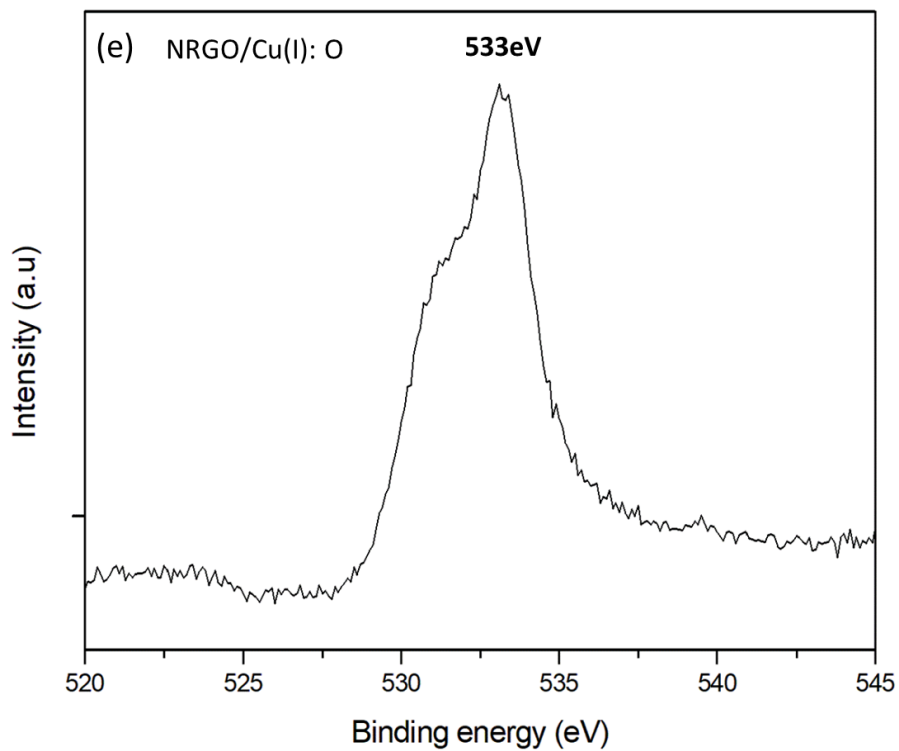
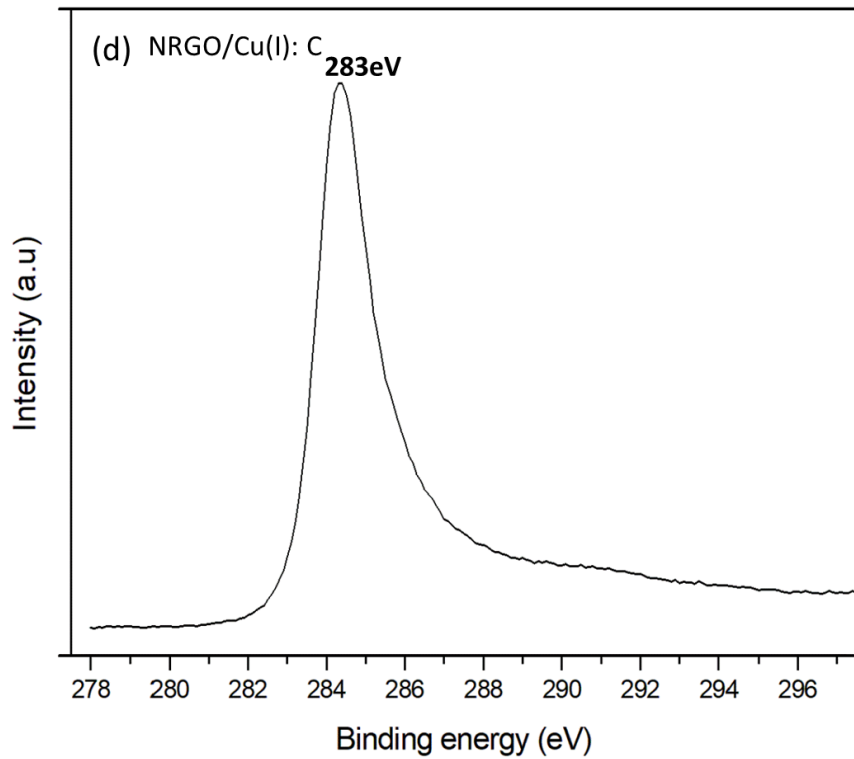


Figure 3.6 (a) XPS of NRGO/Cu(I). (b) High resolution XPS of element N. (c) High resolution XPS of element Cu. (d) High resolution XPS of element C. (e) High resolution XPS element of O.

3.6 SYNTHESIS OF AZIDE FUNCTIONALIZED POLY DIMETHYLSILOXANE

A solution of sodium azide (1.93 g, 9.1mmol) in distilled water (3.4 mL) was added to a solution of epoxy-terminated PDMS ($M_n=800$) (DP ~7, 2 g, 2.5 mmol) in propan-2-ol (13 mL). Then the solution was adjusted to pH 6 with glacial acetic acid (to control acid concentration). The reaction mixture was stirred at 50 °C up to the complete disappearance of the starting material, followed by TLC (toluene/ethyl acetate (9:1)). After dilution with diethyl ether and successive washings with saturated Sodium bicarbonate (NaHCO_3) and water, the organic layer was dried on Sodium sulfate (Na_2SO_4) to obtain azide functionalized PDMS as a yellowish oil [233].

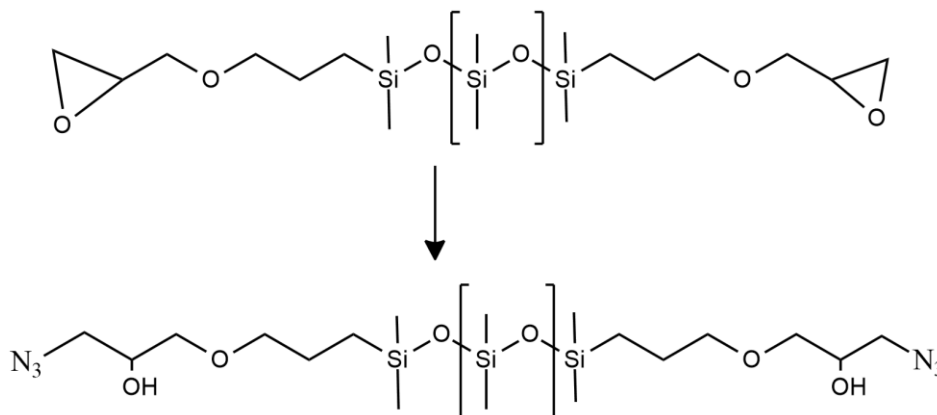


Figure 3.7 Scheme of azide functionalized PDMS

3.7 SYNTHESIS OF ALKYNE FUNCTIONALIZED PDMS

The synthesis was carried out under a dry atmosphere of nitrogen. A three-necked round bottom flask equipped with mechanical stirrer, reflux condenser and an silicon rubber septum was heated under vacuum and flushed with nitrogen several times [233]. Hydroxyl terminated PDMS ($M_n=550$) (DP~9 ,0.4 mmol, 220.0 mg), sodium hydroxide (6.0 eq, 2.4 mmol, 96 mg) and Tetrabutylammonium bromide (TBAB) (0.04 eq, 0.01 mmol, 51 mg) were dissolved in distilled water (1.0 mL). Later on, propargyl bromide (6.0 eq, 2.4 mmol, 280 mg, 80.0-wt % solution in toluene) was added dropwise over a period of one hour and then the

temperature was increased to 60 °C and the reaction mixture was heated for 41 h at 60 °C. After the reaction has finished (TLC control, Chloroform (CHCl₃) the reaction, mixture was cooled down to room temperature. Afterwards, the solution was diluted with Dichloromethane (DCM) (150.0 mL) and centrifuged (three times, 10 °C, 5000 rpm, and 5 min) to separate the formed salt. The combined organic phases were extracted with distilled water (five times, 500.0 mL) and dried over Na₂SO₄. After filtration, the solvent was removed in vacuo and the crude product was purified by column chromatography (SiO₂, 230–400 mesh, Merck (Darmstadt, Germany), CHCl₃, R_f = 0.62, blue stain) to obtain alkyne functionalized PDMS as a light-yellow liquid in a yield of 75%.

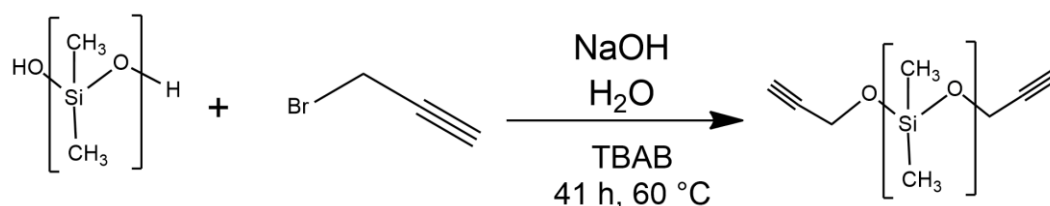


Figure 3.8 Scheme of alkyne functionalized PDMS

3.8 TESTING OF CATALYTIC ACTIVITY

The catalytic activity of the NTRGO/Cu and TRGO/Cu was investigated via a click model reaction between phenyl acetylene and benzyl azide (Table 3.2). In a 10ml flask, phenyl acetylene (0.0826 mmol, 1.1eq), benzyl azide (0.0751 mmol) and NTRGO/Cu(I) were added in 1.5 ml of THF. Using freeze-thaw cycle (2 times) the reaction mixture was degassed. The obtained mixture was bath sonicated for better dispersion of catalyst and allowed to stir for 55 h at 40 °C. Afterwards, the obtained reaction mixture was filtered and washed with 30 ml THF. The solvent was evaporated at reduced pressure (minimal of 200 mbar applied to avoid flashing of starting materials). Then the mixture was allowed to dry at high vacuum for 30 min and recovered catalyst is used for the next cycle.

A 100% reaction yield was achieved for the NTRGO/Cu(I) catalyst with only 2 mol% catalyst loading in THF, whereas with a similar amount of loading only 70% conversion was obtained for the TRGO/Cu(I) catalyst after 48 h at room

temperature. As a reference, the click reaction was also performed in the presence of commercially available copper catalyst Cu₂O powder and Cu on charcoal (Cu/C), and in that case only very little conversion was observed (Table 3.2).

As shown in Table 3.2, compared to TRGO/Cu(I) a higher reaction rate was observed for NRGO/Cu(I) (after 12 h; Table 3.2, 17% and 3 % for NRGO/Cu(I) and TRGO/Cu(I), respectively). The initially observed higher efficiency for NRGO/Cu(I) may be attributed to the formation of coordination of N-doped rGO with Cu⁺ ions,⁴⁰ including a high binding energy of the Cu nanoparticles to N-doping carbon support. The N-doping is also helpful to reduce the surface energy as well as generates the active sites, obliging to enhance the catalytic performance. Surprisingly, 70% and 100% reaction yield was obtained after 48 h for TRGO/Cu(I) and NRGO/Cu(I), respectively. The enhancement in catalytic activity with time could be due to formation of N-ligands (triazole) as a source of autocatalysis, as discussed earlier.

Table 3.2 Performance of different Cu-catalysts: phenyl acetylene and benzylazide in THF at room temperature

Entry	Conditions	Yield (%)
1	Cu ₂ O (2 mol%) in THF, 48 h, r.t.	0
2	Copper on charcoal (2 mol%), in THF, 48 h, r.t.	0
3	TRGO without copper, in THF, 48h, r.t.	0
4	TRGO/Cu (I) (2 mol%), in THF, 12h, r.t.	3
5	TRGO/Cu (I) (2 mol%), in THF, 48h, r.t.	70
6	NRGO/Cu (I) (2 mol%), in THF, 12h, r.t.	17
7	NRGO/Cu (I) (2 mol%), in THF, 48h, r.t.	100

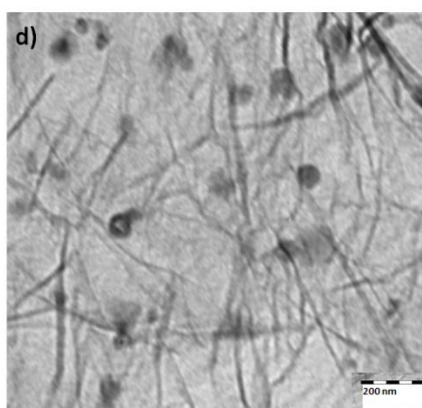
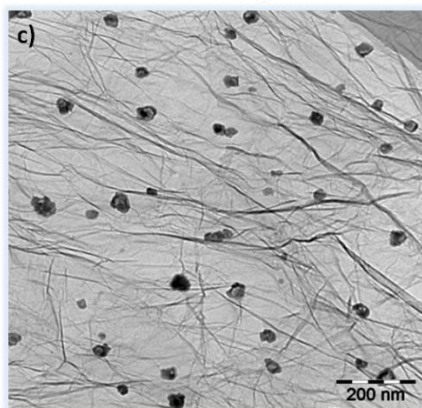
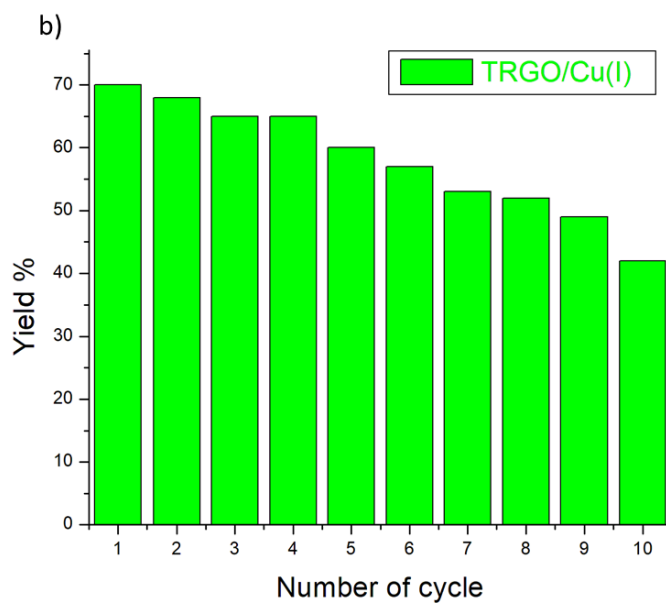
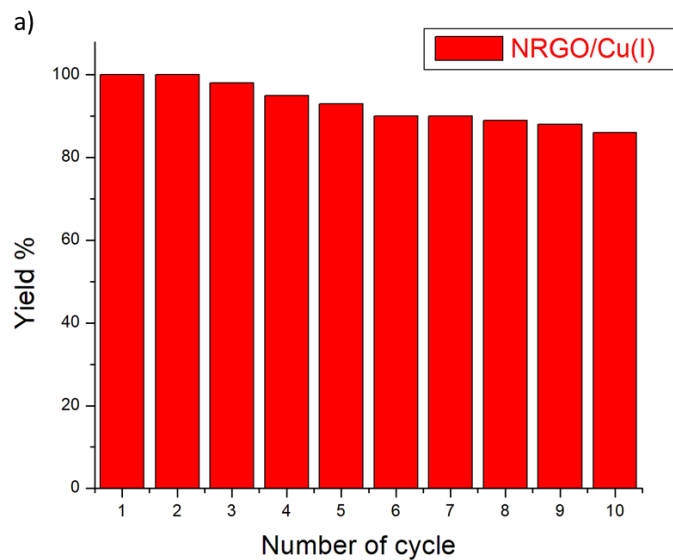


Figure 3.9 (a,b) catalyst recycling within ten reaction cycles for NRGO/Cu(I) and TRGO/Cu(I), respectively. (c,d) TEM image of Cu particles after 10 cycles for NRGO/Cu(I) and TRGO/Cu(I), respectively

The recyclability and reusability testing for the synthesized catalyst (NRGO-Cu(I)) was carried out using the azide/alkyne ‘click’ model reaction under the optimized conditions. The NRGO-Cu(I) catalyst was reused ten times without any noticeable change in its catalytic activity, whereas washing and recyclability of catalyst was performed under open air environment. However, almost 40% reduction was observed for the nitrogen free TRGO-Cu(I) catalyst. TEM images were observed to check the morphology of the recycled catalyst (Figure 3.9).

An unchanged morphology of NRGO-Cu(I) was observed after 10 cycles (Figure 3.9c), whereas agglomeration of Cu particles was observed for TRGO-Cu(I) (Figure 3.8d), which might be the key factor for the reduction of catalytic activity for the synthesized catalyst (TRGO/Cu(I)). Again, the high binding energy of Cu particles to N-doping graphene might be the reason to prevent the agglomeration of copper nanoparticles for nitrogen doped graphene oxide sheets. Metal leaching for reaction product (after 5, and 10 cycles) was studied by FAAS measurements including hot filtration; however, the detectable amount of copper was too low for accurate detection.

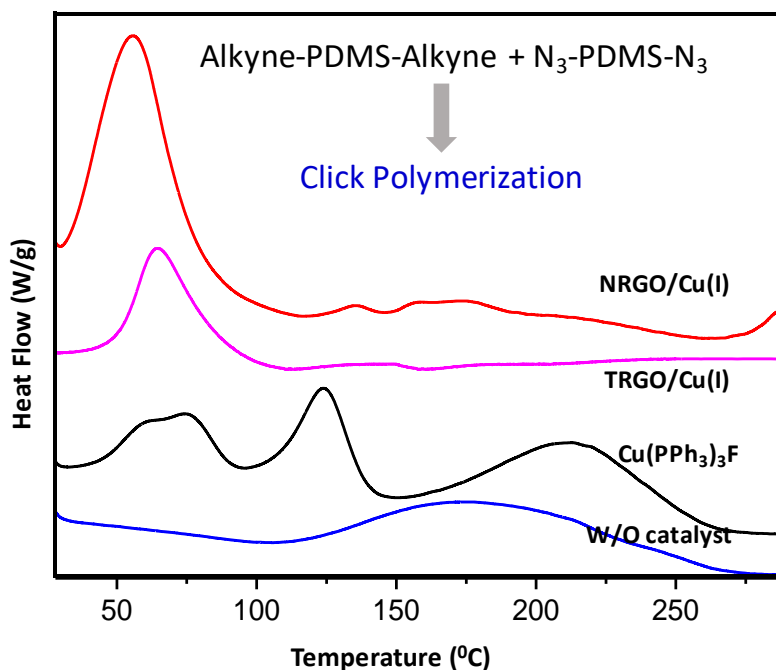


Figure 3.10 DSC measurements for the bulk ‘click’ reaction with different catalysts at 5 °C/min heating rate

To evaluate the performance of synthesized catalysts, bulk ‘click chemistry’ was also evaluated by differential scanning calorimetry (DSC) (Figure 3.10). For the formation of a covalent network, sufficient molecular mobility is required. In order to keep diffusion high, PDMS based liquid components (bivalent azide and alkyne with high mobility; low molecular weights) were prepared. DSC thermograms at 5 °C/min for different catalysts are plotted in Figure 4.9 (1 mol% of catalyst per functional group). Thermal ‘click’ crosslinking (W/O catalyst) happened at a high temperature with a T_{onset} at 110 °C and a T_p at 173 °C, whereas, a lower T_{onset} (at 45 °C) was observed for homogeneous commercial catalyst ($\text{Cu}(\text{PPh}_3)_3\text{F}$). However, crosslinking reaction was not completed at a certain temperature, which might be related to the inhomogeneous dispersion of catalyst in PDMS matrix. The TRGO/Cu(I) catalyst reduced the reaction temperatures to 50 °C (T_{onset}) and 65 °C (T_p), respectively, whereas, a room temperature T_{onset} and 59 °C (T_p) was observed for NRGO/Cu(I) catalyst. The DSC data again confirms the better catalytic activity of NRGO/Cu(I) catalyst.

3.9 DENSITY FUNCTIONAL THEORY (DFT) ANALYSIS

To definitive, the effect of N-doping on the ‘click’ reaction has also been verified through Density Functional Theory (DFT) based calculations. DFT [234], [235] investigations have been performed using Synopsis Atomistix Toolkit (ATK) virtual nanolab (VNL) [236] for understanding the interaction of Cu^+ ion with the pristine as well as NRGO at one hand and on other hand also to observe the impact of size of Cu^+ ion cluster on the NGRO for CuAAC reaction. The 5x5 optimized graphene has been investigated for copper ion (Cu^+) adsorption on three different sites bridge (B), at top of carbon atom (C), and hollow (H). The computed adsorption energies are -8.545eV, -8.537eV, and -8.427 eV for B, C and H site respectively which inferred that bridge site is energetically most favorable adsorption site at graphene sheet (Figure. 3.11(a,b), Appendix 1). It has been observed that on interaction with Cu^+ ion, fermi level shifts into conduction band (Figure 3.11 c) and peaks appeared at the fermi level in TDOS profile (Appendix

2) which inferred that Cu^+ ion adsorbed sheet is electron rich and may act as a catalyst in CuAAC reaction as reported in earlier studies, [237] whereas, Cu^+ ion is adsorbed on NRGO with adsorption energy -8.77 eV which infer strong interaction between NRGO and Cu^+ ions (Figure 3.11 b), validates our experimental studies. On adsorption of Cu^+ ion, a bond of bond length 2\AA has been formed between carbon and ion.

The analysis found that by doping with nitrogen, Fermi level shifts into the conduction band which is in good agreement with earlier studies [234] and on adsorption of Cu^+ ion indirect band gap of ~ 0.29 eV has been introduced (Figure 3.10 d; Appendix 3). In order to understand the high reaction rate that obtained experimentally Mulliken charge population has been calculated, infer that the charge transfer of 0.073 e takes place on N after adsorption of Cu^+ ion and that could be one reason for high reaction rate.

Further studies have been extended to understand the interaction of cluster containing 3 Cu^+ ions (CU-3) and 5 Cu^+ ions (CU-5) (Figure 3.11 e,f). On adsorption of CU-3, cluster shows physisorption with adsorption energy -31.07 eV and binding distance 2.76 Å while for adsorption of CU-5, shows physisorption with adsorption energy and binding distance -59.31 eV and 2.79 Å respectively. Further, the band structure and density of states have also been explored in Appendix 4. It has been found that the band gap has reduced on increasing the size of the cluster given in Table 3.3. Similar results have been observed from density of state profile of the system as well. Mulliken population has been calculated to understand the reaction rate for CU-3 and CU-5, and it is found that 0.156 e and 0.094 e charge has been transferred on nitrogen respectively shows high reaction rates.

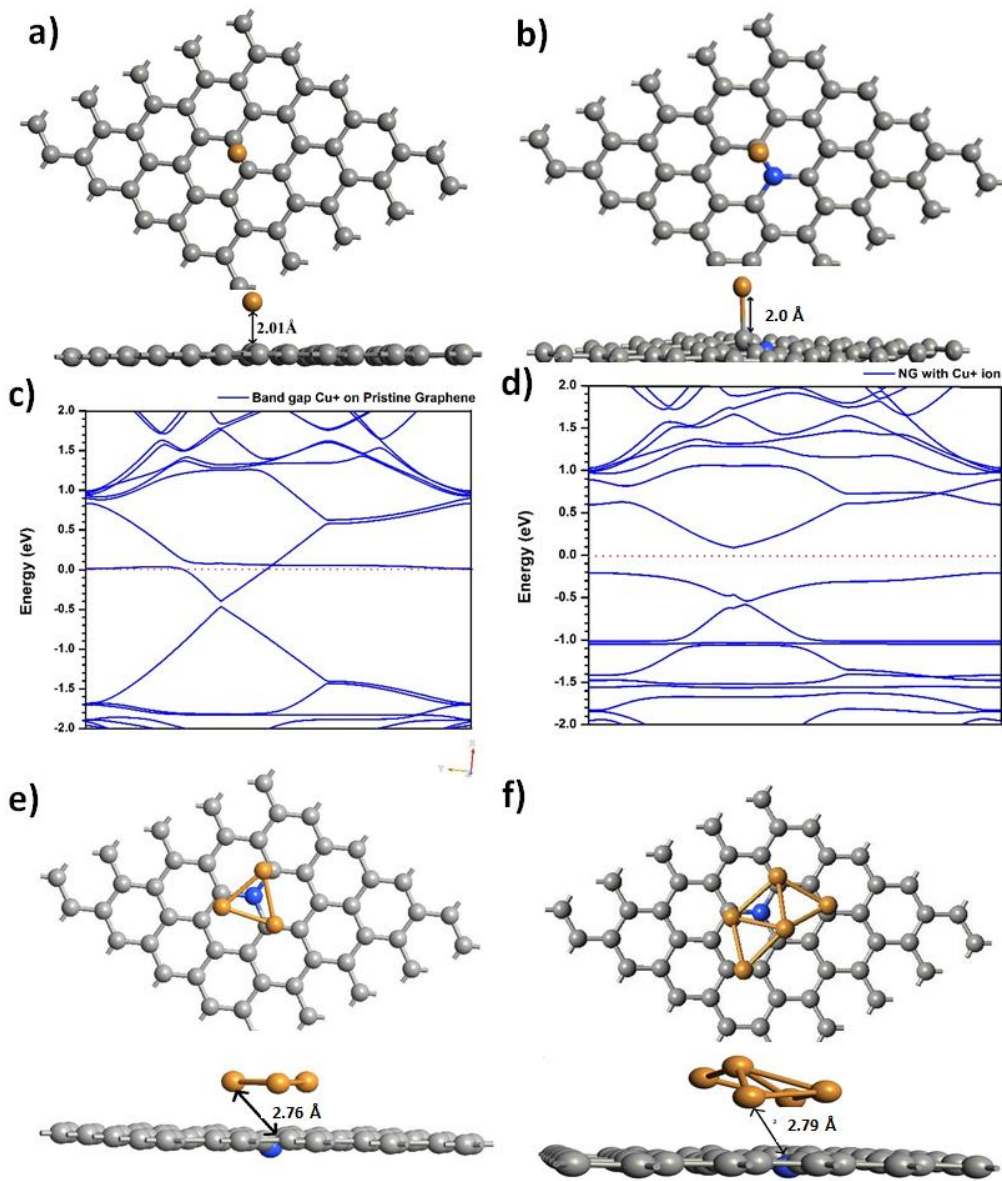


Figure 3.11 (a, b) Cu^+ adsorption on TRGO and NRGO, respectively. (c, d) Band structure of Cu^+ adsorption on TRGO and NRGO, respectively. (e, f) NRGO with a cluster of 3 and 5 Cu^+ ions, respectively.

Table 3.3 Comparison of band gap with increasing size of Cu^+ ion cluster

System	Band Gap (eV)
NG with Cu^+ ion	0.29
NG with CU-3	0.28
NG with CU-5	0.17

3.10 SUMMARY

In this chapter, we have developed highly stable and recyclable heterogeneous catalyst (NRGO/Cu(I)), performs 'click' reaction (designed for the development of self-healing nanocomposites) under both solvent and bulk conditions. Due to increase in electron density on the nitrogen atom doping including the formation of coordination of N-doped rGO with Cu^+ ions, nitrogen doped graphene supported copper particles demonstrate a higher reaction yield at room temperature without adding any external ligand/base. The incorporation of graphene based catalyst can also be advantageous to enhance the physical, mechanical and conductive properties of the cross-linked materials.

CHAPTER 4: DEVELOPMENT OF SELF-HEALING NANOCOMPOSITES

4.1 INTRODUCTION

Material fatigue is one of the most challenging issue, although there are several strategies to improve fatigue strength by the use of nano-fillers or else by introducing self-healing in materials[238]. The material fatigue strength can be increased even with self-healing mechanism like embedding of nano capsules containing healing agents into the material matrix [27]. The healing agent contained in capsules undergo crosslinking in the presence of catalyst when the capsule gets rupture due to loading conditions. The capsule based self-healing witnessed 100% restoration of mechanical properties. Moreover, the addition of nano capsules in matrix reduces the material performance especially the tensile strength[239]. Carbon based nano materials as nano-fillers such as carbon black, CNT and graphene show better in mechanical properties when incorporated in polymeric matrix [240]. Graphene among the nano-fillers has a large effect in performance of a material by enhancing conductive and mechanical properties including strength and toughness even with small addition of nano-filler [241].

In this chapter, we discuss the development of capsule based self-healing materials. Graphene is used as a nano-filler to counter balance the decrease in tensile strength by the addition also graphene can serve as a catalyst to trigger the self-healing mechanism. The chemistry involved behind the self-healing is “click” based chemistry [242], which is prominently used methodology for efficient crosslinking even at ambient conditions. The following sections describe the development of capsules based self-healing using the ‘click’ reactions *via* NRGO/Cu(I) acts as reinforcement agent to compensate the reduced tensile strength by embedding the capsules in material and catalytic activity for self-healing. The capsules contains the trivalent azide and alkyne as healing/crosslinking agents used for healing after the occurrence of rupture on the surface of capsules leading to the ‘click’ reaction in presence of Cu₂O on the

graphene surface. The healing agents encapsulated using in-situ condensation process and the stability of healing agents inside the capsules observed for several months. Moreover, the copper particles with the graphene believes in enhancing the catalytic dispersion and mechanical properties by graphene reinforcement [243].

4.2 PREPARATION OF SELF-HEALING AGENTS

4.2.1 PREPARATION OF TRIVALENT ALKYNE MOIETY

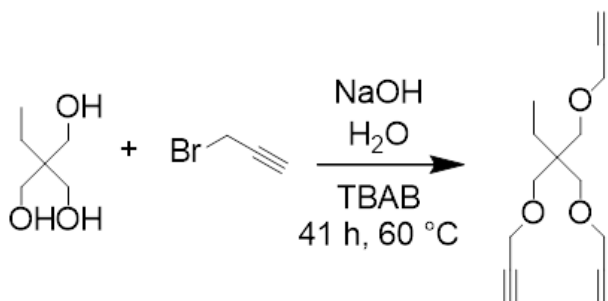


Figure 4.1 Synthesis of trimethylolpropane tripropargyl ether (TMPTPE)

The synthesis of trimethylolpropane tripropargyl ether (TMPTPE) was done according to literature [244] with slight modifications. The synthesis was carried out under a dry atmosphere of nitrogen. A three-necked round bottom flask equipped with mechanical stirrer, reflux condenser and rubber septum was heated under vacuum and flushed several times with nitrogen. Trimethylol propane (149.1 mmol, 20.0 g), sodium hydroxide (6.0 eq, 894.4 mmol, 35.8 g) and Tetra-N-Butylammonium Bromide (TBAB) (0.04 eq, 7.0 mmol, 2.4 g) were dissolved in distilled water (4.0 mL). Afterwards, propargyl bromide (6.0 eq, 894.4 mmol, 85.4 mL, 134.1 g, 80.0 wt % solution in toluene) was added dropwise over a period of one hour and then the temperature was increased to 60 °C and the reaction mixture was heated for 41 h at 60 °C. On completion of reaction (TLC control, CHCl₃, R_f = 0.85, blue stain) the reaction mixture was cooled down to room temperature. Thereafter, the solution was diluted with DCM (150.0 mL) and centrifuged (three times, 10 °C, 5000 rpm, 5 min) to separate the formed salt. The combined organic phases were extracted with distilled water (five times, 500.0 mL) and dried over Na₂SO₄. After filtration, the solvent was removed in vacuum and the crude product

was purified by column chromatography (SiO₂, 230–400 mesh, Merck (Darmstadt, Germany), to obtain trivalent alkyne as a light-yellow liquid in a yield of 75%.

4.2.2 PREPARATION OF TRIVALENT AZIDE MOIETY

The preparation of trivalent azide compound is made according to the literature with slight modifications[245]. The procedure opted for preparation is by, 2,4- pyridinedicarboxylic acid monohydrate (10.9 mmol, 2.0 g) was suspended in methanol (12.0 mL) and subsequently concentrated sulfuric acid (12.0 mmol, 640 μ L) was added. The solution was refluxed for 48 h and then allowed to cool down to room temperature. The mixture was treated with saturated aqueous sodium bicarbonate solution until it was neutral (pH = 7). The solvent was removed under reduced pressure, after which the residue was dissolved in chloroform (30.0 mL). The obtained solution was filtered and the organic layer was washed with a saturated solution of sodium chloride for several times until the water layer was neutral (pH = 7). The organic layer was dried over magnesium sulfate and concentrated under reduced pressure to provide 2,4-pyridinedicarboxylic acid dimethyl ester. ¹H-NMR (CDCl₃, 400 MHz): δ = 8.90 (dd, 1H, 3JH,H = 4.9 Hz, 5JH,H = 0.6 Hz, CH), 8.65 (dd, 1H, 4JH,H = 1.5 Hz, 5JH,H = 0.8 Hz, CH), 8.03 (dd, 1H, 3JH,H = 4.9 Hz, 4JH,H = 1.6 Hz, CH), 4.03 (s, 3H, CH₃), 3.98 (s, 3H, CH₃) ppm; ¹³C-NMR (CDCl₃, 100 MHz): δ = 165.1, 164.8, 150.8, 149.1, 138.8, 126.4, 124.4, 53.2, 53.0 ppm.

In second step, 2,5-Pyridinedicarboxylic acid dimethyl ester (3.8 mmol, 750 mg) and ultra-dry calcium chloride (99.99%, 17.1 mmol, 1.9 g) were dissolved in anhydrous tetrahydrofuran (6.0 mL) and anhydrous methanol (12.0 mL). The solution was cooled to -5 °C and subsequently sodium borohydride was added in small portions (5.6 mmol, 225 mg, (3 \times 75 mg)). The reaction was accomplished after ~2 h 40 minutes and quenched with ice-cold water (15.0 mL). The solution was extracted with chloroform (3 \times 40.0 mL) and the combined organic layers were dried over magnesium sulfate. The solvent was removed under reduced pressure to afford 2-(6-hydroxymethyl)-pyridine- 5-carboxylic acid methyl ester. ¹H-NMR (CDCl₃, 400 MHz): δ = 8.70 (d, 1H, 3JH,H = 5.1 Hz, CH), 7.83 (s, 1H, CH), 7.75

(dd, 1H, 3JH,H = 5.1 Hz, 4JH,H = 0.7 Hz, CH), 4.83 (s, 2H, CH₂), 3.96 (s, 3H, CH₃) ppm; ¹³C-NMR (CDCl₃, 100 MHz): δ = 165.5, 160.4, 149.4, 138.1, 121.6, 119.8, 64.2, 52.7 ppm.

2-(6-Hydroxymethyl)-pyridine-5-carboxylic acid methyl ester (0.3 mmol, 50 mg) was dissolved in anhydrous dichloro-methane (6.6 mL), followed by the addition of N,N,N-triethyl-amine (1.5 mmol, 207 μL) and para-toluenesulfonyl chloride (0.5 mmol, 87 mg). After stirring for 2h the solvent was removed under reduced pressure. The residue was dissolved in anhydrous tetrahydrofuran (3.3 mL) and sodium azide (3.0 mmol, 193 mg) was added. The reaction was stirred for a further 24 h at room temperature, later on it was diluted with ethyl acetate (30.0 mL) and water (30.0 mL). After extraction of the aqueous layer with ethyl acetate (three times 30.0 mL), the combined organic layers were washed with a saturated solution of sodium chloride and dried over magnesium sulphate. The crude product was purified by silica chromatography (n-Hex : EtOAc, 4 : 1), providing 2-(6-azidomethyl)-pyridine-5-carboxylic acid methyl ester. ¹H-NMR (CDCl₃, 400 MHz): δ = 8.74 (d, 1H, 3JH,H = 5.0 Hz, CH), 7.89 (s, 1H, CH), 7.79 (dd, 1H, 3JH,H = 5.0 Hz, 4JH,H = 1.4 Hz, CH), 4.56 (s, 2H, CH₂), 3.96 (s, 3H, CH₃) ppm; ¹³C-NMR (CDCl₃, 100 MHz): δ = 165.3, 157.0, 150.5, 138.4, 122.1, 121.1, 55.4, 52.8 ppm.

2-(6-Azidomethyl)-pyridine-5-carboxylic acid methyl ester (2.6 mmol, 500 mg) was dissolved in methanol (10.0 mL), followed by the addition of a 1.0 M aqueous solution of lithium hydroxide (7.8 mmol, 7.8 mL). The reaction was stirred for 25 minutes at room temperature. Neutralization was achieved with the addition of a 1.0 M solution of hydrogen chloride. The solvent was removed under reduced pressure and the product was dried under high vacuum until constant weight is obtained 2-(6-azidomethyl)-pyridine-5-carboxylic acid. ¹H-NMR (DMSO-d₆, 400 MHz): δ = 8.99 (s, 1H, CH), 8.18 (dd, 1H, 3JH,H = 7.9 Hz, 4JH,H = 2.0 Hz, CH), 7.34 (d, 1H, 3JH,H = 7.9 Hz, CH), 4.49 (s, 2H, CH₂) ppm; ¹³C-NMR (DMSO-d₆, 100 MHz): δ = 167.6, 156.0, 151.0, 137.9, 134.7, 121.7, 54.8 ppm.

2-(6-Azidomethyl)-pyridine-5-carboxylic acid (674 μmol , 120 mg, 11.6 equiv.), N,N-dimethylpyridin-4-amine (88 μmol , 14 mg, 1.5 equiv.) and finally N,N'-methanediylidenedicyclohexanamine (263 μmol , 50 mg, 4.5 equiv.) were dissolved in anhydrous dichloromethane (5.0 mL) with 2-ethyl-2-(hydroxymethyl)propane-1,3-diol (58 μmol , 350 mg, 1 equiv.). The reaction was allowed at room temperature for 24h by stirring and then solution was diluted with dichloromethane (30.0 mL) and filtered. The organic layer was washed with a saturated solution of ammonium chloride and dried over sodium sulfate. The solvent was evaporated under reduced pressure to afford the crude product, which was purified by dissolving in n-hexane and precipitated with an excess of methanol. ($M_n(\text{GPC}) = 5780 \text{ g mol}^{-1}$, $M_w/M_n = 1.3$). $^1\text{H-NMR}$ (CDCl_3 , 400 MHz): $\delta = 9.20$ (s, 3H, CH), 8.34 (dd, 3H, 3JH,H = 8.1 Hz, 4JH,H = 2.1 Hz, CH), 7.46 (d, 3H, 3JH,H = 8.1 Hz, CH), 7.14 (s, 3H, CH of initiator), 4.58 (s, 6H, CH₂), 4.34 (t, 6H, 3JH,H = 6.7 Hz, CH₂), 1.86 (s, 6H, CH₂), 1.43 (s, CH₂ of repetitive unit), 1.12 (s, CH₃ of repetitive unit), 0.81 (s, 18H, CH₃ of initiator) ppm.

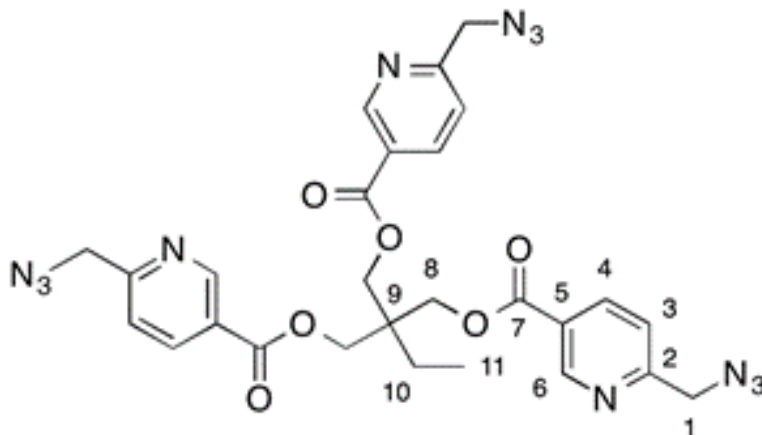


Figure 4.2 Structure of 2-(((6-(azidomethyl)nicotinoyl)oxy)methyl)-2-(hydroxymethyl)propane-1,3-diyl bis(6-(azidomethyl)nicotinate)

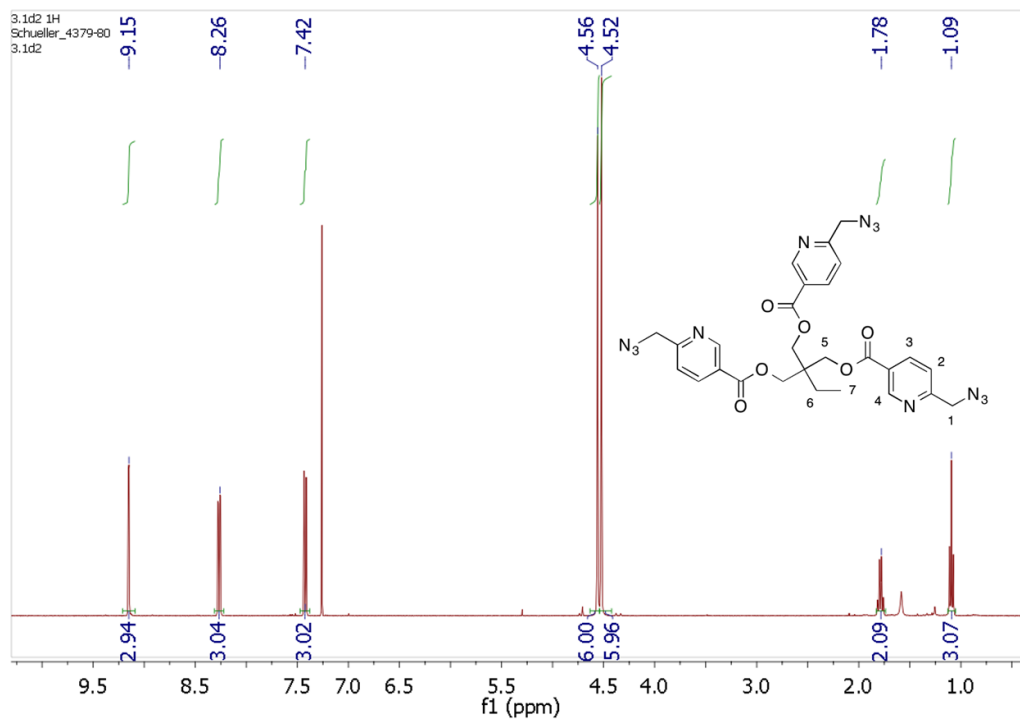


Figure 4.3 ^1H NMR for 2-(((6-(azidomethyl)nicotinoyl)oxy)methyl)-2-(hydroxymethyl)propane-1,3-diyl bis(6-(azidomethyl)nicotinate)

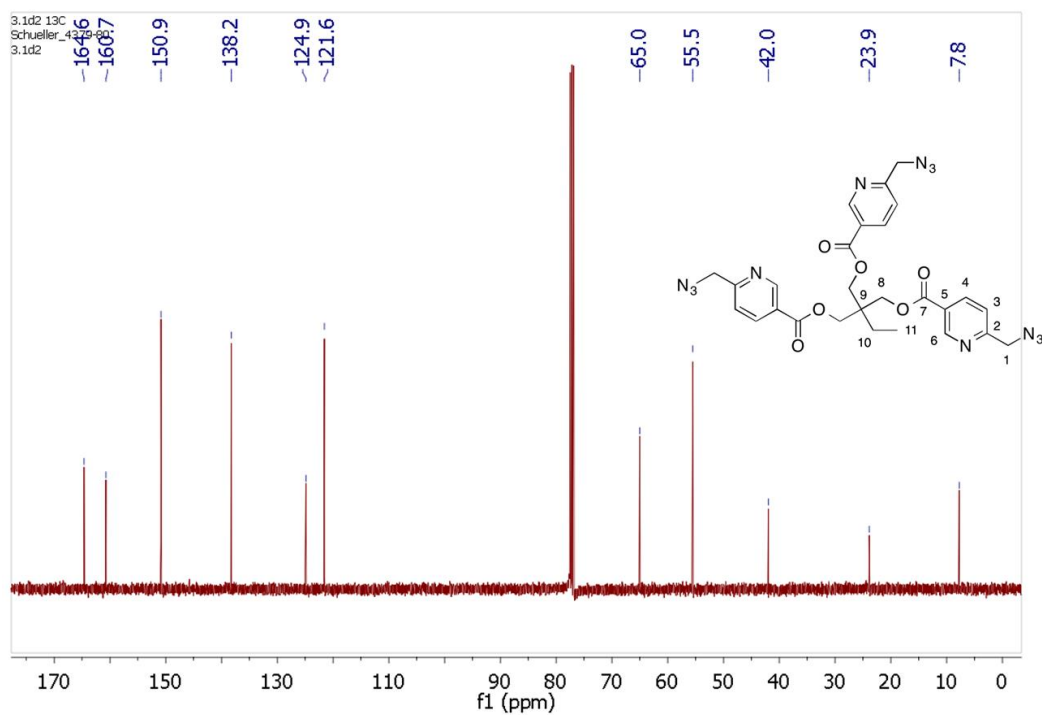


Figure 4.4 ^{13}C NMR for 2-(((6-(azidomethyl)nicotinoyl)oxy)methyl)-2-(hydroxymethyl)propane-1,3-diyl bis(6-(azidomethyl)nicotinate)

4.2 FABRICATION OF ENCAPSULATION

The preparation of encapsulation procedure was adopted as per the literature [246] with slight modifications. The preparation of capsules procedure as follows:

4.2.1 PREPARATION OF PRE-POLYMER SOLUTION

A solution of 37% formaldehyde (0.1 mol) and urea (0.05 mol) were mixed with 20mL distilled water in a 250 mL three-necked round bottom flask fitted with a magnetic stirring bar and reflux condenser. The reaction mixture pH was adjusted to ~8 by the addition of trimethylamine in dropwise manner. The obtained mixture was allowed to heat at 70 °C for 1h by continuous stirring. The reaction was stopped only after checking the formation of turbidity in reaction mixture. The turbidity of the reaction mixture was monitored by adding a drop of mixture to the water.

4.2.2 PREPARATION OF EMULSION

A reaction mixture of 0.8 g sodium dodecyl benzene sulphonate (SDBS) is mixed with distilled water (70 mL) was prepared and 1% (W/V) PVA of 10 mL was added to the mixture. Subsequently, 8mL of trimethylolpropane tripropargyl ether (TMPTE) (Figure 4.1) was added slowly to the prepared solution for 30 minutes in dropwise manner. Further, the solution is allowed to stir at a rate of 1200 rpm for 1 h to get stable oil in water emulsion.

4.2.3 PREPARATION OF MICROCAPSULES

The stirring rate of above prepared emulsion reduced to 500rpm, further the pre-polymer solution was slowly added to it. The temperature was increased to 70 °C from room temperature and concurrently pH was lowered down to ~4 in a span of three steps for every 15 minutes. The pH adjustments was performed by using 1% formic acid. After achieving the final pH the stirring process is continued for additional 1hr. Lastly, the reaction mixture allowed to cool down slowly to room temperature and further the obtained slurry was neutralized by the addition of 10% NaHCO₃ solution. Therefore, the formed microcapsules were washed many times with water and acetone and finally the washed microcapsules undergo filtration and

air-drying methods. The prepared microcapsules were observed using SEM image (Figure 4.5). The average microcapsule size is around 20 μ m which was observed from SEM images.

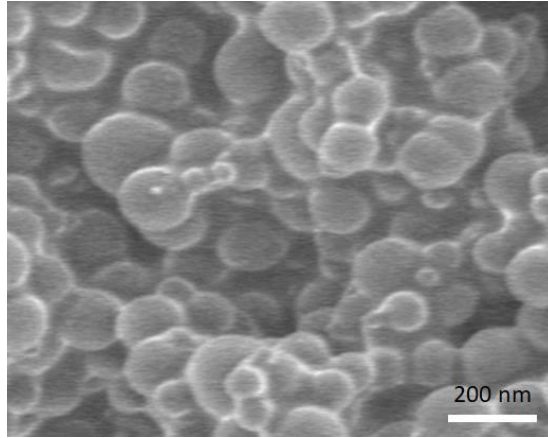


Figure 4.5 FE-SEM image for the synthesized capsules containing healing agent

4.3 COMPOSITE PREPARATION

The preparation of epoxy based self-healing nanocomposite was adopted according to literature [27]. Initially, diglycidylether of bisphenol A (DGEBA) is well known as EPON 828 epoxy resin of 500 mg was taken into the flask and the solution was mixed manually for almost 15 min and thereafter the entrapped air was removed using degassing technique. The calculated amount of nano capsules containing trivalent alkyne components of 5-20wt% in total (azide +alkyne) were taken into consideration for preparing the samples. The calculated amount of nano-capsules were then manually introduced into the mixture, followed by mixing using a vortex and a bath sonicator for 15 min. Subsequently the azide component introduced into the mixture and allowed to mix until it gets finely dispersed in matrix. Later on the required amount of NRGO/Cu(I) catalysts (5 mol% per functional group of azide/alkyne) were mixed into the resin followed by addition of diethylenetriamine (DETA) (12 pph) was manually mixed together for 10 min. The final mixture was poured into a silicon mold of standard size (30 \times 5 \times 2 mm) and allowed specimens to cure at room temperature for 24 h (Figure 4.6(b)).

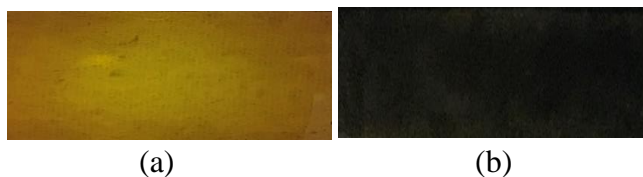


Figure 4.6 (a) Pure Epoxy and (b) Epoxy composite

Further, we have fabricated different specimens with different loading of capsules (5wt%, 10wt%, 15wt% and 20wt %) and catalysts ((CuPPH₃)₃F, TRGO/Cu(I) and NRG0/Cu(I)). The dispersion of capsules in the epoxy matrix was further investigated with the help of SEM (Figure 4.7) which clearly states the agglomeration of microrcapsules with the addition of capsules.

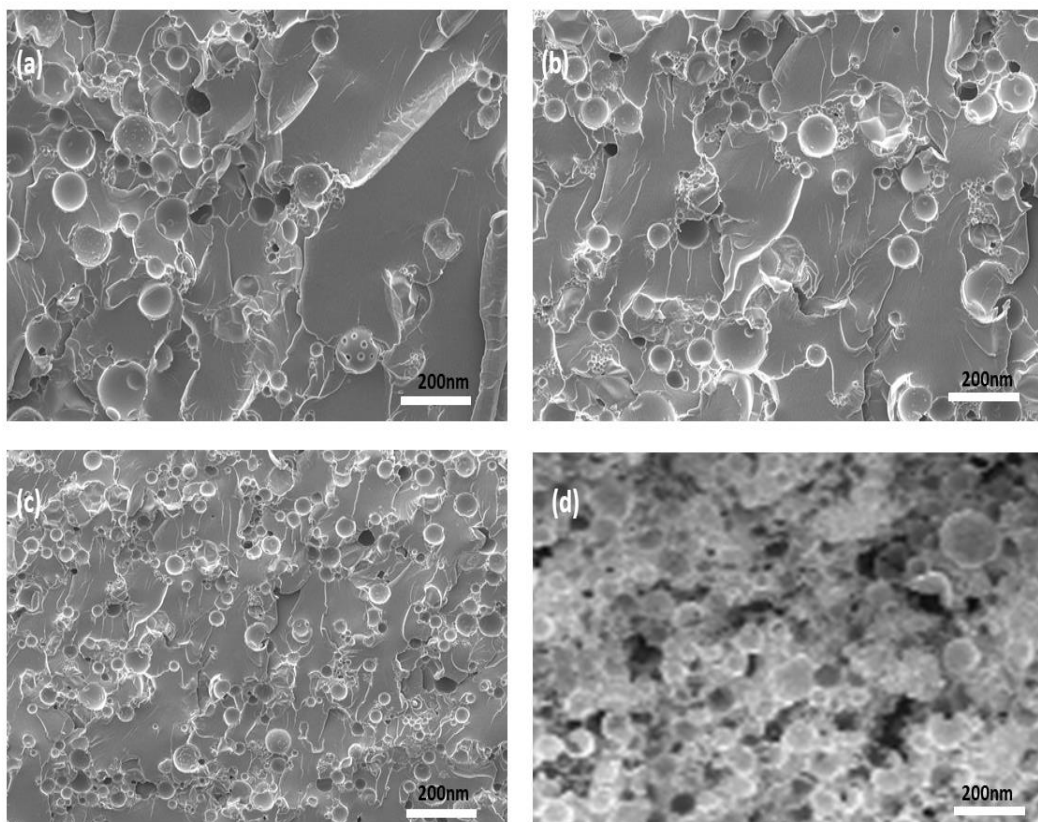


Figure 4.7 SEM image of capsules with a) 5wt%, b) 10wt%, c) 15wt% and d) 20wt%.

4.4 RESULTS AND DISCUSSION

We have fabricated self-healing nanocomposite systems, where alkyne (Figure 4.1) was encapsulated and azide (Figure 4.2) was directly dispersed in epoxy matrix during the preparation (Figure 4.8). To enhance the catalytic activity

of copper and mechanical properties of the specimen the nitrogen doped copper immobilized reduced graphene oxide (NRGO/Cu(I)) was also synthesized. TEM and XPS analysis of the prepared catalyst confirms the presence of nitrogen and copper in the form of Cu(I), require for the “click” reactions.

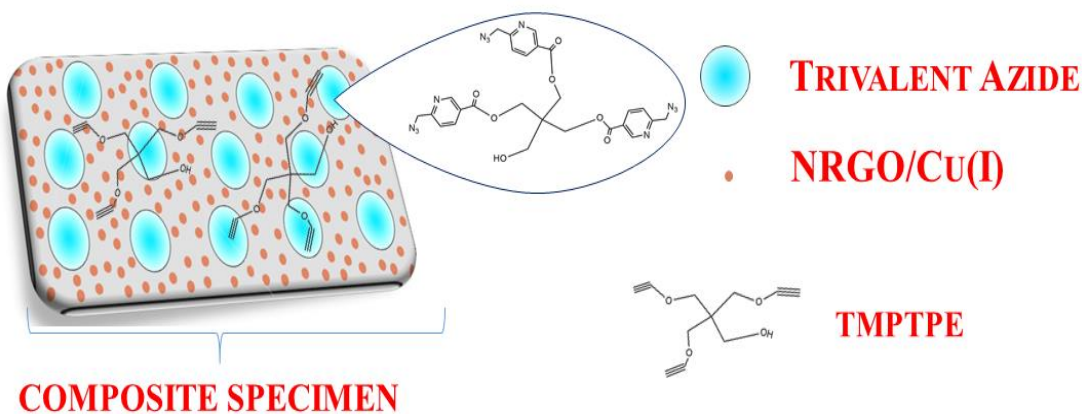


Figure 4.8 Presence of healing agents and catalyst in epoxy matrix

Further, to analyze the ‘click’-based reaction for the formation of polymer network and to confirm the activity of catalyst in the epoxy matrix, Differential Scanning Calorimetry (DSC) was performed for the azide and alkyne components in the presence of catalyst. DSC thermograms at 5 °C /min with and without catalyst is plotted in Figure 4.9 (1 mol% of catalyst per functional group). The obtained results from the DSC confirms that, thermal ‘click’ crosslinking (W/O catalyst) happened at a high temperature with a T_{onset} at 110 °C and a T_p at 173 °C, whereas, a lower T_{onset} (at around 40 °C) was observed for NRGO/Cu(I) catalyst. Moreover, the azide and alkyne components in the epoxy matrix were stable even after several weeks, which confirms the stability of healing agents in the epoxy matrix for life long applications.

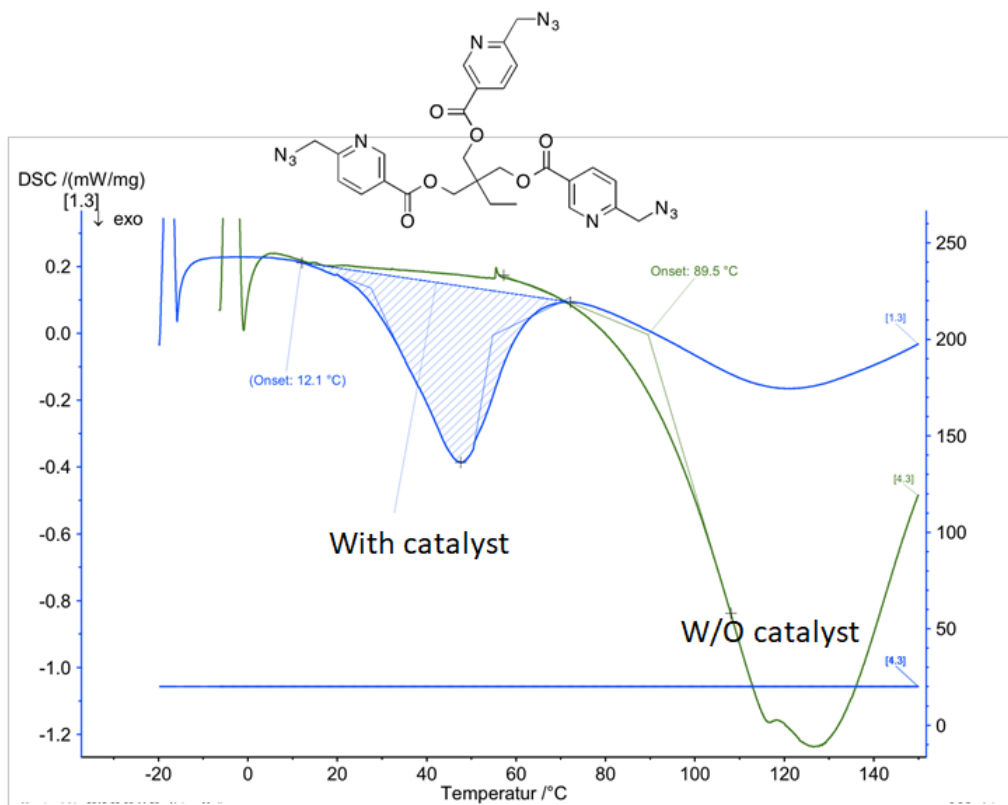


Figure 4.9 'click' reactions measured by DSC at 5 °C/min heating rate

Striving by these results, we further investigated the polymer network formation using 'click chemistry' by crosslinking the azide and alkyne components in the presence of catalysts like homogenous and heterogeneous catalyst. The SEM images confirm uniform dispersion of capsules in epoxy matrix and able to identify the average size of capsule (~200nm) (Figure 4.3 and 4.5). Moreover, it indicates that the stability and presence of healing agents in capsules during the fabrication and during the curing of polymer while crosslinking. However, the agglomeration of capsules was observed for the composites containing more than 15wt% capsules. Thus, to investigate the mechanical and self-healing performance, 15wt% concentration of capsules containing healing agents and homogenous and heterogeneous catalyst was considered.

4.4.1 TENSILE TEST

The prepared samples were undergone through tensile testing to obtain the mechanical properties. The prepared samples are as follows neat epoxy, Epoxy

+5wt% capsules, Epoxy +10wt% capsules, Epoxy +15wt% capsules, Epoxy +20wt% capsules, Epoxy +15wt% capsules+ Cu(PPh₃)₃F, Epoxy +TRGO/Cu(I), Epoxy+15wt% capsules +TRGO/Cu(I), Epoxy +NRGO/Cu(I) and Epoxy+15wt% capsules +NRGO/Cu(I) (the composite specimens containing the catalyst are prepared with 2 mol% concentration per functional group). The samples were prepared using silicon mold with a dimension of 35 x 5 x 2mm and measurements were carried out using the tension mode *via* dynamic mechanical analysis (DMA). From the Figure 4.10 and Table 4.1 it shows, the decrease in Young's modulus and tensile strength of specimen containing the Cu(PPh₃)₃F after addition of capsules. Which is very common drawback for capsule based self-healing systems (the loading of capsules behaves as void in the epoxy matrix, thus lower the tensile strength of the prepared composite specimens) [239], [247]. Interestingly and as expected there is an increase in Young's modulus and tensile strength for NRGO/Cu(I) and TRGO/Cu(I) was observed (Figure 4.10 and Table 4.1). Therefore, the immobilization of TRGO/Cu(I) and NRGO/Cu(I) to specimen increases strain at break point and Young's modulus of specimen as well. This is due to the effective load transfer between the GO and epoxy *via* interfacial adhesion based on earlier reports [248], where the unique feature of GO contribute towards the enhanced in dispersion of TRGO/Cu(I) and NRGO/Cu(I) in epoxy matrix.

Table 4.1 Mechanical performance of prepared specimens

Sample	Tensile Strength (MPa)	Strain-at-break (%)	Young's modulus
Pure Epoxy	25.0 ±1	2.8±0.1	892 ±10
Epoxy +15wt% capsules	11.7 ±2	2.4 ±0.3	487 ±20
Epoxy +15wt% capsules+ Cu(PPh ₃) ₃ F	9.8 ±1	2.3 ±0.1	426 ±20
Epoxy +TRGO/Cu(I)	38 ±1	3.75 ±0.2	1013 ±10
Epoxy+15wt% capsules +TRGO/CU(I)	30.2 ±2	3.15 ±0.3	958 ±20
Epoxy +NRGO/Cu(I)	36.8 ±2	3.6 ±0.2	1022 ±10

Epoxy+15wt% capsules +NRGO/CU(I)	28.9 ±2	3.0 ±0.2	963 ±20
-------------------------------------	---------	----------	---------

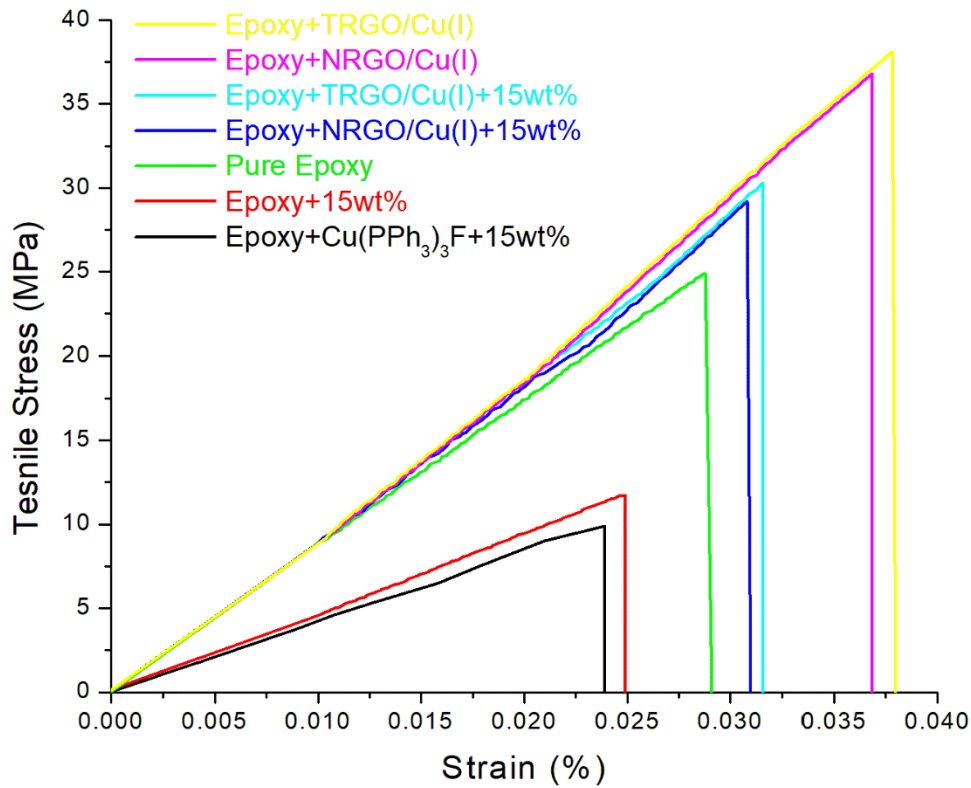


Figure 4.10 Plot for Tensile stress Vs strain for prepared pure epoxy and composite samples measured at strain rate: 0.1mm/min, 25 °C

There is a decrease in mechanical performance after the addition of capsules to the specimens containing TRGO/Cu(I) and NRGO/Cu(I), which states that the excess addition of capsules can contribute in reduction of interfacial adhesion between the epoxy and reinforcing agent. Moreover, the results obtained for specimen exhibited better mechanical properties with pure epoxy compared with other prepared specimens as given in Table 4.1. Even though, there is slight decrease in mechanical performance for NRGO/Cu(I) compared to TRGO/Cu(I) was observed in Table 4.1, it clearly states the strong load transfer between the carbon-carbon comparatively.

Motivated by these results, we further analyzed the effect of mechanical performance based on the capsule loading, a series of test specimens with 5wt%, 10wt%, 15wt% and 2wt% were fabricated containing NRGO/Cu(I) as catalyst. To

investigate the influence of capsule loading on the mechanical performance, tensile testing was carried out. As per the stress-strain curves and tensile strength of prepared specimens, shown in Figure 4.11 and Table 4.2. it shows decrease in tensile strength with increase in capsule loading from 25 of pure epoxy to 11.5 MPa for 20wt% of capsules and in the similar way the strain at break point decreased from 2.8 for pure epoxy to 2.3 for 20wt% of capsules. Moreover, with the addition of NRGO/Cu(I) observed increase in tensile strength and strain at break as discussed earlier.

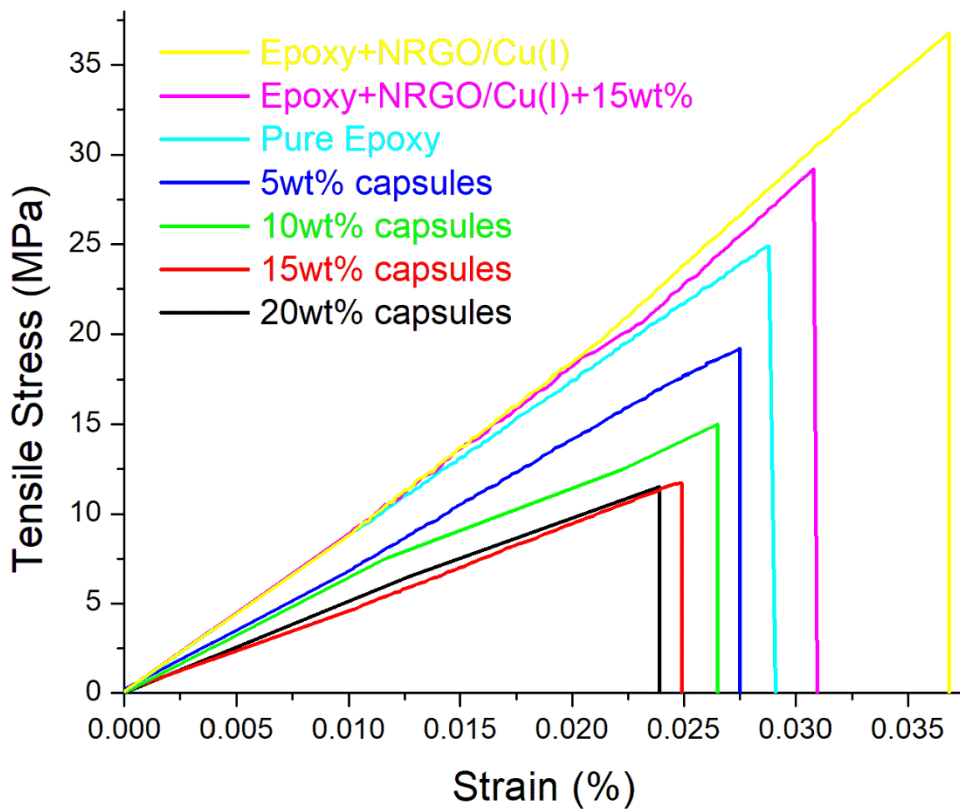


Figure 4.11 plot for tensile stress Vs strain curve for prepared pure epoxy and composite samples with different capsule loading (strain rate: 0.1mm min^{-1} , $25\text{ }^{\circ}\text{C}$)

Table 4.2 Mechanical performance of prepared specimens with different wt% loading of capsules

Sample	Tensile Strength (Mpa)	Strain-at-break (%)	Young's modulus
Epoxy	25.0 ± 1	2.8 ± 0.1	892 ± 10

Epoxy+ NRGO/Cu(I)	36.8 ±2	3.6 ±0.2	1022 ±10
Epoxy+ NRGO/CU(I)+15wt% capsules	28.9 ±2	3.0 ±0.2	963 ±20
5wt% capsules	19.1 ±1	2.7 ±0.2	707 ±20
10wt% capsules	14.8 ±1	2.6 ±0.2	569 ±10
15wt% capsules	11.7 ±2	2.4 ±0.3	487 ±10
20wt% capsules	11.5±1	2.3 ±0.1	500 ±20

4.4.2 SELF-HEALING PERFORMANCE

The self-healing performance of fabricated nanocomposite was evaluated via Dynamic Mechanical Analysis (DMA; single-notch impact testing) (Figure 4.12 & 4.13). The specimens were fabricated with the dimension of 35 x 5 x 2mm, and were evaluated through three point bending test procedure (as per ASTM D7264) performed to evaluate their tensile storage modulus (E'). Initially a sharp “V” shaped notch of 1mm depth was made at the centre of the specimen (specimen made of NRGO- Cu(I) (2 mol%) and 15 wt% capsules) was considered for the evaluation. The E' (2270 MPa) was obtained for the notched specimen of pure epoxy (Figure 4.13). An impulsive load of 10N was applied on the notched specimen via tensile force in 3D bending mode (Figure 4.13) for allowing the crack to propagate. From the Figure 4.10 clearly shows the deformation of curve, indicates the occurrence of delamination in the specimen because of crack propagation [249]. During the delamination period we have observed a sudden drop in E' (1780MPa) from DMA (Figure 4.13), confirms the propagation of crack in the specimen. The recovery of storage modulus (2250MPa) was observed from DMA, after allowing the specimen at 25°C for 36 h, where almost 96% of recovery was observed at room temperature prevail a triazole formation with the presence of NRGO/Cu(I).

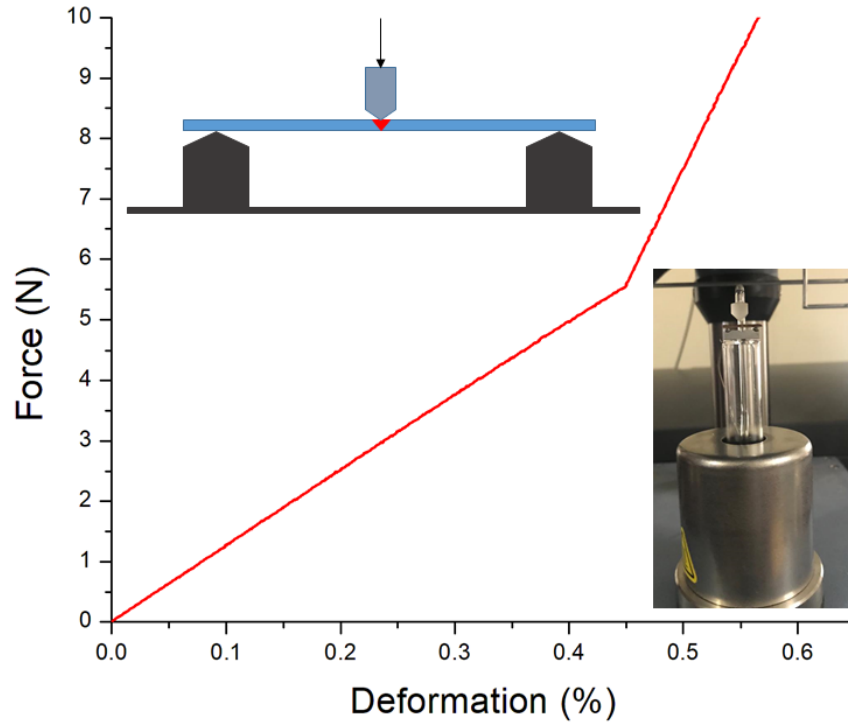


Figure 4.12 Deformation curve for the applied load

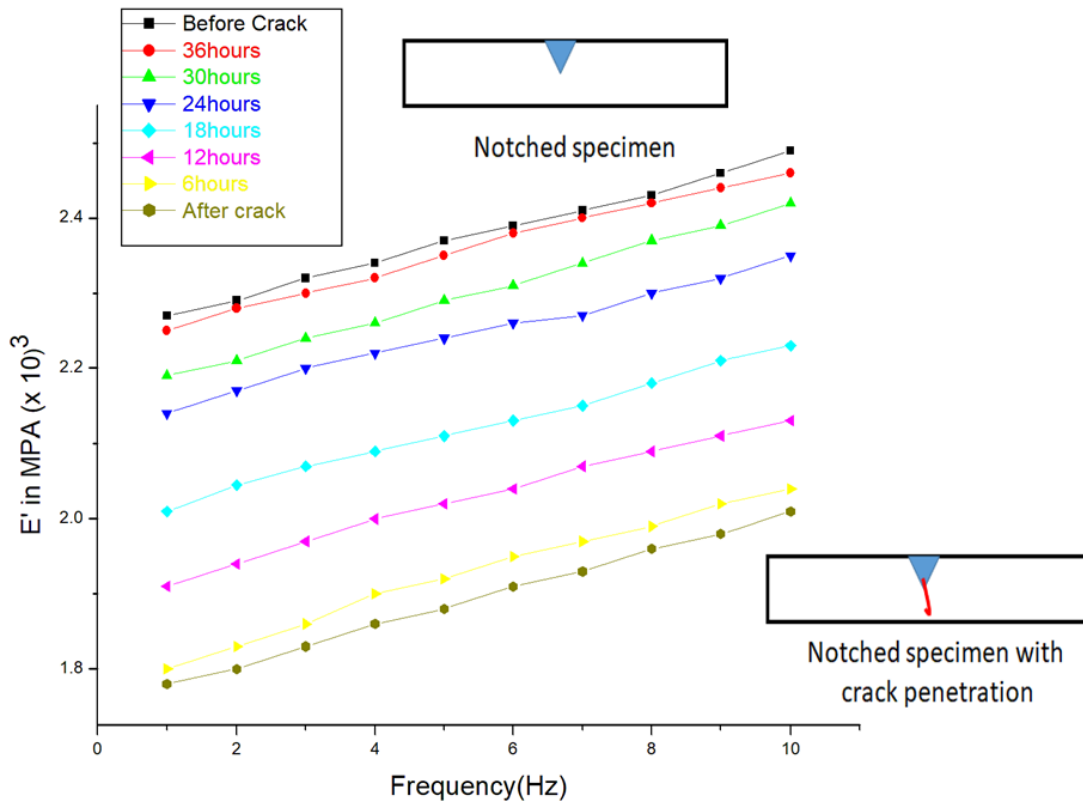


Figure 4.13 DMA analysis (before and after crack) for the prepared nanocomposites (contain 15 wt% azide capsules) at 25 °C

The specimens prepared with absence of healing agents, showed no significant change in E' were observed for all the prepared specimens, i.e., neat epoxy, epoxy with different homogeneous and heterogeneous catalyst without capsules (Figure 4.14). Further, the epoxy with 15wt% capsules also showed no progress in E' due to the absence of copper catalyst. Interestingly, the specimen with homogenous catalyst $\text{Cu}(\text{PPh}_3)_3\text{F}$ and 15wt% capsules showed quick recovery of 40% at 60 °C within 1h, but failed to achieve the full recovery even after 24h at 70 °C (Figure 4.14).

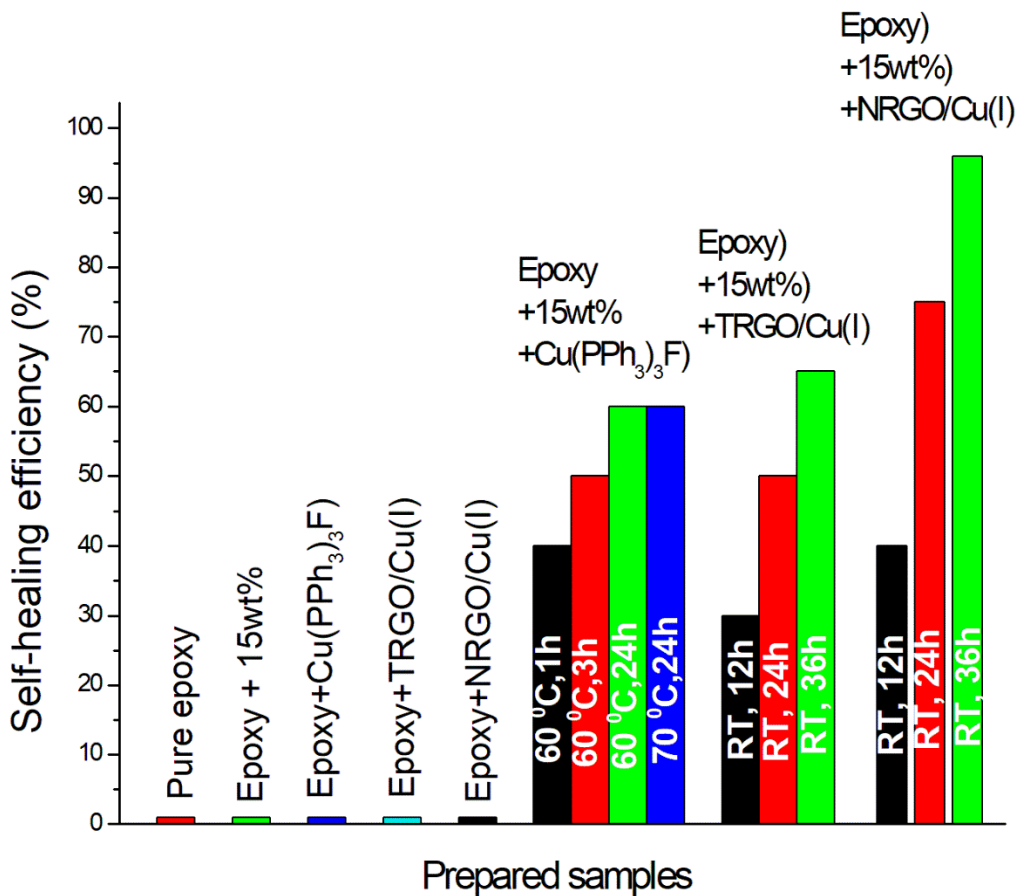


Figure 4.14 Self-healing efficiency of prepared specimens obtained from DMA results

However, the specimen with Epoxy+15wt%+TRGO/Cu(I) showed better results up to 85% recovery at 60 °C even after 36h (Figure 4.15), whereas the specimen with Epoxy+15wt%+NRGO/Cu(I) displayed 100% recovery at 60 °C

even after 6h and 95% recovery at room temperature after 36h, which further showed excellent efficiency of NRGO/Cu(I) with 15wt% capsules impregnated in epoxy matrix (Figure 4.15).

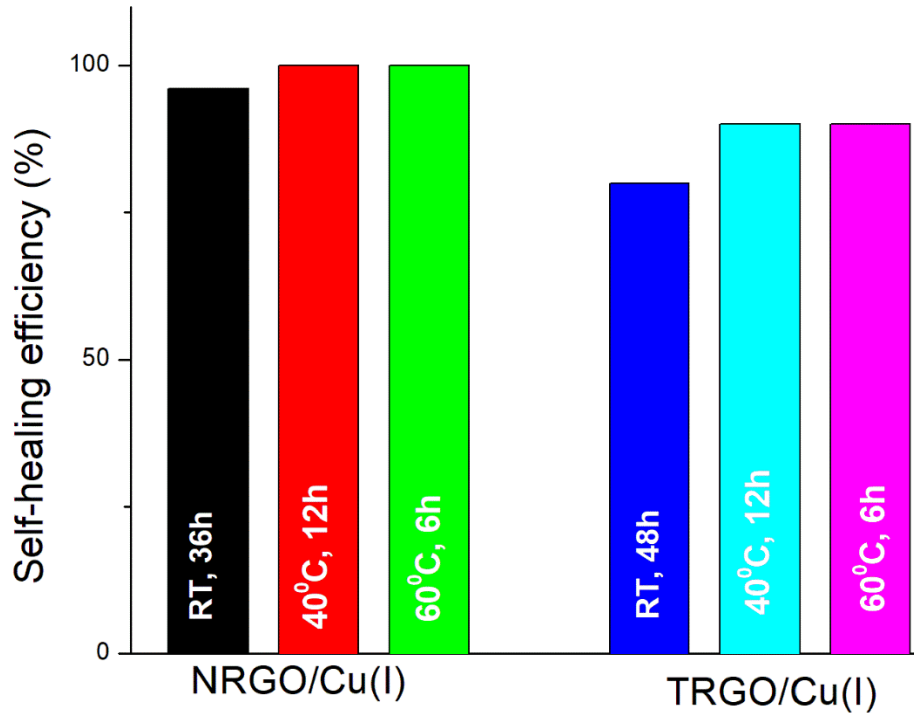


Figure 4.15 Self-healing efficiency of epoxy specimen with heterogeneous catalyst determined at different temperature with time dependent

With these interesting results exhibited by NRGO/Cu(I), further investigation was carried out with different loading concentration of capsules containing 5wt%, 10wt%, 15wt% and 20wt% (Figure 4.16). The results states the self-healing at room temperature is even possible with 20wt% loading along with 15wt%. There is no improvement (96%) in self-healing efficiency for both specimens even after 36h. whereas; 5wt% and 10wt% couldn't even obtain 50% of self-healing due to the unavailability healing agents at site.

The results demonstrates the higher catalytic activity for NRGO/Cu(I) compared to commercially available catalyst and TRGO/Cu(I), due to scaffold properties of graphene sheets. It promotes the prevention of agglomeration by copper particles (Figure 3.5 and 3.9) due to the formation of coordination of N-

doped rGO with Cu^+ , including high binding energy of Cu nanoparticles to N-doped carbon support [229]. Further, the exclusive interactions of copper particles with N-doped reduced graphene sheet, along with ability for electron transfer and capture were extremely supportive to enhance the catalytic activity [250].

The microscopic evidence in the form of TEM analysis (Figure 4.17), where the results demonstrate the agglomeration of homogenous catalyst ($\text{Cu}(\text{PPh}_3)_3 \text{F}$) in epoxy matrix, whereas a highly dispersed catalyst image was captured for heterogeneous catalyst TRGO/Cu(I), required to achieve self-healing behavior for the prepared composites. The agglomeration of $\text{Cu}(\text{PPh}_3)_3 \text{F}$ in epoxy matrix leads to limited self-healing in comparative to heterogeneous catalyst. Therefore the results strongly support the significance of NRGO/Cu(I) for its high stability and uniform dispersion in polymer matrix over the homogenous ($\text{Cu}(\text{PPh}_3)_3 \text{F}$) and heterogeneous catalyst TRGO/Cu(I).

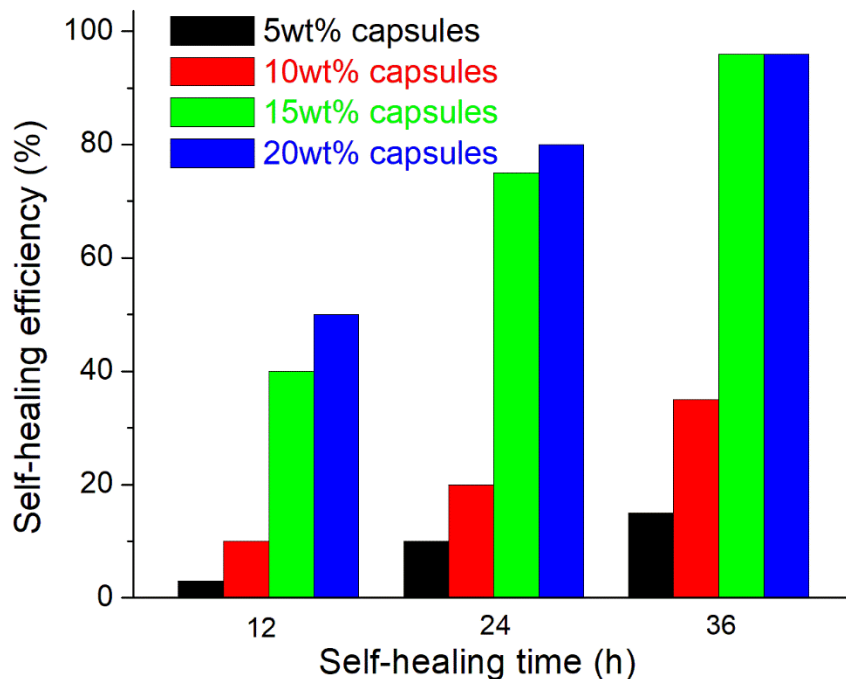


Figure 4.16 Self-healing efficiency of epoxy specimen with NRGO/Cu(I) and different wt% of capsules available at room temperature with time dependent

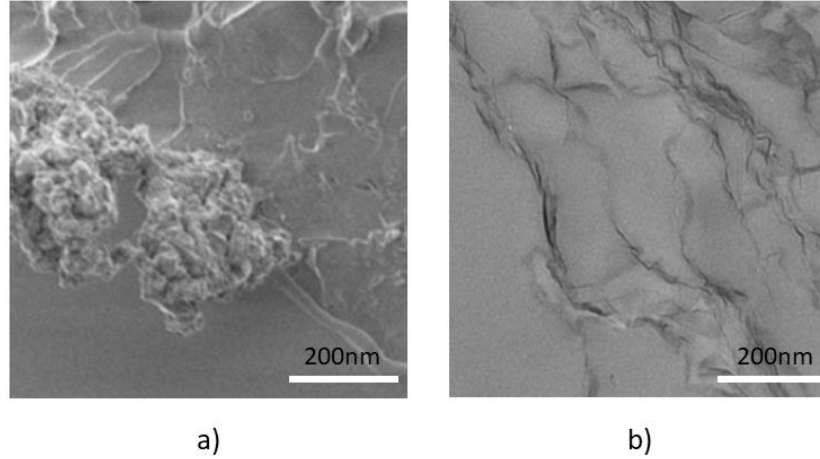


Figure 4.17 TEM images of a) homogenous ($\text{Cu(PPh}_3)_3\text{ F}$) and b) heterogeneous catalyst TRGO/Cu(I) dispersion in epoxy matrix

4.4.2 CONDUCTIVITY

The conductivity of the prepared specimen was carried out by standard four-point probe method, here direct current conductivity (σ) of prepared composite materials as a function of graphene volume fraction (p) which was determined, where composite conductivity is determined by σ , p determines the SPFG volume fraction. From the obtained results, NRGO/Cu (I) and TRGO/Cu(I) specimen displayed the conductivity of 5×10^{-2} and 8×10^{-3} S/cm respectively as showed in Figure 4.18. The increase in conductivity for NRGO/Cu(I) is due to the presence of Nitrogen, strongly promoting the conductivity of a composite material.

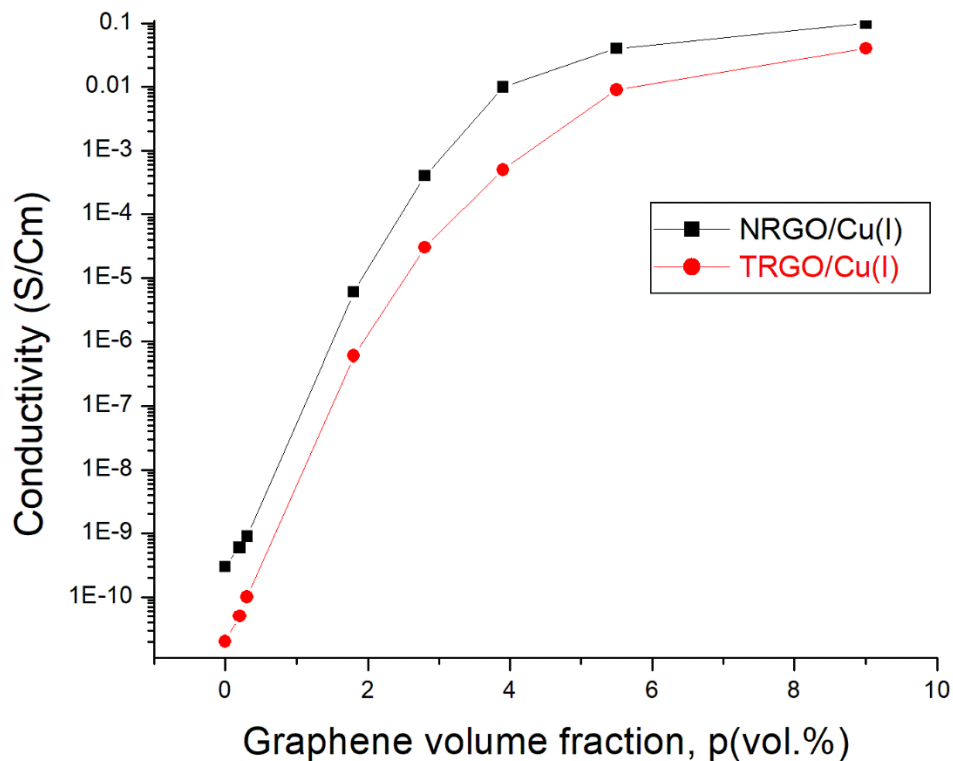


Figure 4.18 Conductivity Vs Graphene volume fraction

4.5 SUMMARY

In summary, we have developed an efficient graphene-based epoxy self-healing nanocomposites, which can heal at room temperature in the presence of synthesized catalyst NRGO/Cu(I) and TRGO/Cu(I). Self-healing is made possible by ‘click’ reactions between alkyne (present in capsule) and azide (dispersed directly on epoxy matrix) triggered by homogenous and heterogeneous Cu catalyst. In addition, the presence of nitrogen doped copper immobilized reduced graphene oxide (NRGO/Cu(I)) displayed enhanced catalytic activity, require to make healing possible at room temperature, and also fulfill the requirement of tensile strength and conductivity by acting as reinforcement agent inside the ,matrix.

CHAPTER 5: CONCLUSION AND FUTURE PERSPECTS

Inspired from natural healing process and replacement of damaged tissue, many self-repairing materials have been successfully developed, which is revolutionizing the project of artificial materials for easy maintenance with improved safety. For structural applications, many realistic strategies have been formulated till today in the development of self-healing materials. However, in all cases the stability of the components/catalysts is limited. This work is focused on development of novel self-healing composite materials based on graphene and capsule-based system, where the catalytic system able to achieve self-healing through well dispersion of nano fillers, stable catalytic activity and healing components.

This work is first dedicated to prepare a highly stable and recyclable heterogeneous catalyst (NRGO/Cu(I)), which performs the ‘click’ reaction under both solvent and bulk conditions. Due to an increase in electron density on nitrogen atom doping including the formation of coordination of N-doped rGO with Cu^+ ions, nitrogen doped graphene supported copper particles demonstrate a higher reaction yield at room temperature without adding any external ligand/base, and is reusable ten times and observed around 90% yield after 10th cycle.

A very interesting self-healing properties were obtained for the composites with the incorporation of a graphene based catalyst, where a room-temperature self-healing graphene-based epoxy nanocomposite with enhanced tensile and conductive properties were developed. Applying a simple capsule-based self-healing concept, network formation via a Cu(I)-catalyzed azide–alkyne “click” reaction using heterogeneous copper(I) catalysts introduces self-healing. The addition of highly dispersible graphene-immobilized Cu_2O (NRGO- Cu_2O)-based catalyst demonstrates an excellent combination of high catalytic performance for ‘click’-based network formation (crack healing) at room temperature along with required reinforcement within the material, in turn allowing compensation of tensile-strength reduction exerted by the embedded capsules. Along with tensile

strength the conductivity of TRGO/Cu(I) displayed an improved conductivity comparatively.

5.1 FUTURE PERSPECTS

There are consistent efforts in recovery of functional properties of material after healing at damage sites using different composite materials and self-healing mechanisms. All though the area of self-healing still facing complications in understanding the behavior/functionality of healing mechanism. The major concern areas are identifying the damage sites and healing for self-healing composites. The research in this field is still in initial phase and different combinations of composite materials with graphene i.e. graphene with polymers (natural, synthetic and conducting) and metals (alloys and oxides), needs to be studied to explore the properties to full extent. Even the mechanism of self-healing needs the deeper investigations for controlled optimization of fabrication methods, likely usage of materials with graphene and other physical parameters like pressure and temperature. The area of graphene based self-healing materials has diverse field of applications. The performance of graphene promoted self-healing composites exhibited improved results, indeed it is has become a challenge in making the composite in practical application. Individually, there is good progress in self-healing capabilities and mechanical properties, in spite of facing many challenges in balancing both in graphene/polymer laminates. It is evident that it can happen when there is an improved compatibility between graphene and polymer after modifying graphene without disrupting the natural properties of graphene.

3D printing is most advanced manufacturing technology which profound in numerous applications in electronic, robotics, construction aerospace, etc., [251]–[255]. This 3D printing is used to manufacture complicated/intercalated shapes, which are quite difficult to manufacture using conventional manufacturing techniques. In general, it is stem branch of additive manufacturing, where the 3D model is designed in computer and fabricated using layer-by-layer deposition of liquid ink, which is simple and has diversified features. Due to its unique features of 3D printing, the use of self-healing nanocomposite materials has a scope in

various applications. Impressive results of self-healing polymer nanocomposites with improved properties and applications will have a prosperous scope in commercialization near future.

REFERENCES

- [1] V. D. Punetha *et al.*, “Functionalization of carbon nanomaterials for advanced polymer nanocomposites: A comparison study between CNT and graphene,” *Prog. Polym. Sci.*, vol. 67, pp. 1–47, 2017.
- [2] Z. Spitalsky, D. Tasis, K. Papagelis, and C. Galiotis, “Carbon nanotube–polymer composites: Chemistry, processing, mechanical and electrical properties,” *Prog. Polym. Sci.*, vol. 35, no. 3, pp. 357–401, 2010.
- [3] N. Gopal, S. Rana, J. Whan, L. Li, and S. Hwa, “Polymer nanocomposites based on functionalized carbon nanotubes,” *Prog. Polym. Sci.*, vol. 35, pp. 837–867, 2010.
- [4] L. Guadagno *et al.*, “Cure behavior and mechanical properties of structural self-healing epoxy resins,” *J. Polym. Sci. Part B Polym. Phys.*, vol. 48, no. 23, pp. 2413–2423, Dec. 2010.
- [5] S. Anandan, N. Hebalkar, B. V Sarada, and T. N. Rao, “Aerospace Materials and Material Technologies,” pp. 85–101, 2017.
- [6] J. Baur and E. Silverman, “Challenges and Structures for Aerospace,” vol. 32, no. April, pp. 328–334, 2007.
- [7] H. Kim, A. A. Abdala, and C. W. MacOsco, “Graphene/polymer nanocomposites,” *Macromolecules*, vol. 43, no. 16, pp. 6515–6530, 2010.
- [8] B. J. Blaiszik, S. L. B. Kramer, S. C. Olugebefola, J. S. Moore, N. R. Sottos, and S. R. White, “Self-Healing Polymers and Composites,” *Annu. Rev. Mater. Res.*, vol. 40, no. 1, pp. 179–211, 2010.
- [9] B. J. Blaiszik, S. L. B. Kramer, S. C. Olugebefola, J. S. Moore, N. R. Sottos, and S. R. White, “Self-Healing Polymers and Composites,” *Annu. Rev. Mater. Res.*, vol. 40, no. 1, pp. 179–211, Jun. 2010.
- [10] R. P. Wool and K. M. O’Connor, “A theory of crack healing in polymers,” *J. Appl. Phys.*, vol. 52, no. 10, pp. 5953–5963, 1981.
- [11] V. K. Thakur and M. R. Kessler, “Self-healing polymer nanocomposite materials: A review,” *Polymer (Guildf.)*, 2015.
- [12] M. Samadzadeh, S. H. Boura, M. Peikari, S. M. Kasiriha, and A. Ashrafi, “A review on self-healing coatings based on micro/nanocapsules,” *Prog. Org. Coatings*, vol. 68, no. 3, pp. 159–164, 2010.
- [13] E. Koh, S.-Y. Baek, N.-K. Kim, S. Lee, J. Shin, and Y.-W. Kim, “Microencapsulation of the triazole derivative for self-healing anticorrosion coatings,” *New J. Chem.*, vol. 38, no. 9, pp. 4409–4419, 2014.
- [14] E. N. Brown, M. R. Kessler, N. R. Sottos, and S. R. White, “*In situ* poly(urea-formaldehyde) microencapsulation of dicyclopentadiene,” *J. Microencapsul.*, vol. 20, no. 6, pp. 719–730, 2003.
- [15] E. N. Brown, N. R. Sottos, and S. R. White, “Fracture testing of a self-healing polymer composite,” *Exp. Mech.*, vol. 42, no. 4, pp. 372–379, Dec. 2002.
- [16] E. N. Brown, S. R. White, and N. R. Sottos, “Retardation and repair of fatigue cracks in a microcapsule toughened epoxy composite - Part II: *In situ* self-healing,” *Compos. Sci. Technol.*, vol. 65, no. 15-16 SPEC. ISS., pp. 2474–2480, 2005.
- [17] E. N. Brown, M. R. Kessler, N. R. Sottos, and S. R. White, “*In situ* poly(urea-formaldehyde) microencapsulation of dicyclopentadiene,” *J. Microencapsul.*, vol. 20, no. 6, pp. 719–730, Jan. 2003.
- [18] G. O. Wilson, J. S. Moore, S. R. White, N. R. Sottos, and H. M. Andersson, “Autonomic healing of epoxy vinyl esters via ring opening metathesis polymerization,” *Adv. Funct. Mater.*, vol. 18, no. 1, pp. 44–52, 2008.

- [19] M. R. Kessler, N. R. Sottos, and S. R. White, "Self-healing structural composite materials," *Compos. Part A Appl. Sci. Manuf.*, vol. 34, no. 8, pp. 743–753, 2003.
- [20] M. D. Chipara, M. Chipara, E. Shansky, and J. M. Zaleski, "Self-healing of high elasticity block copolymers," *Polym. Adv. Technol.*, vol. 20, no. 4, pp. 427–431, 2009.
- [21] G. O. Wilson, K. A. Porter, H. Weissman, S. R. White, N. R. Sottos, and J. S. Moore, "Stability of Second Generation Grubbs' Alkylidenes to Primary Amines: Formation of Novel Ruthenium-Amine Complexes," *Adv. Synth. Catal.*, vol. 351, no. 11-12, pp. 1817–1825, 2009.
- [22] X. Liu, J. K. Lee, S. H. Yoon, and M. R. Kessler, "Characterization of diene monomers as healing agents for autonomic damage repair," *J. Appl. Polym. Sci.*, vol. 101, no. 3, pp. 1266–1272, 2006.
- [23] J. M. Kamphaus, J. D. Rule, J. S. Moore, N. R. Sottos, and S. R. White, "A new self-healing epoxy with tungsten (VI) chloride catalyst," *J. R. Soc. Interface*, vol. 5, no. 18, pp. 95–103, 2007.
- [24] B. J. D. Rule, E. N. Brown, N. R. Sottos, S. R. White, and J. S. Moore, "Wax-Protected Catalyst Microspheres for Efficient Self-Healing Materials **," no. 2, pp. 205–208, 2005.
- [25] J. L. Moll, S. R. White, and N. R. Sottos, "A Self-sealing Fiber-reinforced Composite," *J. Compos. Mater.*, vol. 44, no. 22, pp. 2573–2585, Jan. 2010.
- [26] M. Z. Rong, M. Q. Zhang, and W. Zhang, "A novel self-healing epoxy system with microencapsulated epoxy and imidazole curing agent," pp. 167–172, 2007.
- [27] S. R. White *et al.*, "correction: Autonomic healing of polymer composites," *Nature*, vol. 415, no. 6873, pp. 817–817, 2002.
- [28] N. R. Sottos *et al.*, "Multidimensional Vascularized Polymers using Degradable Sacrificial Templates," *Adv. Mater.*, vol. 25, no. 7, pp. 1043–1052, 2014.
- [29] J. H. Huang *et al.*, "Rapid fabrication of bio-inspired 3D microfluidic vascular networks," *Adv. Mater.*, vol. 21, no. 35, pp. 3567–3571, 2009.
- [30] C. M. Dry and N. R. Sottos, "Passive smart self-repair in polymer matrix composite materials," *1993 North Am. Conf. Smart Struct. Mater.*, vol. 1916, pp. 438–444, 1993.
- [31] M. Motuku, U. K. Vaidya, and G. M. Janowski, "Parametric studies on self-repairing approaches for resin infused composites subjected to low velocity impact," *Smart Mater. Struct.*, vol. 8, no. 5, pp. 623–638, 1999.
- [32] S. M. Bleay, C. B. Loader, V. J. Hawyes, L. Humberstone, and P. T. Curtis, "A smart repair system for polymer matrix composites," *Compos. Part A Appl. Sci. Manuf.*, vol. 32, no. 12, pp. 1767–1776, 2001.
- [33] H. R. Williams, R. S. Trask, and I. P. Bond, "Self-healing composite sandwich structures," *Smart Mater. Struct.*, vol. 16, no. 4, pp. 1198–1207, 2007.
- [34] K. S. Toohey, N. R. Sottos, J. A. Lewis, J. S. Moore, and S. R. White, "Self-healing materials with microvascular networks," *Nat. Mater.*, vol. 6, no. 8, pp. 581–585, 2007.
- [35] K. S. Toohey, C. J. Hansen, J. A. Lewis, S. R. White, and N. R. Sottos, "Delivery of two-part self-healing chemistry via microvascular networks," *Adv. Funct. Mater.*, vol. 19, no. 9, pp. 1399–1405, 2009.
- [36] C. J. Hansen, W. Wu, K. S. Toohey, N. R. Sottos, S. R. White, and J. A. Lewis, "Self-healing materials with interpenetrating microvascular networks," *Adv. Mater.*, vol. 21, no. 41, pp. 4143–4147, 2009.
- [37] Y. C. Yuan, T. Yin, M. Z. Rong, and M. Q. Zhang, "Self healing in polymers and polymer composites. Concepts, realization and outlook: A review," *Express Polym. Lett.*, vol. 2, no. 4, pp. 238–250, 2008.

- [38] S. J. Garcia, "Effect of polymer architecture on the intrinsic self-healing character of polymers," *Eur. Polym. J.*, vol. 53, no. 1, pp. 118–125, 2014.
- [39] W. H. Binder and R. Zirbs, "Supramolecular Polymers and Networks with Hydrogen Bonds in the Main- and Side-Chain," in *Hydrogen Bonded Polymers*, W. Binder, Ed. Berlin, Heidelberg: Springer Berlin Heidelberg, 2007, pp. 1–78.
- [40] G. M. L. van Gemert, J. W. Peeters, S. H. M. Söntjens, H. M. Janssen, and A. W. Bosman, "Self-Healing Supramolecular Polymers In Action," *Macromol. Chem. Phys.*, vol. 213, no. 2, pp. 234–242, 2012.
- [41] S. Imaizumi, H. Kokubo, and M. Watanabe, "Polymer Actuators Using Ion-Gel Electrolytes Prepared by Self-Assembly of ABA-Triblock Copolymers," *Macromolecules*, vol. 45, no. 1, pp. 401–409, Jan. 2012.
- [42] Y. Kitazawa *et al.*, "Polymer Electrolytes Containing Solvate Ionic Liquids: A New Approach To Achieve High Ionic Conductivity, Thermal Stability, and a Wide Potential Window," *Chem. Mater.*, vol. 30, no. 1, pp. 252–261, Jan. 2018.
- [43] Y. Huang, P. G. Lawrence, and Y. Lapitsky, "Self-Assembly of Stiff, Adhesive and Self-Healing Gels from Common Polyelectrolytes," *Langmuir*, vol. 30, no. 26, pp. 7771–7777, Jul. 2014.
- [44] F. Herbst, D. Döhler, P. Michael, and W. H. Binder, "Self-Healing Polymers via Supramolecular Forces," *Macromol. Rapid Commun.*, vol. 34, no. 3, pp. 203–220, Feb. 2013.
- [45] J. P. Gong, "Why are double network hydrogels so tough?," *Soft Matter*, vol. 6, no. 12, pp. 2583–2590, 2010.
- [46] Q. Chen, H. Chen, L. Zhu, and J. Zheng, "Fundamentals of double network hydrogels," *J. Mater. Chem. B*, vol. 3, no. 18, pp. 3654–3676, 2015.
- [47] Z. Feng, H. Zuo, W. Gao, N. Ning, M. Tian, and L. Zhang, "A Robust, Self-Healable, and Shape Memory Supramolecular Hydrogel by Multiple Hydrogen Bonding Interactions," *Macromol. Rapid Commun.*, vol. 39, no. 20, pp. 1–7, 2018.
- [48] B. C.-K. Tee, C. Wang, R. Allen, and Z. Bao, "An electrically and mechanically self-healing composite with pressure- and flexion-sensitive properties for electronic skin applications," *Nat. Nanotechnol.*, vol. 7, no. 12, pp. 825–832, Nov. 2012.
- [49] S. Dai, X. Zhou, S. Wang, J. Ding, and N. Yuan, "A self-healing conductive and stretchable aligned carbon nanotube/hydrogel composite with a sandwich structure," *Nanoscale*, vol. 10, no. 41, pp. 19360–19366, 2018.
- [50] M. Zhong *et al.*, "Self-healable, tough and highly stretchable ionic nanocomposite physical hydrogels," *Soft Matter*, vol. 11, no. 21, pp. 4235–4241, 2015.
- [51] G. Gao, G. Du, Y. Sun, and J. Fu, "Self-Healable, Tough, and Ultrastretchable Nanocomposite Hydrogels Based on Reversible Polyacrylamide/Montmorillonite Adsorption," *ACS Appl. Mater. Interfaces*, vol. 7, no. 8, pp. 5029–5037, Mar. 2015.
- [52] Y. Li, S. Chen, M. Wu, and J. Sun, "Polyelectrolyte Multilayers Impart Healability to Highly Electrically Conductive Films," *Adv. Mater.*, vol. 24, no. 33, pp. 4578–4582, Aug. 2012.
- [53] M. Zhong, Y.-T. Liu, and X.-M. Xie, "Self-healable, super tough graphene oxide–poly(acrylic acid) nanocomposite hydrogels facilitated by dual cross-linking effects through dynamic ionic interactions," *J. Mater. Chem. B*, vol. 3, no. 19, pp. 4001–4008, 2015.
- [54] H. Jiang *et al.*, "Room-temperature self-healing tough nanocomposite hydrogel crosslinked by zirconium hydroxide nanoparticles," *Compos. Sci. Technol.*, vol. 140, pp. 54–62, 2017.
- [55] L. Han *et al.*, "A Mussel-Inspired Conductive, Self-Adhesive, and Self-Healable

- Tough Hydrogel as Cell Stimulators and Implantable Bioelectronics,” *Small*, vol. 13, no. 2, p. 1601916, Jan. 2017.
- [56] T. Wu and B. Chen, “A mechanically and electrically self-healing graphite composite dough for stencil-printable stretchable conductors,” *J. Mater. Chem. C*, vol. 4, no. 19, pp. 4150–4154, 2016.
- [57] W. Cui, J. Ji, Y. Cai, H. Li, and R. Ran, “Robust, anti-fatigue, and self-healing graphene oxide/hydrophobically associated composite hydrogels and their use as recyclable adsorbents for dye wastewater treatment †,” *Jounral Mater. Chem. A*, vol. 3, no. 33, pp. 17445–17458, 2015.
- [58] J. Liu, G. Song, C. He, and H. Wang, “Self-Healing in Tough Graphene Oxide Composite Hydrogels,” *Macromol. Rapid Commun.*, vol. 34, no. 12, pp. 1002–1007, 2013.
- [59] J. R. McKee, E. A. Appel, J. Seitsonen, E. Kontturi, O. A. Scherman, and O. Ikkala, “Healable, Stable and Stiff Hydrogels: Combining Conflicting Properties Using Dynamic and Selective Three-Component Recognition with Reinforcing Cellulose Nanorods,” *Adv. Funct. Mater.*, vol. 24, no. 18, pp. 2706–2713, May 2014.
- [60] K. Guo *et al.*, “Conductive Elastomers with Autonomic Self-Healing Properties,” *Angew. Chemie Int. Ed.*, vol. 54, no. 41, pp. 12127–12133, Oct. 2015.
- [61] C.-H. Li *et al.*, “A highly stretchable autonomous self-healing elastomer,” *Nat. Chem.*, vol. 8, p. 618, Apr. 2016.
- [62] R. Du, J. Wu, L. Chen, H. Huang, X. Zhang, and J. Zhang, “Hierarchical Hydrogen Bonds Directed Multi-Functional Carbon Nanotube-Based Supramolecular Hydrogels,” *Small*, vol. 10, no. 7, pp. 1387–1393, Apr. 2014.
- [63] Q. Ding *et al.*, “Nanocellulose-Mediated Electroconductive Self-Healing Hydrogels with High Strength, Plasticity, Viscoelasticity, Stretchability, and Biocompatibility toward Multifunctional Applications,” *ACS Appl. Mater. Interfaces*, vol. 10, no. 33, pp. 27987–28002, Aug. 2018.
- [64] S. Thakur, S. Barua, and N. Karak, “Self-healable castor oil based tough smart hyperbranched polyurethane nanocomposite with antimicrobial attributes,” *RSC Adv.*, vol. 5, no. 3, pp. 2167–2176, 2015.
- [65] S. Thakur and N. Karak, “Tuning of sunlight-induced self-cleaning and self-healing attributes of an elastomeric nanocomposite by judicious compositional variation of the TiO₂–reduced graphene oxide nano hybrid,” *J. Mater. Chem. A*, vol. 3, no. 23, pp. 12334–12342, 2015.
- [66] G. Deng *et al.*, “Dynamic Hydrogels with an Environmental Adaptive Self-Healing Ability and Dual Responsive Sol – Gel Transitions,” *ACS Macro Lett.*, vol. 1, no. 2, pp. 275–279, 2012.
- [67] R. K. Bose, J. Köttteritzsch, S. J. Garcia, M. D. Hager, U. S. Schubert, and S. van der Zwaag, “A rheological and spectroscopic study on the kinetics of self-healing in a single-component diels–alder copolymer and its underlying chemical reaction,” *J. Polym. Sci. Part A Polym. Chem.*, vol. 52, no. 12, pp. 1669–1675, Jun. 2014.
- [68] A. Fuhrmann *et al.*, “Conditional repair by locally switching the thermal healing capability of dynamic covalent polymers with light,” *Nat. Commun.*, vol. 7, p. 13623, 2016.
- [69] R. R. Kohlmeyer, M. Lor, and J. Chen, “Remote, Local, and Chemical Programming of Healable Multishape Memory Polymer Nanocomposites,” *Nano Lett.*, vol. 12, no. 6, pp. 2757–2762, Jun. 2012.
- [70] J. Bai and Z. Shi, “Dynamically Cross-linked Elastomer Hybrids with Light-Induced Rapid and Efficient Self-Healing Ability and Reprogrammable Shape

- Memory Behavior,” *ACS Appl. Mater. Interfaces*, vol. 9, no. 32, pp. 27213–27222, Aug. 2017.
- [71] J. Bai *et al.*, “Self-assembled elastomer nanocomposites utilizing C60 and poly(styrene-*b*-butadiene-*b*-styrene) via thermally reversible Diels-Alder reaction with self-healing and remolding abilities,” *Polymer (Guildf.)*, vol. 116, pp. 268–277, 2017.
- [72] A. Nasresfahani and P. M. Zelisko, “Synthesis of a self-healing siloxane-based elastomer cross-linked via a furan-modified polyhedral oligomeric silsesquioxane investigation of a thermally reversible silicon-based cross-link,” *Polym. Chem.*, vol. 8, no. 19, pp. 2942–2952, 2017.
- [73] C. Shao, M. Wang, H. Chang, F. Xu, and J. Yang, “A Self-Healing Cellulose Nanocrystal-Poly(ethylene glycol) Nanocomposite Hydrogel via Diels-Alder Click Reaction,” *ACS Sustain. Chem. Eng.*, vol. 5, no. 7, pp. 6167–6174, 2017.
- [74] J. Li *et al.*, “Three-Dimensional Graphene Structure for Healable Flexible Electronics Based on Diels–Alder Chemistry,” *ACS Appl. Mater. Interfaces*, vol. 10, no. 11, pp. 9727–9735, Mar. 2018.
- [75] J. Bai and Z. Shi, “Dynamically Cross-linked Elastomer Hybrids with Light-Induced Rapid and Efficient Self-Healing Ability and Reprogrammable Shape Memory Behavior,” *ACS Appl. Mater. Interfaces*, vol. 9, no. 32, pp. 27213–27222, Aug. 2017.
- [76] B. Lu *et al.*, “One-Pot Assembly of Microfibrillated Cellulose Reinforced PVA–Borax Hydrogels with Self-Healing and pH-Responsive Properties,” *ACS Sustain. Chem. Eng.*, vol. 5, no. 1, pp. 948–956, Jan. 2017.
- [77] A. J. R. Amaral, M. Emamzadeh, and G. Pasparakis, “Transiently malleable multi-healable hydrogel nanocomposites based on responsive boronic acid copolymers,” *Polym. Chem.*, vol. 9, no. 4, pp. 525–537, 2018.
- [78] T. Wu and B. Chen, “Synthesis of Multiwalled Carbon Nanotube-Reinforced Polyborosiloxane Nanocomposites with Mechanically Adaptive and Self-Healing Capabilities for Flexible Conductors,” *ACS Appl. Mater. Interfaces*, vol. 8, no. 36, pp. 24071–24078, Sep. 2016.
- [79] A. Gantar *et al.*, “Injectable and self-healing dynamic hydrogel containing bioactive glass nanoparticles as a potential biomaterial for bone regeneration,” *RSC Adv.*, vol. 6, no. 73, pp. 69156–69166, 2016.
- [80] C. Xu, R. Cui, L. Fu, and B. Lin, “Recyclable and heat-healable epoxidized natural rubber/bentonite composites,” *Compos. Sci. Technol.*, vol. 167, pp. 421–430, 2018.
- [81] J. Canadell, H. Goossens, and B. Klumperman, “Self-Healing Materials Based on Disulfide Links,” *Macromolecules*, vol. 44, no. 8, pp. 2536–2541, Apr. 2011.
- [82] N. Huebsch *et al.*, “Ultrasound-triggered disruption and self-healing of reversibly cross-linked hydrogels for drug delivery and enhanced chemotherapy,” *Proc. Natl. Acad. Sci.*, vol. 111, no. 27, pp. 9762–9767, 2014.
- [83] Q. Liu *et al.*, “A Supramolecular Shear-Thinning Anti-Inflammatory Steroid Hydrogel,” *Adv. Mater.*, vol. 28, no. 31, pp. 6680–6686, Aug. 2016.
- [84] P. Y. W. Dankers *et al.*, “Hierarchical Formation of Supramolecular Transient Networks in Water: A Modular Injectable Delivery System,” *Adv. Mater.*, vol. 24, no. 20, pp. 2703–2709, May 2012.
- [85] M. M. C. Bastings *et al.*, “A Fast pH-Switchable and Self-Healing Supramolecular Hydrogel Carrier for Guided, Local Catheter Injection in the Infarcted Myocardium,” *Adv. Healthc. Mater.*, vol. 3, no. 1, pp. 70–78, Jan. 2014.
- [86] A. K. Gaharwar *et al.*, “Shear-Thinning Nanocomposite Hydrogels for the Treatment of Hemorrhage,” *ACS Nano*, vol. 8, no. 10, pp. 9833–9842, Oct. 2014.

- [87] L. Han, Y. Zhang, X. Lu, K. Wang, Z. Wang, and H. Zhang, "Polydopamine Nanoparticles Modulating Stimuli-Responsive PNIPAM Hydrogels with Cell/Tissue Adhesiveness," *ACS Appl. Mater. Interfaces*, vol. 8, no. 42, pp. 29088–29100, Oct. 2016.
- [88] Y. Shi, M. Wang, C. Ma, Y. Wang, X. Li, and G. Yu, "A Conductive Self-Healing Hybrid Gel Enabled by Metal–Ligand Supramolecule and Nanostructured Conductive Polymer," *Nano Lett.*, vol. 15, no. 9, pp. 6276–6281, Sep. 2015.
- [89] M. A. Darabi *et al.*, "Skin-Inspired Multifunctional Autonomic-Intrinsic Conductive Self-Healing Hydrogels with Pressure Sensitivity, Stretchability, and 3D Printability," *Adv. Mater.*, vol. 29, no. 31, p. 1700533, Aug. 2017.
- [90] T. Sun, X. Shen, C. Peng, H. Fan, M. Liu, and Z. Wu, "A novel strategy for the synthesis of self-healing capsule and its application," *Compos. Sci. Technol.*, vol. 171, no. September 2018, pp. 13–20, 2019.
- [91] C. Li, J. Tan, J. Gu, L. Qiao, B. Zhang, and Q. Zhang, "Rapid and efficient synthesis of isocyanate microcapsules via thiol-ene photopolymerization in Pickering emulsion and its application in self-healing coating," *Compos. Sci. Technol.*, vol. 123, no. 8, pp. 250–258, 2016.
- [92] Z. He, S. Jiang, Q. Li, J. Wang, Y. Zhao, and M. Kang, "Facile and cost-effective synthesis of isocyanate microcapsules via polyvinyl alcohol-mediated interfacial polymerization and their application in self-healing materials," *Compos. Sci. Technol.*, 2016.
- [93] P. Engineering, L. Guadagno, M. Raimondo, C. Naddeo, and P. Longo, "Self-Healing Materials for Structural Applications," *Polym. Eng. Sci.*, vol. 54, no. 4, 2014.
- [94] T. S. Coope, D. F. Wass, R. S. Trask, and I. P. Bond, "Metal Triflates as Catalytic Curing Agents in Self-Healing Fibre Reinforced Polymer Composite Materials a," *Macromol. Mater. Eng.*, pp. 1–11, 2013.
- [95] P. A. Bolimowski, I. P. Bond, and D. F. Wass, "Robust synthesis of epoxy resin-filled microcapsules for application to self-healing materials," *Philos. Trans. R. Soc. A Math. Phys. Eng. Sci.*, vol. 374, no. February, 2016.
- [96] S. P. Panagiota Polydoropoulou, Christos Vasilios Katsiropoulos, Andreas Loukopoulos, "Mechanical behavior of aeronautical composites containing self-healing microcapsules," *Int. J. Struct. Integr.*, vol. 9, no. 6, pp. 753–767, 2018.
- [97] B. Soo, H. Cho, H. M. Andersson, S. R. White, N. R. Sottos, and P. V. Braun, "Polydimethylsiloxane-Based Self-Healing Materials **," *Adv. Mater.*, vol. 18, pp. 997–1000, 2006.
- [98] S. H. Cho, S. R. White, and P. V. Braun, "Self-healing polymer coatings," *Adv. Mater.*, vol. 21, no. 6, pp. 645–649, 2009.
- [99] H. Search, C. Journals, A. Contact, M. Iopscience, S. Mater, and I. P. Address, "Micromechanical characterization of single-walled carbon nanotube reinforced ethylidene norbornene nanocomposites for self-healing applications," *Smart Mater. Struct.*, vol. 105028, no. 21, 2012.
- [100] D. T. Everitt, R. Luterbacher, T. S. Coope, R. S. Trask, D. F. Wass, and I. P. Bond, "Optimisation of epoxy blends for use in extrinsic self-healing fibre-reinforced composites," *Polymer (Guildf.)*, vol. 69, pp. 283–292, 2015.
- [101] L. Raimondo, M., De Nicola, F., Volponi, R., Binder, W., Michael, P., Russo, S. and Guadagno, "Self-Repairing CFRPs targeted towards structural aerospace applications," *Int. J. Struct. Integr.*, vol. 7, no. 5, pp. 656–670, 2016.
- [102] X. Hu, R. Liang, J. Li, Z. Liu, and G. Sun, "Highly Stretchable Self-Healing Nanocomposite Hydrogel Reinforced by 5 nm Particles," *ES Mater. Manuf.*, vol. 2, pp. 1–8, 2018.

- [103] C. Shao *et al.*, “Mussel-Inspired Cellulose Nanocomposite Tough Hydrogels with Synergistic Self-Healing, Adhesive, and Strain-Sensitive Properties,” *Chem. Mater.*, vol. 30, no. 9, pp. 3110–3121, May 2018.
- [104] X. Liu, B. He, Z. Wang, H. Tang, T. Su, and Q. Wang, “Tough nanocomposite ionogel-based actuator exhibits robust performance,” *Sci. Rep.*, vol. 4, pp. 1–7, 2014.
- [105] M. Sabzi, M. Babaahmadi, N. Samadi, G. R. Mahdavinia, M. Keramati, and N. Nikfarjam, “Graphene network enabled high speed electrical actuation of shape memory nanocomposite based on poly(vinyl acetate),” *Polym. Int.*, vol. 66, no. 5, pp. 665–671, 2017.
- [106] L. Zhao, J. Huang, T. Wang, W. Sun, and Z. Tong, “Multiple Shape Memory, Self-Healable, and Supertough PAA-GO-Fe₃+Hydrogel,” *Macromol. Mater. Eng.*, vol. 302, no. 2, pp. 1–9, 2017.
- [107] Y. Zhao *et al.*, “A Self-Healing Aqueous Lithium-Ion Battery,” *Angew. Chemie - Int. Ed.*, vol. 55, no. 46, pp. 14384–14388, 2016.
- [108] G. Cai, J. Wang, K. Qian, J. Chen, S. Li, and P. S. Lee, “Extremely Stretchable Strain Sensors Based on Conductive Self-Healing Dynamic Cross-Links Hydrogels for Human-Motion Detection,” *Adv. Sci.*, vol. 4, no. 2, p. 1600190, Feb. 2017.
- [109] J. Li, G. Zhang, R. Sun, and C.-P. Wong, “A covalently cross-linked reduced functionalized graphene oxide/polyurethane composite based on Diels–Alder chemistry and its potential application in healable flexible electronics,” *J. Mater. Chem. C*, vol. 5, no. 1, pp. 220–228, 2017.
- [110] Y. T. Rengui Peng, Yang Yu, Sheng Chen, Yingkui Yang, “Conductive nanocomposite hydrogels with self-healing property,” *RSC Adv.*, vol. 4, no. 66, pp. 35149–35155, 2014.
- [111] Y.-J. Liu, W.-T. Cao, M.-G. Ma, and P. Wan, “Ultrasensitive Wearable Soft Strain Sensors of Conductive, Self-healing, and Elastic Hydrogels with Synergistic ‘Soft and Hard’ Hybrid Networks,” *ACS Appl. Mater. Interfaces*, vol. 9, no. 30, pp. 25559–25570, Aug. 2017.
- [112] S. Wu *et al.*, “Ultrafast self-healing nanocomposites via infrared laser and their application in flexible electronics,” *ACS Appl. Mater. Interfaces*, vol. 9, no. 3, pp. 3040–3049, 2017.
- [113] S. Roy, A. Baral, and A. Banerjee, “An amino-acid-based self-healing hydrogel: Modulation of the self-healing properties by incorporating carbon-based nanomaterials,” *Chem. - A Eur. J.*, vol. 19, no. 44, pp. 14950–14957, 2013.
- [114] L. Han *et al.*, “Mussel-Inspired Adhesive and Tough Hydrogel Based on Nanoclay Confined Dopamine Polymerization,” *ACS Nano*, vol. 11, no. 3, pp. 2561–2574, 2017.
- [115] E. Zhang, T. Wang, L. Zhao, W. Sun, X. Liu, and Z. Tong, “Fast self-healing of graphene oxide-hectorite clay-poly(N,N -dimethylacrylamide) hybrid hydrogels realized by near-infrared irradiation,” *ACS Appl. Mater. Interfaces*, vol. 6, no. 24, pp. 22855–22861, 2014.
- [116] P. Chen *et al.*, “Double network self-healing graphene hydrogel by two step method for anticancer drug delivery,” *Mater. Technol.*, vol. 29, no. 4, pp. 210–213, 2014.
- [117] H. P. Cong, P. Wang, and S. H. Yu, “Stretchable and self-healing graphene oxide-polymer composite hydrogels: A dual-network design,” *Chem. Mater.*, vol. 25, no. 16, pp. 3357–3362, 2013.
- [118] L. Han *et al.*, “Tough, self-healable and tissue-adhesive hydrogel with tunable multifunctionality,” *NPG Asia Mater.*, vol. 9, no. 4, p. e372, 2017.

- [119] X. Jing, H. Y. Mi, B. N. Napiwocki, X. F. Peng, and L. S. Turng, "Mussel-inspired electroactive chitosan/graphene oxide composite hydrogel with rapid self-healing and recovery behavior for tissue engineering," *Carbon N. Y.*, vol. 125, pp. 557–570, 2017.
- [120] Y. Chen *et al.*, "Graphene Oxide Hybrid Supramolecular Hydrogels with Self-Healable, Bioadhesive and Stimuli-Responsive Properties and Drug Delivery Application," *Macromol. Mater. Eng.*, vol. 303, no. 8, pp. 1–11, 2018.
- [121] and G. S. Yuxi Xu, Qiong Wu, Yiqing Sun, Hua Bai, "Three-Dimensional Self-Assembly of Graphene Oxide and DNA into Multifunctional Hydrogels," *ACS Nano*, vol. 4, no. 12, pp. 7358–7362, 2010.
- [122] C. Hou, T. Huang, H. Wang, H. Yu, Q. Zhang, and Y. Li, "A strong and stretchable self-healing film with self-activated pressure sensitivity for potential artificial skin applications," *Sci. Rep.*, vol. 3, no. 1, pp. 21–25, 2013.
- [123] Y. M. Wang, M. Pan, X. Y. Liang, B. J. Li, and S. Zhang, "Electromagnetic Wave Absorption Coating Material with Self-Healing Properties," *Macromol. Rapid Commun.*, vol. 38, no. 23, pp. 1–8, 2017.
- [124] S. I. Seyed Shahabadi, J. Kong, and X. Lu, "Aqueous-Only, Green Route to Self-Healable, UV-Resistant, and Electrically Conductive Polyurethane/Graphene/Lignin Nanocomposite Coatings," *ACS Sustain. Chem. Eng.*, vol. 5, no. 4, pp. 3148–3157, 2017.
- [125] Z. Wei *et al.*, "Autonomous self-healing of poly(acrylic acid) hydrogels induced by the migration of ferric ions," *Polym. Chem.*, vol. 4, no. 17, pp. 4601–4605, 2013.
- [126] Q. Zheng, Z. Ma, and S. Gong, "Multi-stimuli-responsive self-healing metallo-supramolecular polymer nanocomposites," *J. Mater. Chem. A*, vol. 4, no. 9, pp. 3324–3334, 2016.
- [127] X. K. D. Hillewaere and F. E. Du Prez, "Fifteen chemistries for autonomous external self-healing polymers and composites," *Prog. Polym. Sci.*, vol. 49–50, pp. 121–153, 2015.
- [128] W.-L. Song *et al.*, "Flexible graphene/polymer composite films in sandwich structures for effective electromagnetic interference shielding," *Carbon N. Y.*, vol. 66, pp. 67–76, 2014.
- [129] X. Shen, R. Z. Gong, Y. Nie, and J. H. Nie, "Preparation and electromagnetic performance of coating of multiwall carbon nanotubes with iron nanogranule," *J. Magn. Magn. Mater.*, vol. 288, pp. 397–402, 2005.
- [130] G. Wang *et al.*, "Reduced Graphene Oxide–Polyurethane Nanocomposite Foam as a Reusable Photoreceiver for Efficient Solar Steam Generation," *Chem. Mater.*, vol. 29, no. 13, pp. 5629–5635, Jul. 2017.
- [131] C. Berger *et al.*, "Ultrathin Epitaxial Graphite: 2D Electron Gas Properties and a Route toward Graphene-based Nanoelectronics," *J. Phys. Chem. B*, vol. 108, no. 52, pp. 19912–19916, Dec. 2004.
- [132] K. S. Novoselov *et al.*, "Electric Field Effect in Atomically Thin Carbon Films," *Science (80-.)*, vol. 306, no. 5696, pp. 666–669, 2004.
- [133] X. Li *et al.*, "Large-Area Synthesis of High-Quality and Uniform Graphene Films on Copper Foils," *Science (80-.)*, vol. 324, no. 5932, pp. 1312–1314, 2009.
- [134] L. Zhang, J. Liang, Y. Huang, Y. Ma, Y. Wang, and Y. Chen, "Size-controlled synthesis of graphene oxide sheets on a large scale using chemical exfoliation," *Carbon N. Y.*, vol. 47, no. 14, pp. 3365–3368, 2009.
- [135] W. S. Hummers and R. E. Offeman, "Preparation of Graphitic Oxide," *J. Am. Chem. Soc.*, vol. 80, no. 6, p. 1339, Mar. 1958.
- [136] Y. Yue *et al.*, "Highly Self-Healable 3D Microsupercapacitor with MXene–

- Graphene Composite Aerogel,” *ACS Nano*, vol. 12, no. 5, pp. 4224–4232, May 2018.
- [137] Y.-G. Luan, X.-A. Zhang, S.-L. Jiang, J.-H. Chen, and Y.-F. Lyu, “Self-healing Supramolecular Polymer Composites by Hydrogen Bonding Interactions between Hyperbranched Polymer and Graphene Oxide,” *Chinese J. Polym. Sci.*, vol. 36, no. 5, pp. 584–591, May 2018.
- [138] C. Luo, C.-N. Yeh, J. M. L. Baltazar, C.-L. Tsai, and J. Huang, “A Cut-and-Paste Approach to 3D Graphene-Oxide-Based Architectures,” *Adv. Mater.*, vol. 30, no. 15, p. 1706229, 2018.
- [139] Z. Xiang, L. Zhang, Y. Li, T. Yuan, W. Zhang, and J. Sun, “Reduced Graphene Oxide-Reinforced Polymeric Films with Excellent Mechanical Robustness and Rapid and Highly Efficient Healing Properties,” *ACS Nano*, vol. 11, no. 7, pp. 7134–7141, Jul. 2017.
- [140] Y. Zhu, C. Yao, J. Ren, C. Liu, and L. Ge, “Graphene improved electrochemical property in self-healing multilayer polyelectrolyte film,” *Colloids Surfaces A Physicochem. Eng. Asp.*, vol. 465, pp. 26–31, 2015.
- [141] Y. Peng *et al.*, “Hydrothermal Synthesis of MoS₂ and Its Pressure-Related Crystallization,” *J. Solid State Chem.*, vol. 159, no. 1, pp. 170–173, 2001.
- [142] L. Huang *et al.*, “Multichannel and Repeatable Self-Healing of Mechanical Enhanced Graphene-Thermoplastic Polyurethane Composites,” *Adv. Mater.*, vol. 25, no. 15, pp. 2224–2228, Apr. 2013.
- [143] M. Noack *et al.*, “Light-Fueled, Spatiotemporal Modulation of Mechanical Properties and Rapid Self-Healing of Graphene-Doped Supramolecular Elastomers,” *Adv. Funct. Mater.*, vol. 27, no. 25, p. 1700767, 2017.
- [144] H. Cheng, Y. Huang, Q. Cheng, G. Shi, L. Jiang, and L. Qu, “Self-Healing Graphene Oxide Based Functional Architectures Triggered by Moisture,” *Adv. Funct. Mater.*, vol. 27, no. 42, p. 1703096, 2017.
- [145] T. Yu, G. S. Wang, L. Liu, P. Wang, Z. Y. Wei, and M. Qi, “Synthesis of PCL / Graphene Oxide Composites by In Situ Polymerization,” in *Advances in Environmental Science and Engineering*, 2012, vol. 518, pp. 837–840.
- [146] S. Wu, J. Li, G. Zhang, R. Sun, and C. Wong, “High mechanical strength and high dielectric graphene/polyurethane composites healed by near infrared laser,” in *2016 17th International Conference on Electronic Packaging Technology (ICEPT)*, 2016, pp. 157–161.
- [147] C. Lin *et al.*, “A self-healable nanocomposite based on dual-crosslinked Graphene Oxide/Polyurethane,” *Polymer (Guildf.)*, vol. 127, pp. 241–250, 2017.
- [148] J. Li *et al.*, “In situ polymerization of mechanically reinforced, thermally healable graphene oxide/polyurethane composites based on Diels–Alder chemistry,” *J. Mater. Chem. A*, vol. 2, no. 48, pp. 20642–20649, 2014.
- [149] C. Hou, Y. Duan, Q. Zhang, H. Wang, and Y. Li, “Bio-applicable and electroactive near-infrared laser-triggered self-healing hydrogels based on graphene networks,” *J. Mater. Chem.*, vol. 22, no. 30, pp. 14991–14996, 2012.
- [150] Z. Li, Z. Xu, Y. Liu, R. Wang, and C. Gao, “Multifunctional non-woven fabrics of interfused graphene fibres,” *Nat. Commun.*, vol. 7, p. 13684, Nov. 2016.
- [151] Y. Liu *et al.*, “Solder-free electrical Joule welding of macroscopic graphene assemblies,” *Mater. Today Nano*, vol. 3, pp. 1–8, 2018.
- [152] V. K. A. S. Ghosh, D. Sanghamitra, M. V. P. Kumar, and A. Amit, “Self-healing phenomena of graphene: potential and applications,” *Open Physics*, vol. 14, p. 364, 2016.
- [153] C. S. Boland *et al.*, “Sensitive electromechanical sensors using viscoelastic graphene-polymer nanocomposites,” *Science (80-.)*, vol. 354, no. 6317, pp.

- 1257–1260, 2016.
- [154] L. Chen, L. Si, F. Wu, S. Y. Chan, P. Yu, and B. Fei, “Electrical and mechanical self-healing membrane using gold nanoparticles as localized ‘nano-heaters,’” *J. Mater. Chem. C*, vol. 4, no. 42, pp. 10018–10025, 2016.
- [155] C. Lin *et al.*, “NIR induced self-healing electrical conductivity polyurethane/graphene nanocomposites based on Diels–Alder reaction,” *Polymer (Guildf)*, vol. 140, pp. 150–157, 2018.
- [156] N. Samadi, M. Sabzi, and M. Babaahmadi, “Self-healing and tough hydrogels with physically cross-linked triple networks based on Agar/PVA/Graphene,” *Int. J. Biol. Macromol.*, vol. 107, pp. 2291–2297, 2018.
- [157] C. Wang *et al.*, “A Rapid and Efficient Self-Healing Thermo-Reversible Elastomer Crosslinked with Graphene Oxide,” *Adv. Mater.*, vol. 25, no. 40, pp. 5785–5790, Oct. 2013.
- [158] F. Fan, C. Zhou, X. Wang, and J. Szpunar, “Layer-by-Layer Assembly of a Self-Healing Anticorrosion Coating on Magnesium Alloys,” *ACS Appl. Mater. Interfaces*, vol. 7, no. 49, pp. 27271–27278, Dec. 2015.
- [159] N. Kargarfard, N. Diedrich, H. Rupp, D. Döhler, and H. W. Binder, “Improving Kinetics of ‘Click-Crosslinking’ for Self-Healing Nanocomposites by Graphene-Supported Cu-Nanoparticles,” *Polymers*, vol. 10, no. 1. 2018.
- [160] E. D’Elia, S. Barg, N. Ni, V. G. Rocha, and E. Saiz, “Self-Healing Graphene-Based Composites with Sensing Capabilities,” *Adv. Mater.*, vol. 27, no. 32, pp. 4788–4794, 2015.
- [161] S. Rana, D. Döhler, A. S. Nia, M. Nasir, M. Beiner, and W. H. Binder, “‘Click’-Triggered Self-Healing Graphene Nanocomposites,” *Macromol. Rapid Commun.*, vol. 37, no. 21, pp. 1715–1722, 2016.
- [162] L. Yuan, G. Liang, J. Xie, L. Li, and J. Guo, “Preparation and characterization of poly(urea-formaldehyde) microcapsules filled with epoxy resins,” *Polymer (Guildf)*, vol. 47, no. 15, pp. 5338–5349, 2006.
- [163] D. Y. Wu, S. Meure, and D. Solomon, “Self-healing polymeric materials: A review of recent developments,” *Prog. Polym. Sci.*, vol. 33, no. 5, pp. 479–522, 2008.
- [164] J. M. Asua, “Miniemulsion polymerization,” *Prog. Polym. Sci.*, vol. 27, no. 7, pp. 1283–1346, 2002.
- [165] Q. Li, A. K. Mishra, N. H. Kim, T. Kuila, K. Lau, and J. H. Lee, “Effects of processing conditions of poly(methylmethacrylate) encapsulated liquid curing agent on the properties of self-healing composites,” *Compos. Part B Eng.*, vol. 49, pp. 6–15, 2013.
- [166] A. Shulkin and H. D. H. Stöver, “Polymer microcapsules by interfacial polyaddition between styrene–maleic anhydride copolymers and amines,” *J. Memb. Sci.*, vol. 209, no. 2, pp. 421–432, 2002.
- [167] Z. Yang, J. Hollar, X. He, and X. Shi, “A self-healing cementitious composite using oil core/silica gel shell microcapsules,” *Cem. Concr. Compos.*, vol. 33, no. 4, pp. 506–512, 2011.
- [168] E. B. Murphy and F. Wudl, “The world of smart healable materials,” *Prog. Polym. Sci.*, vol. 35, no. 1, pp. 223–251, 2010.
- [169] J. E. Flinn and H. Nack, “What is happening in microencapsulation,” *Chem. Eng.*, vol. 171, no. 8, 1967.
- [170] P. B. O’Donnell and J. W. McGinity, “Preparation of microspheres by the solvent evaporation technique,” *Adv. Drug Deliv. Rev.*, vol. 28, no. 1, pp. 25–42, 1997.
- [171] R. Dubey, “Microencapsulation technology and applications,” *Def. Sci. J.*, vol. 59, no. 1, pp. 82–95, 2009.

- [172] Q. Li, Siddaramaiah, N. H. Kim, D. Hui, and J. H. Lee, "Effects of dual component microcapsules of resin and curing agent on the self-healing efficiency of epoxy," *Compos. Part B Eng.*, vol. 55, pp. 79–85, 2013.
- [173] Y. Zhao, J. Fickert, K. Landfester, and D. Crespy, "Encapsulation of Self-Healing Agents in Polymer Nanocapsules," *Small*, vol. 8, no. 19, pp. 2954–2958, Oct. 2012.
- [174] D. Y. Zhu, M. Z. Rong, and M. Q. Zhang, "Self-healing polymeric materials based on microencapsulated healing agents: From design to preparation," *Prog. Polym. Sci.*, vol. 49–50, pp. 175–220, 2014.
- [175] S. Neuser, E. Manfredi, and V. Michaud, "Characterization of solvent-filled polyurethane/urea–formaldehyde core–shell composites," *Mater. Chem. Phys.*, vol. 143, no. 3, pp. 1018–1025, 2014.
- [176] X. Liu, X. Sheng, J. K. Lee, and M. R. Kessler, "Synthesis and Characterization of Melamine-Urea-Formaldehyde Microcapsules Containing ENB-Based Self-Healing Agents," *Macromol. Mater. Eng.*, vol. 294, no. 6-7, pp. 389–395, Jul. 2009.
- [177] B. Di Credico, M. Levi, and S. Turri, "An efficient method for the output of new self-repairing materials through a reactive isocyanate encapsulation," *Eur. Polym. J.*, vol. 49, no. 9, pp. 2467–2476, 2013.
- [178] H. Wei *et al.*, "Advanced micro/nanocapsules for self-healing smart anticorrosion coatings," *J. Mater. Chem. A*, vol. 3, no. 2, pp. 469–480, 2015.
- [179] B. C. Dave, B. Dunn, J. S. Valentine, and J. I. Zink, "Sol-gel encapsulation methods for biosensors," *Anal. Chem.*, vol. 66, no. 22, pp. 1120A-1127A, Nov. 1994.
- [180] H. Zhang, X. Wang, and D. Wu, "Silica encapsulation of n-octadecane via sol–gel process: A novel microencapsulated phase-change material with enhanced thermal conductivity and performance," *J. Colloid Interface Sci.*, vol. 343, no. 1, pp. 246–255, 2010.
- [181] A. C. Pierre, "The sol-gel encapsulation of enzymes," *Biocatal. Biotransformation*, vol. 22, no. 3, pp. 145–170, May 2004.
- [182] K. P. Peterson, C. M. Peterson, and E. J. A. Pope, "Silica Sol-Gel Encapsulation of Pancreatic Islets," *Proc. Soc. Exp. Biol. Med.*, vol. 218, no. 4, pp. 365–369, Sep. 1998.
- [183] G. O. Wilson, M. M. Caruso, N. T. Reimer, S. R. White, N. R. Sottos, and J. S. Moore, "Evaluation of Ruthenium Catalysts for Ring-Opening Metathesis Polymerization-Based Self-Healing Applications," no. 3, pp. 3288–3297, 2008.
- [184] J. D. Rule and J. S. Moore, "ROMP Reactivity of endo - and exo - Dicyclopentadiene," pp. 7878–7882, 2002.
- [185] X. Sheng, M. R. Kessler, and J. K. Lee, "The influence of cross-linking agents on ring-opening metathesis polymerized thermosets," *J. Therm. Anal. Calorim.*, vol. 89, no. 2, pp. 459–464, 2007.
- [186] J. K. Lee, X. Liu, S. H. Yoon, and M. R. Kessler, "Thermal analysis of ring-opening metathesis polymerized healing agents," *J. Polym. Sci. Part B Polym. Phys.*, vol. 45, no. 14, pp. 1771–1780, Jul. 2007.
- [187] G. E. Larin, N. Bernklau, M. R. Kessler, and J. C. DiCesare, "Rheokinetics of ring-opening metathesis polymerization of norbornene-based monomers intended for self-healing applications," *Polym. Eng. Sci.*, vol. 46, no. 12, pp. 1804–1811, Dec. 2006.
- [188] M. Raimondo, L. Guadagno, V. Ponte, D. Melillo, and I. Industriale, "Healing Efficiency of Epoxy-Based Materials for Structural Applications," vol. 84084, no. C1, 2013.

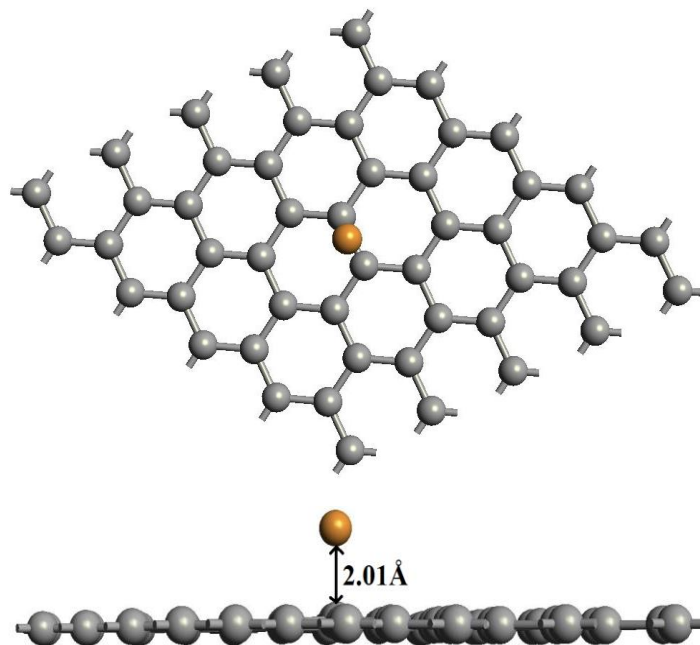
- [189] C. Dry, "Procedures Developed for Self-Repair of Polymeric Matrix Composite Materials," *Compos. Struct.*, vol. 35, pp. 263–269, 1996.
- [190] Y. C. Yuan, M. Z. Rong, M. Q. Zhang, B. Chen, G. C. Yang, and X. M. Li, "Healing Polymeric Materials Using Epoxy/Mercaptan as the Healant," *Macromolecules*, no. 41, pp. 5197–5202, 2008.
- [191] X. K. D. Hillewaere, R. F. A. Teixeira, L. T. T. Nguyen, J. A. Ramos, H. Rahier, and F. E. Du Prez, "Autonomous self-healing of epoxy thermosets with thiol-isocyanate chemistry," *Adv. Funct. Mater.*, vol. 24, no. 35, pp. 5575–5583, 2014.
- [192] D. Döhler, P. Michael, and W. H. Binder, "Autocatalysis in the room temperature copper(I)-catalyzed alkyne-azide 'click' cycloaddition of multivalent poly(acrylate)s and poly(isobutylene)s," *Macromolecules*, vol. 45, no. 8, pp. 3335–3345, 2012.
- [193] H. C. Kolb, M. G. Finn, and K. B. Sharpless, "Click Chemistry: Diverse Chemical Function from a Few Good Reactions," *Angew. Chemie - Int. Ed.*, vol. 40, no. 11, pp. 2004–2021, 2001.
- [194] J. H. Daly, D. Hayward, and R. A. Pethrick, "Prediction of the rheological properties of a curing thermoset system," *Macromolecules*, vol. 46, no. 9, pp. 3621–3630, 2013.
- [195] M. Gragert, M. Schunack, and W. H. Binder, "Azide/alkyne-"Click"-reactions of encapsulated reagents: Toward self-healing materials," *Macromol. Rapid Commun.*, vol. 32, no. 5, pp. 419–425, 2011.
- [196] M. Schunack, M. Gragert, D. Döhler, P. Michael, and W. H. Binder, "Low-temperature Cu(I)-catalyzed 'click' reactions for self-healing polymers," *Macromol. Chem. Phys.*, vol. 213, no. 2, pp. 205–214, 2012.
- [197] S. Matsumura *et al.*, "Ionomers for proton exchange membrane fuel cells with sulfonic acid groups on the end-groups: Novel branched poly(ether-ketone)s," *Am. Chem. Soc. Polym. Prepr. Div. Polym. Chem.*, vol. 49, no. 1, pp. 511–512, 2008.
- [198] Q. Wei *et al.*, "Self-healing hyperbranched poly(aryltriazole)s," *Sci. Rep.*, vol. 3, p. 1093, 2013.
- [199] F. Herbst, D. Döhler, P. Michael, and W. H. Binder, "Self-healing polymers via supramolecular forces," *Macromol. Rapid Commun.*, vol. 34, no. 3, pp. 203–220, 2013.
- [200] J. -M Lehn, "Supramolecular Chemistry—Scope and Perspectives Molecules, Supermolecules, and Molecular Devices (Nobel Lecture)," *Angew. Chemie Int. Ed. English*, vol. 27, no. 1, pp. 89–112, 1988.
- [201] G. Armstrong and M. Buggy, "Hydrogen-bonded supramolecular polymers: A literature review," *J. Mater. Sci.*, vol. 40, no. 3, pp. 547–559, 2005.
- [202] N. Roy, B. Bruchmann, and J. M. Lehn, "DYNAMERS: dynamic polymers as self-healing materials," *Chem. Soc. Rev.*, vol. 44, no. 11, pp. 3786–3807, 2015.
- [203] F. Herbst and W. H. Binder, "Comparing solution and melt-state association of hydrogen bonds in supramolecular polymers," *Polym. Chem.*, vol. 4, p. 3602, 2013.
- [204] G. G. Hammes and a C. Park, "Kinetic studies of hydrogen bonding. 1- Cyclohexyluracil and 9-ethyladenine.," *J. Am. Chem. Soc.*, vol. 90, no. 15, pp. 4151–7, 1968.
- [205] G. M. L. Van Gemert, J. W. Peeters, S. H. M. Söntjens, H. M. Janssen, and A. W. Bosman, "Self-healing supramolecular polymers in action," *Macromol. Chem. Phys.*, vol. 213, no. 2, pp. 234–242, 2012.
- [206] S. Q. Wang, S. Ravindranath, Y. Wang, and P. Boukany, "New theoretical considerations in polymer rheology: Elastic breakdown of chain entanglement network," *J. Chem. Phys.*, vol. 127, no. 6, 2007.

- [207] S. Sivakova, D. A. Bohnsack, M. E. Mackay, P. Suwanmala, and S. J. Rowan, "Utilization of a combination of weak hydrogen-bonding interactions and phase segregation to yield highly thermosensitive supramolecular polymers," *J. Am. Chem. Soc.*, vol. 127, no. 51, pp. 18202–18211, 2005.
- [208] F. Herbst *et al.*, "Aggregation and chain dynamics in supramolecular polymers by dynamic rheology: Cluster formation and self-Aggregation," *Macromolecules*, vol. 43, no. 23, pp. 10006–10016, 2010.
- [209] F. Herbst, S. Seiffert, and W. H. Binder, "Dynamic supramolecular poly(isobutylene)s for self-healing materials," *Polym. Chem.*, vol. 3, no. 11, p. 3084, 2012.
- [210] S. Burattini *et al.*, "A self-repairing, supramolecular polymer system: healability as a consequence of donor-acceptor pi-pi stacking interactions," *Chem. Commun.*, no. 44, pp. 6717–6719, 2009.
- [211] S. Burattini, B. W. Greenland, W. Hayes, M. E. MacKay, S. J. Rowan, and H. M. Colquhoun, "A supramolecular polymer based on tweezer-type pi-pi stacking interactions: Molecular design for healability and enhanced toughness," *Chem. Mater.*, vol. 23, no. 1, pp. 6–8, 2011.
- [212] R. J. Varley and S. van der Zwaag, "Autonomous damage initiated healing in a thermo-responsive ionomer," *Polym. Int.*, vol. 59, no. 8, pp. 1031–1038, 2010.
- [213] S. D. Bergman and F. Wudl, "Mendable polymers," *J. Mater. Chem.*, vol. 18, no. 1, pp. 41–62, 2008.
- [214] M. M. Caruso, B. J. Blaiszik, S. R. White, N. R. Sottos, and J. S. Moore, "Full recovery of fracture toughness using a nontoxic solvent-based self-healing system," *Adv. Funct. Mater.*, vol. 18, no. 13, pp. 1898–1904, 2008.
- [215] S. H. Cho, S. R. White, and P. V Braun, "Room-Temperature Polydimethylsiloxane-Based Self-Healing Polymers," *Chem. Mater.*, vol. 24, no. 21, pp. 4209–4214, 2012.
- [216] H. Jin, C. L. Mangun, A. S. Griffin, J. S. Moore, N. R. Sottos, and S. R. White, "Thermally stable autonomic healing in epoxy using a dual-microcapsule system," *Adv. Mater.*, vol. 26, no. 2, pp. 282–287, 2014.
- [217] S. Chen and W. H. Binder, "Dynamic Ordering and Phase Segregation in Hydrogen-Bonded Polymers," *Acc. Chem. Res.*, vol. 49, no. 7, pp. 1409–1420, 2016.
- [218] Z. P. Zhang, Y. Lu, M. Z. Rong, and M. Q. Zhang, "A thermally remendable and reprocessible crosslinked methyl methacrylate polymer based on oxygen insensitive dynamic reversible C–ON bonds," *RSC Adv.*, vol. 6, no. 8, pp. 6350–6357, 2016.
- [219] V. A. Online, D. F. Beneito, and J. J. Vilatela, "Real time monitoring of click chemistry self-healing in polymer composites," *J. Mater. Chem. A*, vol. 2, no. 11, pp. 3881–3887, 2014.
- [220] S. Billiet, W. Van Camp, X. K. D. Hillewaere, H. Rahier, and F. E. Du Prez, "Development of optimized autonomous self-healing systems for epoxy materials based on maleimide chemistry," *Polymer (Guildf)*, vol. 53, no. 12, pp. 2320–2326, 2012.
- [221] N. B. Pramanik, G. B. Nando, and N. K. Singha, "Self-healing polymeric gel via RAFT polymerization and Diels-Alder click chemistry," *Polym. (United Kingdom)*, vol. 69, pp. 349–356, 2014.
- [222] Z. Q. Lei, H. P. Xiang, Y. J. Yuan, M. Z. Rong, and M. Q. Zhang, "Room-Temperature Self-Healable and Remoldable Cross-linked Polymer Based on the Dynamic Exchange of Disulfide Bonds," *Chem. Mater.*, vol. 26, no. 6, pp. 2038–2046, 2014.

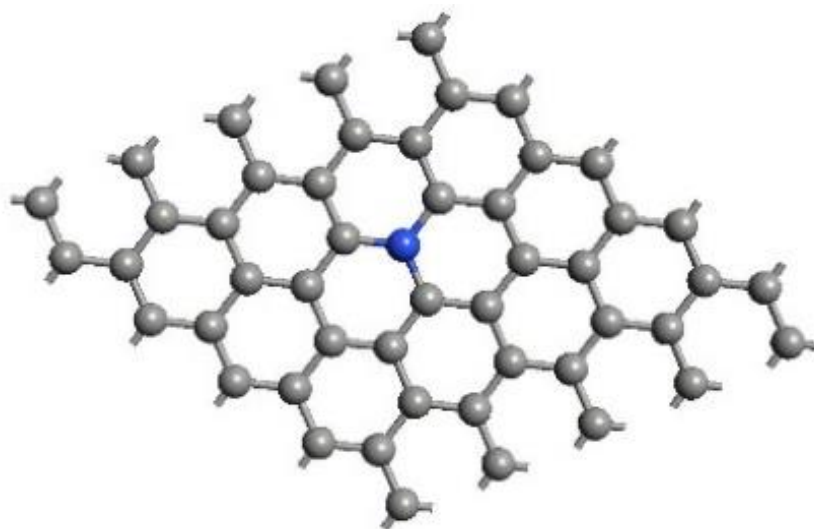
- [223] B. T. Michal, C. A. Jaye, E. J. Spencer, and S. J. Rowan, "Inherently Photohealable and Thermal Shape-Memory Polydisulfide Networks," *ACS Macro Lett.*, vol. 2, no. 8, pp. 694–699, 2013.
- [224] S. Banerjee *et al.*, "Photoinduced smart, self-healing polymer sealant for photovoltaics," *ACS Appl. Mater. Interfaces*, vol. 7, no. 3, pp. 2064–2072, 2015.
- [225] D. E. Bergbreiter, P. N. Hamilton, and N. M. Koshti, "Self-Separating Homogeneous Copper (I) Catalysts," *J. Am. Chem. Soc.*, vol. 129, no. 35, pp. 10666–10667, Sep. 2007.
- [226] Y. Li, H. Wang, L. Xie, Y. Liang, G. Hong, and H. Dai, "MoS₂ Nanoparticles Grown on Graphene: An Advanced Catalyst for the Hydrogen Evolution Reaction," *J. Am. Chem. Soc.*, vol. 133, no. 19, pp. 7296–7299, May 2011.
- [227] L. He, F. Weniger, H. Neumann, and M. Beller, "Synthesis, characterization, and application of metal nanoparticles supported on nitrogen-doped carbon: catalysis beyond electrochemistry," *Angew. Chemie Int. Ed.*, vol. 55, no. 41, pp. 12582–12594, 2016.
- [228] N. S. K. Gowthaman, M. A. Raj, and S. A. John, "Nitrogen-Doped Graphene as a Robust Scaffold for the Homogeneous Deposition of Copper Nanostructures: A Nonenzymatic Disposable Glucose Sensor," *ACS Sustain. Chem. Eng.*, vol. 5, no. 2, pp. 1648–1658, 2017.
- [229] A. Shaygan Nia, S. Rana, D. Döhler, X. Noifalisse, A. Belfiore, and W. H. Binder, "Click chemistry promoted by graphene supported copper nanomaterials," *Chem. Commun.*, vol. 50, no. 97, pp. 15374–15377, 2014.
- [230] D. Jiang *et al.*, "Enhanced non-enzymatic glucose sensing based on copper nanoparticles decorated nitrogen-doped graphene," *Biosens. Bioelectron.*, vol. 54, pp. 273–278, 2014.
- [231] M. K. Rabchinskii *et al.*, "Nanoscale Perforation of Graphene Oxide During Photoreduction Process in Nanoscale Perforation of Graphene Oxide during Photoreduction Process in the Argon Atmosphere," *J. Phys. Chem. C*, vol. 120, no. 49, pp. 28261–28269, 2016.
- [232] A. Shaygannia *et al.*, "Carbon-Supported Copper Nanomaterials: Recyclable Catalysts for Huisgen [3+2] Cycloaddition Reactions," *Chem. - A Eur. J.*, vol. 21, no. 30, pp. 10763–10770, 2015.
- [233] S. Halila, M. Manguian, S. Fort, S. Cottaz, and T. Hamaide, "Syntheses by Chemistry of Polyorganosiloxanes and Their Surfactant Properties," no. Umr 5223, pp. 1–13, 2008.
- [234] W. Koch and M. C. Holthausen, *A chemist's guide to density functional theory*. John Wiley & Sons, 2015.
- [235] K. Capelle, "A bird's-eye view of density-functional theory," *Brazilian Journal of Physics*, vol. 36, scielo, pp. 1318–1343, 2006.
- [236] [Http://www.atomistix.com/](http://www.atomistix.com/), "No Title."
- [237] J. E. Hein and V. V Fokin, "Copper-catalyzed azide–alkyne cycloaddition (CuAAC) and beyond: new reactivity of copper(i) acetylides," *Chem. Soc. Rev.*, vol. 39, no. 4, pp. 1302–1315, 2010.
- [238] N. Domun, H. Hadavinia, T. Zhang, T. Sainsbury, G. H. Liaghat, and S. Vahid, "Improving the fracture toughness and the strength of epoxy using nanomaterials – a review of the current status," *Nanoscale*, vol. 7, no. 23, pp. 10294–10329, 2015.
- [239] B. J. Blaiszik, N. R. Sottos, and S. R. White, "Nanocapsules for self-healing materials," *Compos. Sci. Technol.*, vol. 68, no. 3–4, pp. 978–986, 2008.
- [240] F. Ghadami, M. R. Dadfar, and M. Kazazi, "Hot-cured epoxy-nanoparticle-filled nanocomposites: Fracture toughness behavior," *Eng. Fract. Mech.*, vol. 162,

- pp. 193–200, 2016.
- [241] F. Yavari, M. A. Rafiee, J. Rafiee, Z.-Z. Yu, and N. Koratkar, “Dramatic Increase in Fatigue Life in Hierarchical Graphene Composites,” *ACS Appl. Mater. Interfaces*, vol. 2, no. 10, pp. 2738–2743, Oct. 2010.
- [242] W. H. Binder and R. Sachsenhofer, “‘Click’ Chemistry in Polymer and Materials Science,” *Macromol. Rapid Commun.*, vol. 28, pp. 15–54, 2007.
- [243] A. Shaygan Nia, S. Rana, D. Döhler, W. Osim, and W. H. Binder, “Nanocomposites via a direct graphene-promoted ‘click’-reaction,” *Polym. (United Kingdom)*, vol. 79, pp. 21–28, 2015.
- [244] N. Kargarfard, N. Diedrich, H. Rupp, D. Döhler, and W. H. Binder, “Improving kinetics of ‘Click-Crosslinking’ for self-healing nanocomposites by graphene-supported Cu-nanoparticles,” *Polymers (Basel)*, vol. 10, no. 1, 2017.
- [245] S. Neumann, D. Döhler, D. Ströhl, and W. H. Binder, “Chelation-assisted CuAAC in star-shaped polymers enables fast self-healing at low temperatures,” *Polym. Chem.*, vol. 7, pp. 2342–2351, 2016.
- [246] S. K. Dolui, Bhaskar Jyoti Saikia, “Preparation and characterization of an azide–alkyne cycloaddition based self-healing system via a semiencapsulation method,” *RSC Adv.*, vol. 5, no. 112, pp. 92480–92489, 2015.
- [247] M. Samadzadeh, S. H. Boura, M. Peikari, S. M. Kasiriha, and A. Ashrafi, “A review on self-healing coatings based on micro/nanocapsules,” *Prog. Org. Coatings*, vol. 68, no. 3, pp. 159–164, 2010.
- [248] W. Li *et al.*, “Effectively Exerting the Reinforcement of Dopamine Reduced Graphene Oxide on Epoxy-Based Composites via Strengthened Interfacial Bonding,” *ACS Appl. Mater. Interfaces*, vol. 8, no. 20, pp. 13037–13050, May 2016.
- [249] M. Jalalvand, G. Czél, and M. R. Wisnom, “Numerical modelling of the damage modes in UD thin carbon/glass hybrid laminates,” *Compos. Sci. Technol.*, vol. 94, pp. 39–47, 2014.
- [250] A. Shaygan Nia *et al.*, “Carbon-Supported Copper Nanomaterials: Recyclable Catalysts for Huisgen [3+2] Cycloaddition Reactions,” *Chem. – A Eur. J.*, vol. 21, no. 30, pp. 10763–10770, Jul. 2015.
- [251] N. W. Bartlett *et al.*, “A 3D-printed, functionally graded soft robot powered by combustion,” *Science (80-.)*, vol. 349, no. 6244, pp. 161–165, 2015.
- [252] X. Wang, M. Jiang, Z. Zhou, J. Gou, and D. Hui, “3D printing of polymer matrix composites: A review and prospective,” *Compos. Part B Eng.*, vol. 110, pp. 442–458, 2017.
- [253] Fatemeh Hamidi and Farhad Aslani, “Additive manufacturing of cementitious composites_ Materials, methods, potentials, and challenges — the UWA Profiles and Research Repository,” *Constr. Build. Mater.*, vol. 218, pp. 582–609, 2019.
- [254] S. Bodkhe, G. Turcot, F. P. Gosselin, and D. Therriault, “One-Step Solvent Evaporation-Assisted 3D Printing of Piezoelectric PVDF Nanocomposite Structures,” *ACS Appl. Mater. Interfaces*, vol. 9, no. 24, pp. 20833–20842, Jun. 2017.
- [255] J. H. Martin, B. D. Yahata, J. M. Hundley, J. A. Mayer, T. A. Schaedler, and T. M. Pollock, “3D printing of high-strength aluminium alloys,” *Nature*, vol. 549, no. 7672, pp. 365–369, 2017.

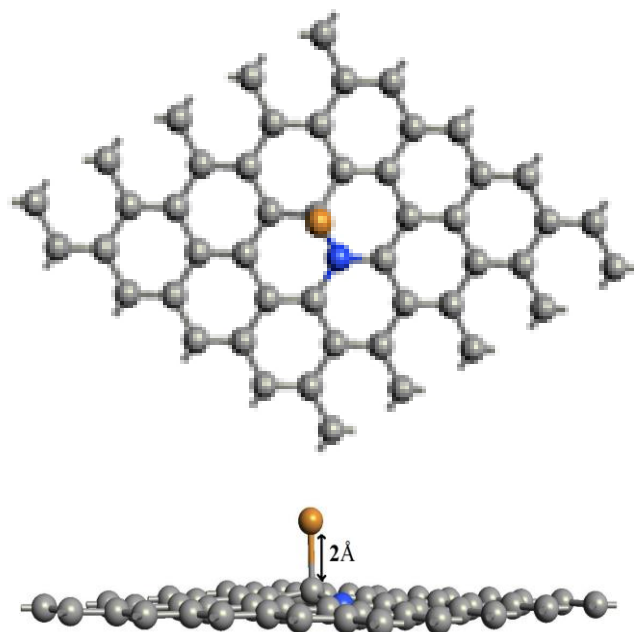
APPENDIX



(a)

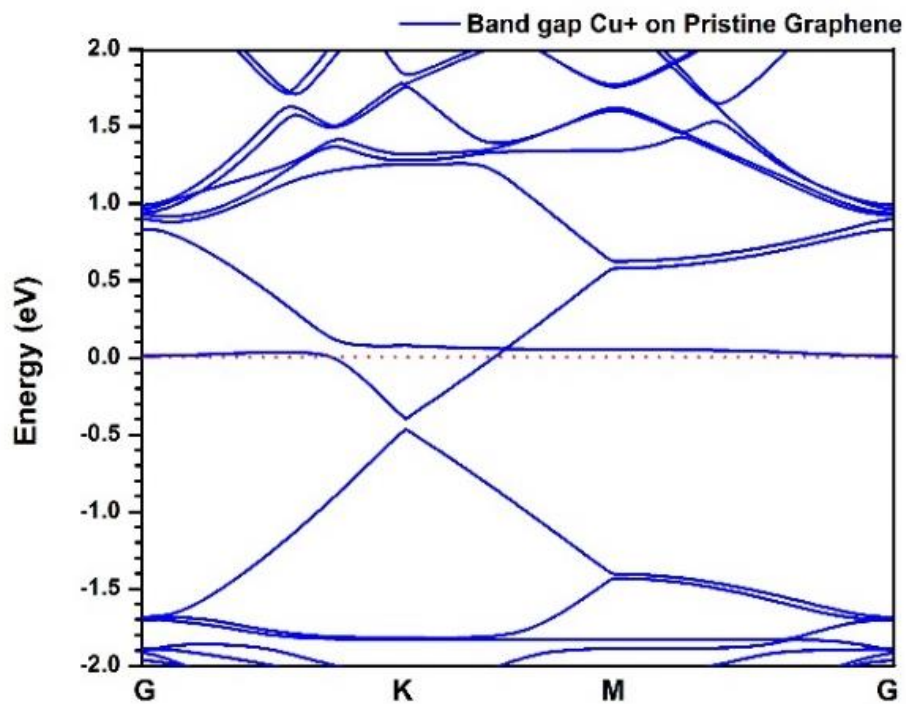


(b)

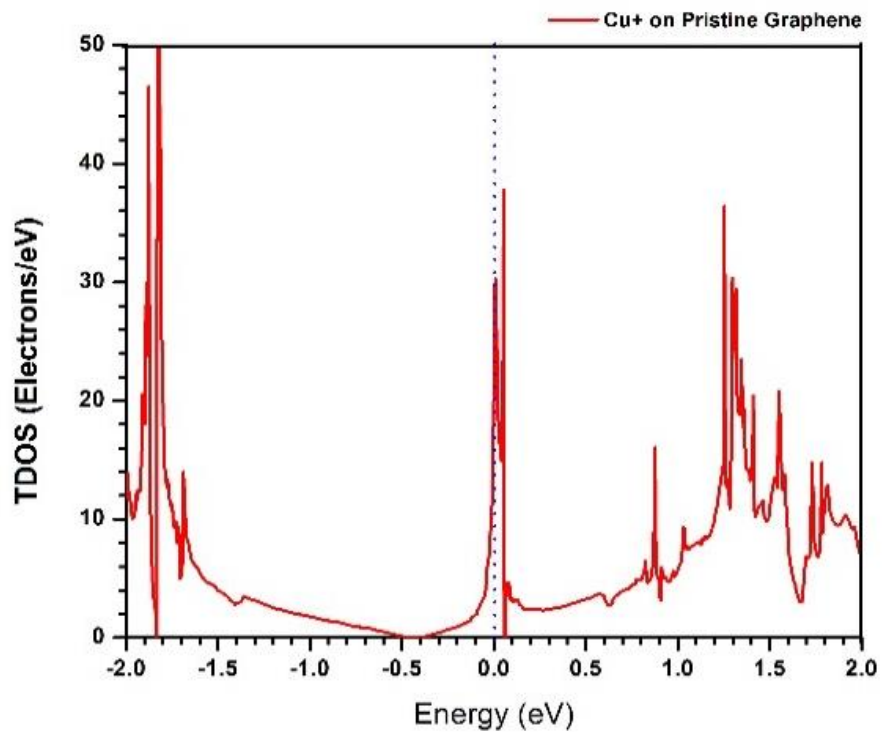


(C)

Appendix 1 (a) Cu^+ adsorption on pristine graphene, (b) NG, (c) Cu^+ adsorption on NG

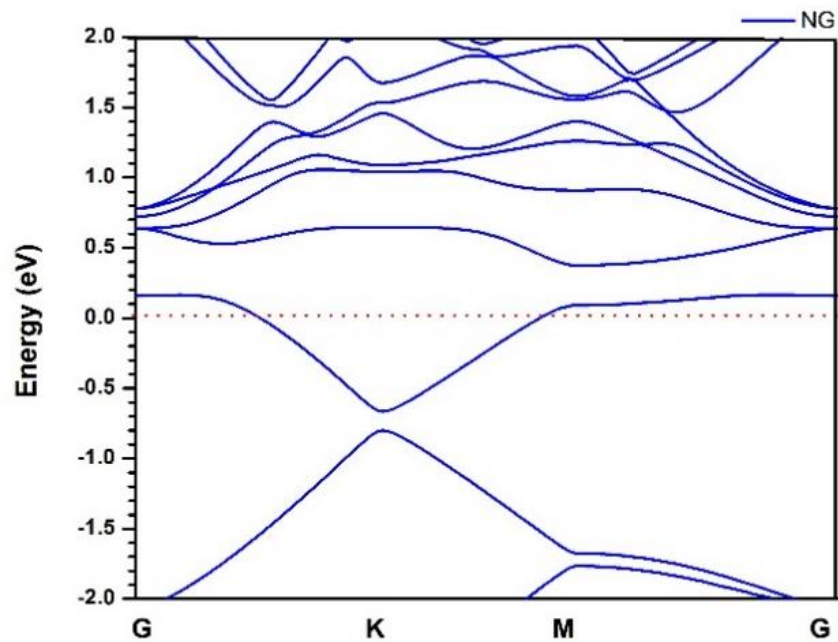


(a)

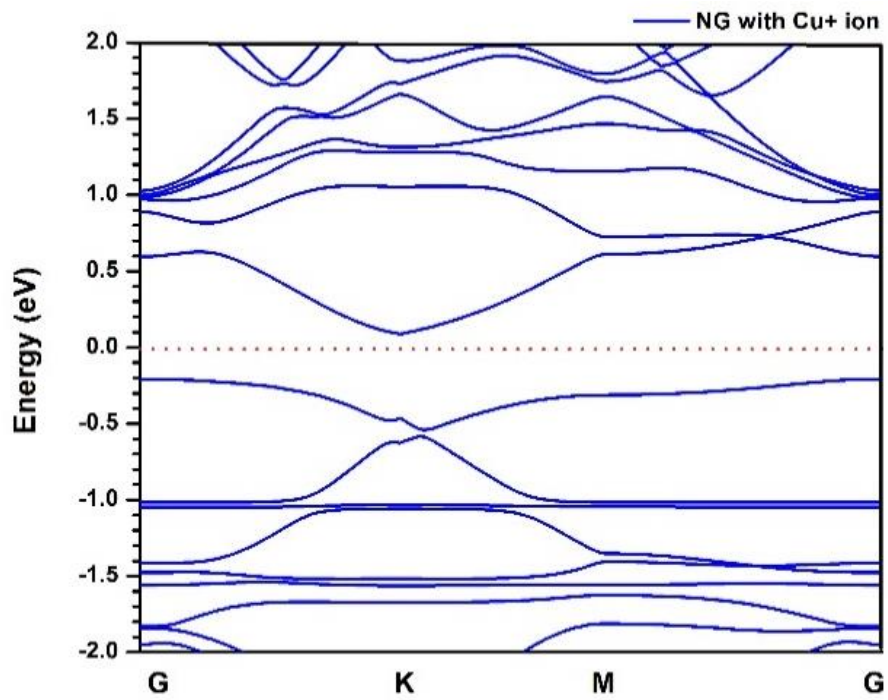


(b)

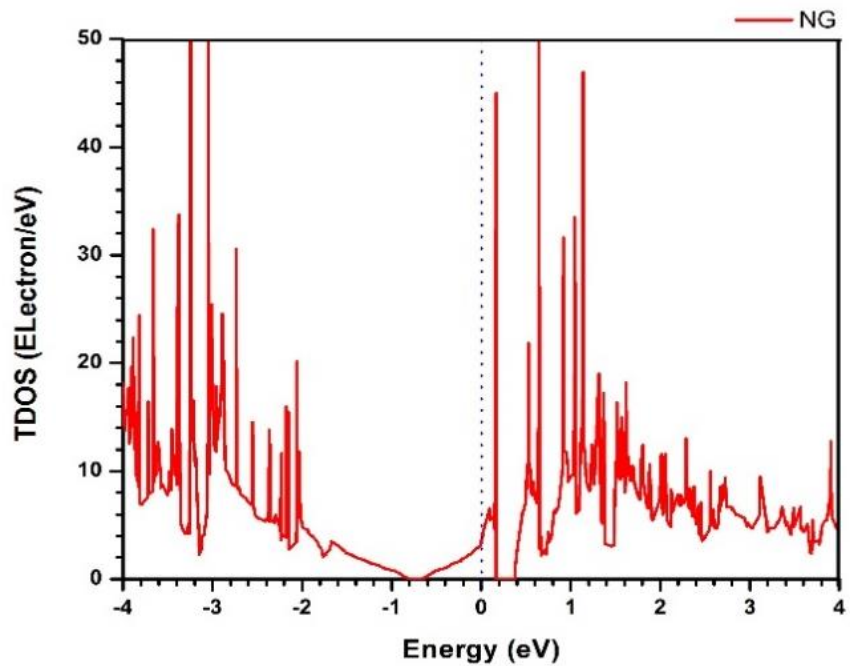
Appendix 2 (a) Bandstructure, (b) TDOS of Cu+ adsorption on pristine graphene.



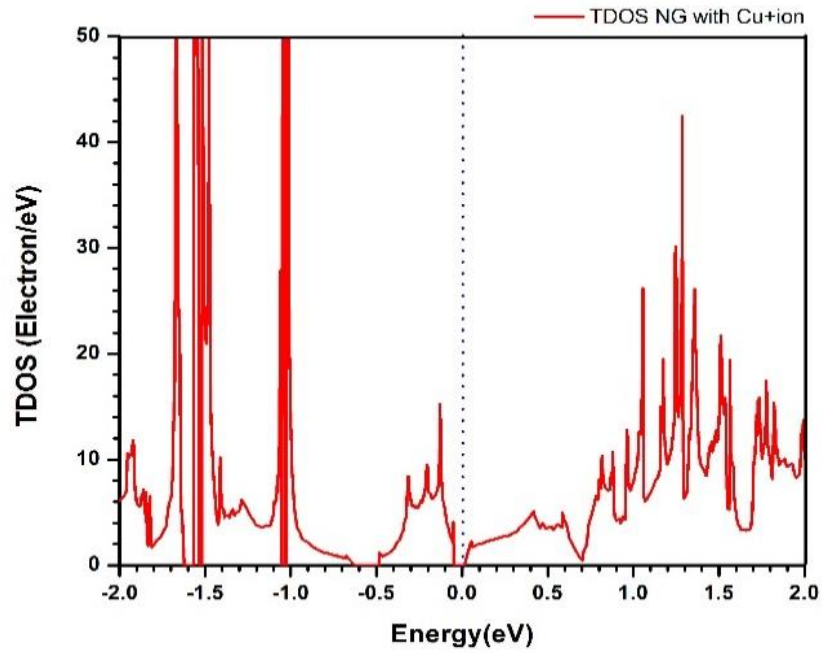
(a)



(b)

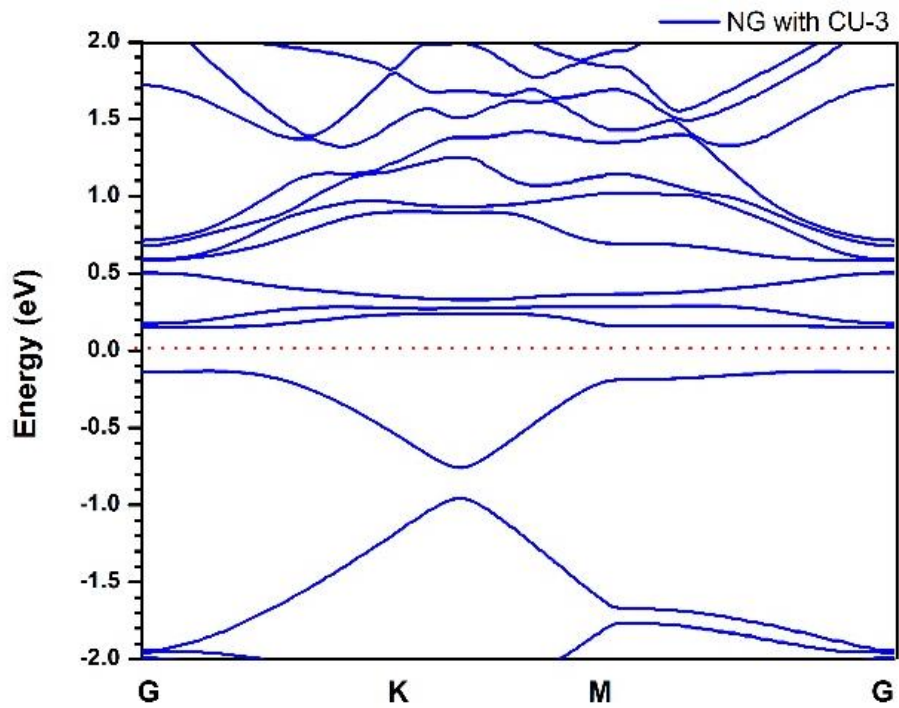


(c)

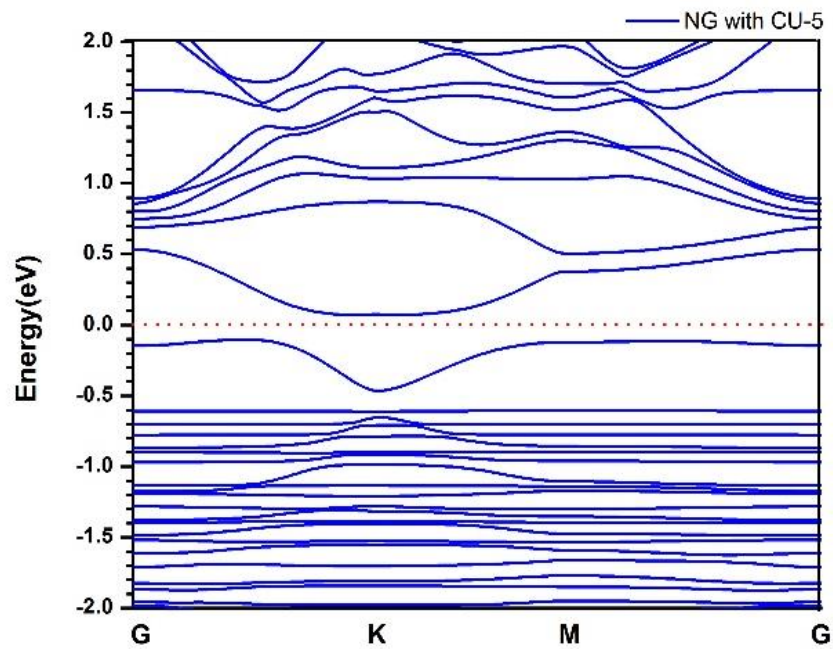


(d)

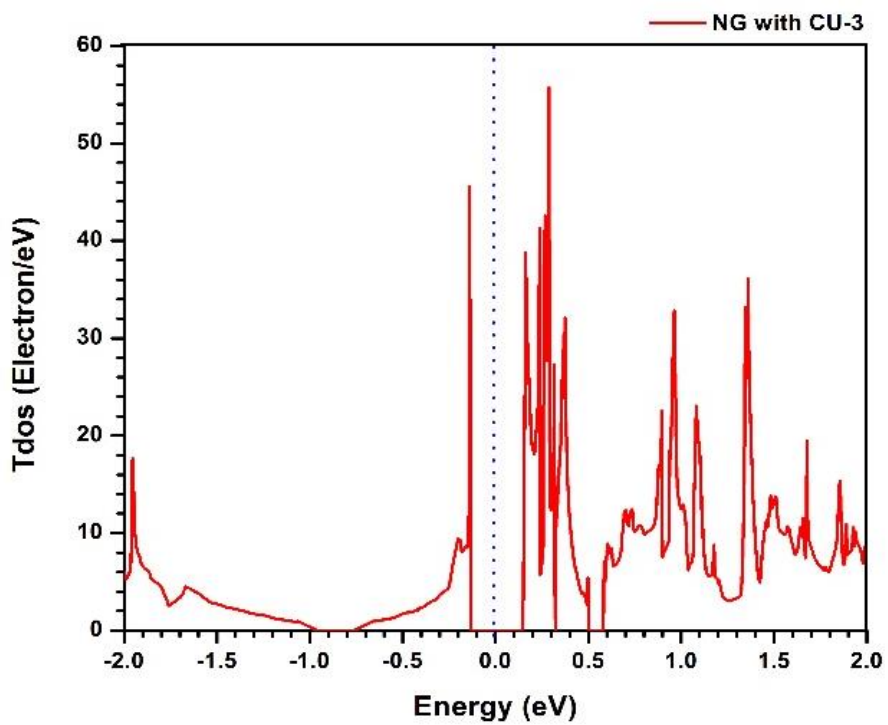
Appendix 3 Bandstructure of (a) NG ,(b) NG with Cu+, Density of states of (c) NG ,(d) NG with Cu+



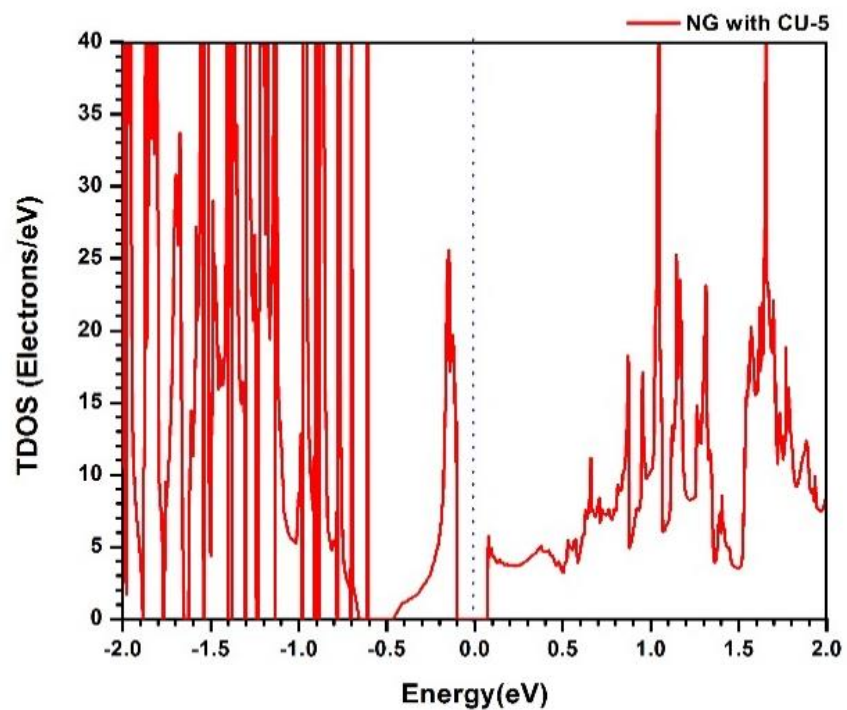
(a)



(b)

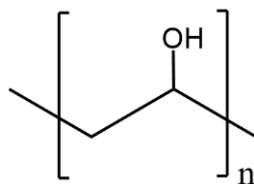


(c)

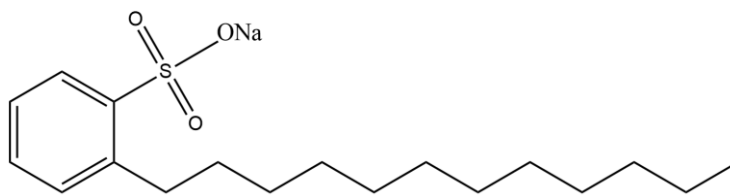


(d)

Appendix 4 Band structure of (a) NG with CU-3, (b) NG with CU-5 and density of states of (a) NG with CU-3, (b) NG with CU-5.



(a)



(b)

Appendix 5 chemical structure (a) Polyvinyl alcohol (b) sodium dodecyl benzene sulphonate (SDBS)

BIO-DATA

Sanka Rama Venkata Siva Prasanna

EDUCATION

- 2014-2016 M.Tech in Pipeline engineering, University of Petroleum & Energy Studies (UPES), Dehradun
- 2010-2013 B.Tech in Mechanical Engineering, Chirala Engineering College, Chirala
- 2007-2010 Diploma in Mechanical Engineering, Bapatla Polytechnic College, Bapatla

JOURNAL PUBLICATIONS

Articles

1. **Sanka, R. V., Siva Prasanna**, Balaji Krishnakumar, Yves Leterrier, Shyam Pandey, Sravendra Rana, and Veronique Michaud. "Soft Self-Healing Nanocomposites." *Frontiers In Materials* 6 (2019):1-20. (I.F:2.27)
2. **Sanka, R. V., Siva Prasanna**, K. Balaji, Yves Leterrier, Shyam Pandey, Monika Srivastava, Anurag Srivastava, Wolfgang H. Binder, Sravendra Rana, and Véronique Michaud. "Nitrogen-doped graphene stabilized copper nanoparticles for Huisgen [3+ 2] cycloaddition "click" chemistry." *Chemical Communications* 44 (2019):6249-6252. (I.F:6.12)
3. B. Krishnakumar, **Sanka, R. V., Siva Prasanna**, W. H. Binder, V. Parthasarthy, S. Rana, and N. Karak, "Vitrimers: Associative dynamic covalent adaptive networks in thermoset polymers," *Chem. Eng. J.*, vol. 385, p. 123820, 2020. (I.F:8.47)
4. B. Krishnakumar, **Sanka, R. V., Siva Prasanna**, W. H. Binder, C. Park, J. Jung, V. Parthasarthy, S. Rana and G. J. Yun, "Catalyst free self-healable vitrimer/graphene oxide nanocomposites," *Compos. Part B Eng.*, vol. 184, p. 107647, 2020. (I.F:7.39)
5. Pandey, Sandeep, **Sanka, R. V., Siva Prasanna**, Manoj Karakoti, Chetna Tewari, Boddepalli SanthiBhushan, Jitendra K. Pandey, Anurag Srivastava, Sravendra Rana, and Nanda Gopal Sahoo. "Dispersion and stability study of carbon nanotubes in pH and temperature responsive polymeric matrix: Experiment and dispersion-corrected DFT study." *Materials Today Communications* 17 (2018): 187-193. (I.F:1.98)

Book Chapters

1. **Sanka, R. V., Siva Prasanna**, K. Balaji, Shyam Pandey, and Sravendra Rana. "Metal Oxide Based Nanomaterials and Their Polymer Nanocomposites." *In Nanomaterials and Polymer Nanocomposites*, pp. 123-144. Elsevier, 2019.
2. Karakoti, Manoj, Sunil Dhali, Sravendra Rana, **Sanka, R. V., Siva Prasanna**, S. P. S. Mehta, and Nanda G. Sahoo. "Surface Modification of Carbon-Based Nanomaterials for Polymer Nanocomposites." *In Carbon-Based Polymer Nanocomposites for Environmental and Energy Applications*, pp. 27-56. 2018.

Conference Presentations

1. “International Conference on Nano for Energy and Water (NEW) & Indo-French Workshop on water Networking” being held at UPES on February 22-24, 2017. Graphene Supported Copper Nanoparticles for Click Triggered Self-healing Nanocomposites. Sravendra Rana, **Sanka, R. V., Siva Prasanna**, Jitendra K. Pandey, Nanda Gopal Sahoo, and Wolfgang H. Binder
2. “International Conference on Nanotechnology: Ideas, Innovation & Initiatives-2017 (ICN:31-2017)”, being held at Indian Institute of Technology Roorkee (IITR) on December 06-08, 2017. Click triggered self-healing graphene nanocomposites Sravendra Rana, **Sanka, R. V., Siva Prasanna**, Balaji K
3. “International Conference on Science and Engineering of Materials-ICSEM 2018” being held at Sharda University on January 06-08, 2018, as an Invited Speaker. Carbon nanofillers based self-healing composite materials **Sanka, R. V., Siva Prasanna**, Balaji K, Sravendra Rana
4. “Sixth International Conference on Recent Advances in Composite Materials” being held at IIT Banaras on February 25-28, 2019. Graphene reinforced self-repairing nanocomposites, Balaji K, **Sanka, R. V., Siva Prasanna**, Sravendra Rana.
5. “Third International Conference on Recent Advances in Material chemistry- ICRAMC 2019” being held at SRM Institute of Science and Technology with Alternative Energies and Atomic Energy Commission (CEA) on February 13-15, 2019. Click Chemistry Promoted by Graphene Immobilized Copper Nanoparticles, Balaji K, **Sanka, R. V., Siva Prasanna**, Sravendra Rana.
6. “International conference on Advances in Polymeric Materials & Human healthcare-APA-STERMI 2019” being held at International Conference Centre, Goa on 16-18, October 2019. Self-healable vitrimer/graphene oxide nanocomposites, Sravendra Rana, Balaji K, Manjeet Singh, **Sanka, R. V., Siva Prasanna**.
7. “International Conference on Advances in Chemical Engineering (ADCHE-2020)” being held at UPES, Dehradun on 05-07-Feb, 2020. Graphene based self-healing vitrimer nanocomposite, Sravendra Rana, Balaji K, **Sanka, R. V., Siva Prasanna**. (Best Presentation award)
8. “International Conference on Advances in Chemical Engineering (ADCHE-2020)” being held at UPES, Dehradun on 05-07-Feb, 2020. Self-healing epoxy graphene oxide vitrimer nanocomposite with disulfide exchanges, Sravendra Rana, Balaji K, **Sanka, R. V., Siva Prasanna**.

Development of Graphene Promoted Click Triggered Self-Healing Nanocomposites

ORIGINALITY REPORT

12% SIMILARITY INDEX **12%** INTERNET SOURCES **0%** PUBLICATIONS **0%** STUDENT PAPERS

MATCH ALL SOURCES (ONLY SELECTED SOURCE PRINTED)

5% ★ d-
nb.info
Internet Source

Exclude quotes On Exclude matches < 8 words

Exclude bibliography On

The plagiarism report was generated using Turnitin software. We have observed a slightly higher similarity index, which seems due to unavoidable chemical names (as they are common chemicals/solvents used for designing the self-healing structures).



Dr. Sravendra Rana



Dr. Shyam Pandey